

Scientific reticence and sea level rise

J E Hansen

NASA Goddard Institute for Space Studies, 2880 Broadway, New York, NY 10025, USA

E-mail: jhansen@giss.nasa.gov

Received 23 March 2007

Accepted for publication 3 May 2007

Published 24 May 2007

Online at stacks.iop.org/ERL/2/024002

Abstract

I suggest that a 'scientific reticence' is inhibiting the communication of a threat of a potentially large sea level rise. Delay is dangerous because of system inertias that could create a situation with future sea level changes out of our control. I argue for calling together a panel of scientific leaders to hear evidence and issue a prompt plain-written report on current understanding of the sea level change issue.

Keywords: sea level, global warming, glaciology, ice sheets

1. Introduction

I suggest that 'scientific reticence', in some cases, hinders communication with the public about dangers of global warming. If I am right, it is important that policy-makers recognize the potential influence of this phenomenon.

Scientific reticence may be a consequence of the scientific method. Success in science depends on objective skepticism. Caution, if not reticence, has its merits. However, in a case such as ice sheet instability and sea level rise, there is a danger in excessive caution. We may rue reticence, if it serves to lock in future disasters.

Barber (1961) describes a 'resistance by scientists to scientific discovery', with a scholarly discussion of several sources of cultural resistance. There are aspects of the phenomenon that Barber discusses in the 'scientific reticence' that I describe, but additional factors come into play in the case of global climate change and sea level rise.

Another relevant discussion is that of 'behavioral discounting' (Hariri *et al* 2006), also called 'delay discounting' (Axtell and McRae 2006). Concern about the danger of 'crying wolf' is more immediate than concern about the danger of 'fiddling while Rome burns'. It is argued in the referenced discussions that there is a preference for immediate over delayed rewards, which may contribute to irrational reticence even among rational scientists.

I can illustrate 'scientific reticence' best via personal experiences. The examples are relevant to the Intergovernmental Panel on Climate Change (IPCC) process of assessing the state of the science, specifically to the issue of possible sea level rise.

2. The court case

'Scientific reticence' leapt to mind as I was being questioned, and boxed-in, by a lawyer for the plaintiff in Automobile Manufacturers versus California Air Resources Board (Auto Manufacturers 2006). I conceded that I was not a glaciologist. The lawyer then, with aplomb, requested that I identify glaciologists who agreed publicly with my assertion that the sea level was likely to rise more than one meter this century if greenhouse gas emissions followed an IPCC business-as-usual (BAU) scenario: 'Name one!'

I could not, instantly. I was dismayed, because, in conversation and e-mail exchange with relevant scientists I sensed a deep concern about likely consequences of BAU global warming for ice sheet stability. What would be the legal standing of such a lame response as 'scientific reticence'? Why would scientists be reticent to express concerns about something so important?

I suspect the existence of what I call the 'John Mercer effect'. Mercer (1978) suggested that global warming from burning of fossil fuels could lead to disastrous disintegration of the West Antarctic ice sheet, with a sea level rise of several meters worldwide. This was during the era when global warming was beginning to get attention from the United States Department of Energy and other science agencies. I noticed that scientists who disputed Mercer, suggesting that his paper was alarmist, were treated as being more authoritative.

It was not obvious who was right on the science, but it seemed to me, and I believe to most scientists, that the scientists preaching caution and downplaying the dangers of climate change fared better in receipt of research funding.

Drawing attention to the dangers of global warming may or may not have helped increase funding for relevant scientific areas, but it surely did not help individuals like Mercer who stuck their heads out. I could vouch for that from my own experience. After I published a paper (Hansen *et al* 1981) that described likely climate effects of fossil fuel use, the Department of Energy reversed a decision to fund our research, specifically highlighting and criticizing aspects of that paper at a workshop in Coolfont, West Virginia and in publication (MacCracken 1983).

I believe there is a pressure on scientists to be conservative. Papers are accepted for publication more readily if they do not push too far and are larded with caveats. Caveats are essential to science, being born in skepticism, which is essential to the process of investigation and verification. But there is a question of degree. A tendency for 'gradualism' as new evidence comes to light may be ill-suited for communication, when an issue with a short time fuse is concerned.

However, these matters are subjective. I could not see how to prove the existence of a 'scientific reticence' about ice sheets and sea level. Score one for the plaintiff, and their ally and 'friend of the court', the United States federal government.

3. On the ice

A field glaciologist, referring to a moulin on Greenland, said: 'the whole damned ice sheet is going to go down that hole!' He was talking about his expectations, under the assumption of continued unchecked growth of global greenhouse gas emissions. Field glaciologists have been doing a good job of reporting current trends on the ice sheets. It is the translation of field data into conclusions needed by the public and policymakers that is at issue.

Ice sheet disintegration, unlike ice sheet growth, is a wet process that can proceed rapidly. Multiple positive feedbacks accelerate the process once it is underway. These feedbacks occur on and under the ice sheets and in the nearby oceans.

A key feedback on the ice sheets is the 'albedo flip' (Hansen *et al* 2007) that occurs when snow and ice begin to melt. Snow-covered ice reflects back to space most of the sunlight striking it. However, as warming causes melting on the surface, the darker wet ice absorbs much more solar energy. Most of the resulting melt water burrows through the ice sheet, lubricates its base, and thus speeds the discharge of icebergs to the ocean (Zwally *et al* 2002).

The area with summer melt on Greenland increased from ~450 000 km² when satellite observations began in 1979 to more than 600 000 km² in 2002 (Steffen *et al* 2004). A linear fit to data for 1992–2005 yields an increase of melt area of 40 000 km²/year (Tedesco 2007), but this rate may be exaggerated by the effect of stratospheric aerosols from the 1991 volcanic eruption of Mount Pinatubo, which reduced the summer melt in 1992. Summer melt on West Antarctica has received less attention than on Greenland, but it is more important. Satellite QuickSCAT radiometer observations reveal increasing areas of summer melt on West Antarctica and

an increasing melt season length during the period 1999–2005 (Nghiem *et al* 2007).

The key role of the ocean, in the matter of ice sheet stability, is as a conduit for excess global-scale heating that eventually leads to the melting of ice. The process begins with increasing human-made greenhouse gases, which cause the atmosphere to be more opaque at infrared wavelengths. The increased atmospheric opacity causes heat radiation to space to emerge from a higher level, where it is colder, thus decreasing the radiation of heat to space. As a result, the Earth is now out of energy balance by between 0.5 and 1 W m⁻² (Hansen *et al* 2005).

This planetary energy imbalance is itself now sufficient to melt ice corresponding to one meter of sea level rise per decade, if the energy were used entirely for that purpose (Hansen *et al* 2005). However, so far most of the excess energy has been going into the ocean. Acceleration of ice sheet disintegration requires tapping into ocean heat, which occurs primarily in two ways (Hansen 2005): (1) increased velocity of outlet glaciers (flowing in rock-walled channels) and ice streams (bordered mainly by slower moving ice), and thus increased flux and subsequent melting of icebergs discharged to the open ocean, and (2) direct contact of ocean and ice sheet (underneath and against fringing ice shelves). Ice loss from the second process has a positive feedback on the first process: as buttressing ice shelves melt, the ice stream velocity increases.

Positive feedback from the loss of buttressing ice shelves is relevant to some Greenland ice streams, but the West Antarctic ice sheet, which rests on bedrock well below sea level (Thomas *et al* 2004), will be affected much more. The loss of ice shelves provides exit routes with reduced resistance for ice from further inland, as suggested by Mercer (1978) and earlier by Hughes (1972). Warming ocean waters are now thinning some West Antarctic ice shelves by several meters per year (Payne *et al* 2004, Shepherd *et al* 2004).

The Antarctic peninsula recently provided a laboratory to study feedback interactions, albeit for ice volumes less than those in the major ice sheets. Combined actions of surface melt (Van den Broeke 2005) and ice shelf thinning from below (Shepherd *et al* 2003) led to the sudden collapse of the Larsen B ice shelf, which was followed by the acceleration of glacial tributaries far inland (Rignot *et al* 2004, Scambos *et al* 2004). The summer warming and melt that preceded the ice shelf collapse (Fahnestock *et al* 2002, Vaughan *et al* 2003) was no more than the global warming expected this century under BAU scenarios, and only a fraction of expected West Antarctic warming with realistic polar amplification of global warming.

Modeling studies yield increased ocean heat uptake around West Antarctica and Greenland due to increasing human-made greenhouse gases (Hansen *et al* 2006b). Observations show a warming ocean around West Antarctica (Shepherd *et al* 2004), ice shelves thinning several meters per year (Rignot and Jacobs 2002, Payne *et al* 2004), and increased iceberg discharge (Thomas *et al* 2004). As the discharge of ice increases from a disintegrating ice sheet, as occurs with all deglaciations, regional cooling by the icebergs is significant, providing a substantial but temporary negative feedback (Hansen 2005). However, this cooling effect is

limited on a global scale as shown by comparison with the planetary energy imbalance, which is now sufficient to melt ice equivalent to about one meter of sea level per decade (table S1 of Hansen *et al* 2005). Yet the planetary energy imbalance should not be thought of as a limit on the rate of ice melt, as increasing iceberg discharge yields both positive and negative feedbacks on planetary energy imbalance via ocean surface cooling and resulting changes of sea ice and cloud cover.

Global warming should also increase snowfall accumulation rates in ice sheet interiors because of the higher moisture content of the warming atmosphere. Despite high variability on interannual and decadal timescales, and limited Antarctic warming to date, observations tend to support this expectation for both Greenland and Antarctica (Rignot and Thomas 2002, Johannessen *et al* 2005, Davis *et al* 2005, Monaghan *et al* 2006). Indeed, some models (Wild *et al* 2003) have ice sheets growing overall with global warming, but those models do not include realistic processes of ice sheet disintegration. Extensive paleoclimate data confirm the common sense expectation that the net effect is for ice sheets to shrink as the world warms.

The most compelling data for the net change of ice sheets is provided by the gravity satellite mission GRACE, which shows that both Greenland (Chen *et al* 2006) and Antarctica (Velicogna and Wahr 2006) are losing mass at substantial rates. The most recent analyses of the satellite data (Klosco) confirm that Greenland and Antarctica are each losing mass at a rate of about 150 cubic kilometers per year, with the Antarctic mass loss primarily in West Antarctica. These rates of mass loss are at least a doubling of rates of several years earlier, and only a decade earlier these ice sheets were much closer to mass balance (Cazenave 2006).

The Antarctic data are the most disconcerting. Warming there has been limited in recent decades, at least in part due to the effects of ozone depletion (Shindell and Schmidt 2004). The fact that West Antarctica is losing mass at a significant rate suggests that the thinning ice shelves are already beginning to have an effect on ice discharge rates. Warming of the ocean surface around Antarctica (Hansen *et al* 2006a) is small compared with the rest of world, consistent with climate model simulations (IPCC 2007), but that limited warming is expected to increase (Hansen *et al* 2006b). The detection of recent, increasing summer surface melt on West Antarctica (Nghiem *et al* 2007) raises the danger that feedbacks among these processes could lead to nonlinear growth of ice discharge from Antarctica.

4. Urgency: this problem is nonlinear!

IPCC business-as-usual (BAU) scenarios are constructs in which it is assumed that emissions of CO₂ and other greenhouse gases will continue to increase year after year. Some energy analysts take it as almost a law of physics that such growth of emissions will continue in the future. Clearly, there is not sufficiently widespread appreciation of the implications of putting back into the air a large fraction of the carbon stored in the ground over epochs of geologic time. Climate forcing due to these greenhouse gases would

dwarf the climate forcing for any time in the past several hundred thousand years, when accurate records of atmospheric composition are available from ice cores.

However, the long-term global cooling and increase of global ice through the Plio–Pleistocene provides an even more poignant illustration of the implications of continued BAU burning of fossil fuels. The global oxygen isotope record of benthic (deep ocean dwelling) foraminifera compiled by Lisiecki and Raymo (2005), repeated in figure 10a of Hansen *et al* (2007) for comparison with solar insolation changes over the same period, reveals long-term cooling and sea level fall, with superposed oscillations at a dominant frequency of 41 ky. The long-term cooling presumably is due, at least in part, to the drawdown of atmospheric CO₂ by weathering that accompanied and followed the rapid growth of the Andes (Ghosh *et al* 2006) and Himalayas (Raymo and Ruddiman 1992), which was most rapid in the late Miocene. Changes in meridional heat transport may have contributed to the climate trend (Rind and Chandler 1991), but the CO₂ amount providing a global positive forcing seems unlikely to have been more than approximately 350–450 ppm (Dowsett *et al* 1994, Raymo *et al* 1996, Crowley 1996). The global mean temperature three million years ago was only 2–3 °C warmer than today (Crowley 1996, Dowsett *et al* 1996), while the sea level was 25 ± 10 m higher (Wardlaw and Quinn 1991, Barrett *et al* 1992, Dowsett *et al* 1994).

The Plio–Pleistocene record compiled by Lisiecki and Raymo (2005) is fascinating to paleoclimatologists as it clearly shows the expected dominance of global climate variations with the 41 ky cyclic variation of the tilt of the Earth's spin axis, increased tilt melting ice at both poles. When the planetary cooling reached a degree that allowed a large mid-latitude Northern Hemisphere (Laurentide) ice sheet, the periodicity necessarily became more complex, because of the absence of land area for a similar ice sheet in the Southern Hemisphere (Hansen *et al* 2007). However, the information of practical importance from the Plio–Pleistocene record is the implication of dramatic global climate change with only moderate global climate forcing. With global warming of only 2–3 °C and CO₂ of perhaps 350–450 ppm it was a dramatically different planet, without Arctic sea ice in the warm seasons and with a sea level 25 ± 10 m higher.

Assuming a nominal 'Charney' climate sensitivity of 3 °C equilibrium global warming for doubled CO₂, BAU scenarios yield a global warming at least of the order of 3 °C by the end of this century. However, the Charney sensitivity is the equilibrium (long-term) global response when only fast feedback processes (changes of sea ice, clouds, water vapor and aerosols in response to climate change) are included (Hansen *et al* 2007). Actual global warming would be larger as slow feedbacks come into play. Slow feedbacks include increased vegetation at high latitudes, ice sheet shrinkage, and terrestrial and marine greenhouse gas emissions in response to global warming.

In assessing the likely effects of a warming of 3 °C, it is useful to note the effects of the 0.7 °C warming in the past century (Hansen *et al* 2006a). This warming already produces large areas of summer melt on Greenland and significant melt

on West Antarctica. Global warming of several more degrees, with its polar amplification, would have both Greenland and West Antarctica bathed in summer melt for extended melt seasons.

The IPCC (2007) midrange projection for sea level rise this century is 20–43 cm (8–17 inches) and its full range is 18–59 cm (7–23 inches). The IPCC notes that they are unable to evaluate possible dynamical responses of the ice sheets, and thus do not include any possible ‘rapid dynamical changes in ice flow’. Yet the provision of such specific numbers for sea level rise encourages a predictable public response that the projected sea level change is moderate, and smaller than in IPCC (2001). Indeed, there have been numerous media reports of ‘reduced’ sea level rise predictions, and commentators have denigrated suggestions that business-as-usual greenhouse gas emissions may cause a sea level rise of the order of meters.

However, if these IPCC projected rates of sea level rise are taken as predictions of actual sea level rise, as they have been by the public, they suggest that the ice sheets can miraculously survive a BAU climate forcing assault for a period of the order of a millennium or longer. This is not entirely a figment of the IPCC decision to provide specific numbers for only a portion of the problem, while demurring from any quantitative statement about the most important (dynamical) portion of the problem. Undoubtedly there are glaciologists who anticipate such long response times, because their existing ice sheet models have been designed to match paleoclimate changes, which occur on millennial timescales.

However, Hansen *et al* (2007) show that the typical ~6 ky timescale for paleoclimate ice sheet disintegration reflects the half-width of the shortest of the weak orbital forcings that drive the climate change, not an inherent timescale of ice sheets for disintegration. Indeed, the paleoclimate record contains numerous examples of ice sheets yielding a sea level rise of several meters per century, with forcings smaller than that of the BAU scenario. The problem with the paleoclimate ice sheet models is that they do not generally contain the physics of ice streams, effects of surface melt descending through crevasses and lubricating basal flow, or realistic interactions with the ocean.

Rahmstorf (2007) has noted that if one uses the observed sea level rise of the past century to calibrate a linear projection of future sea level, BAU warming will lead to a sea level rise of the order of one meter in the present century. This is a useful observation, as it indicates that the sea level change would be substantial even without the nonlinear collapse of an ice sheet. However, this approach cannot be taken as a realistic way of projecting the likely sea level rise under BAU forcing. The linear approximation fits the past sea level change well for the past century only because the two terms contributing significantly to sea level rise were (1) thermal expansion of ocean water and (2) melting of alpine glaciers.

Under BAU forcing in the 21st century, the sea level rise surely will be dominated by a third term: (3) ice sheet disintegration. This third term was small until the past few years, but it is has at least doubled in the past decade and is now close to 1 mm/year, based on the gravity satellite measurements discussed above. As a quantitative example,

let us say that the ice sheet contribution is 1 cm for the decade 2005–15 and that it doubles each decade until the West Antarctic ice sheet is largely depleted. That time constant yields a sea level rise of the order of 5 m this century. Of course I cannot prove that my choice of a ten-year doubling time for nonlinear response is accurate, but I am confident that it provides a far better estimate than a linear response for the ice sheet component of sea level rise under BAU forcing.

An important point is that the nonlinear response could easily run out of control, because of positive feedbacks and system inertias. Ocean warming and thus melting of ice shelves will continue after growth of the forcing stops, because the ocean response time is long and the temperature at depth is far from equilibrium for current forcing. Ice sheets also have inertia and are far from equilibrium: and as ice sheets disintegrate their surface moves lower, where it is warmer, subjecting the ice to additional melt. There is also inertia in energy systems: even if it is decided that changes must be made, it may require decades to replace infrastructure.

The nonlinearity of the ice sheet problem makes it impossible to accurately predict the sea level change on a specific date. However, as a physicist, I find it almost inconceivable that BAU climate change would not yield a sea level change of the order of meters on the century timescale. The threat of a large sea level change is a principal element in our argument (Hansen *et al* 2006a, 2006b, 2007) that the global community must aim to keep additional global warming less than 1 °C above the 2000 temperature, and even 1 °C may be too great. In turn, this implies a CO₂ limit of about 450 ppm, or less. Such scenarios are dramatically different than BAU, requiring almost immediate changes to get on a fundamentally different energy and greenhouse gas emissions path.

5. Reticence

Is my perspective on this problem really so different than that of other members of the relevant scientific community? Based on interactions with others, I conclude that there is not such a great gap between my position and that of most, or at least much, of the relevant community. The apparent difference may be partly a natural reticence to speak out, which I attempt to illuminate via specific examples.

In the late 1980s, an article (Kerr 1989) titled ‘Hansen vs. the World on the Greenhouse Threat’, reported on a scientific conference in Amherst, MA. One may have surmised strong disagreement with my assertion (to Congress) that the world had entered a period of strong warming due to human-made greenhouse gases. But participants told Kerr ‘if there were a secret ballot at this meeting on the question, most people would say the greenhouse warming is probably there’. And ‘what bothers us is that we have a scientist telling Congress things that we are reluctant to say ourselves’.

That article made me notice right away a difference between scientists and ‘normal people’. A non-scientist friend from my hometown, who had congratulated me after my congressional testimony, felt bad after he saw the article by Kerr. He obviously believed that I had been shown to be wrong. However, I thought Kerr did a good job of describing

the various perspectives, and made it clear, at least between the lines, that differences were as much about reticence to speak as about scientific interpretations.

IPCC reports may contain a reticence in the sense of being extremely careful about making attributions. This characteristic is appropriately recognized as an asset that makes the IPCC conclusions authoritative and widely accepted. It is probably a necessary characteristic, given that the IPCC document is produced as a consensus among most nations in the world and represents the views of thousands of scientists.

Kerr (2007) describes a specific relevant example, whether the IPCC should include estimates of dynamical ice sheet loss in their projections: ‘too poorly understood, IPCC authors said’, and ‘overly cautious—(dynamical effects) could raise sea level much faster than IPCC was predicting’ some scientists responded. Kerr goes on to say ‘almost immediately, new findings have emerged to support IPCC’s conservative position’. Glaciologist Richard Alley, an IPCC lead author, said ‘Lots of people were saying we [IPCC authors] should extrapolate into the future, but we dug our heels in at the IPCC and said that we don’t know enough to give an answer’.

6. Our legacy

Reticence is fine for the IPCC. And individual scientists can choose to stay within a comfort zone, not needing to worry that they say something that proves to be slightly wrong. But perhaps we should also consider our legacy from a broader perspective. Do we not know enough to say more?

Confidence in a scientific inference can be built from many factors. For climate change these include knowledge gained from studying paleoclimate changes, analysis of how the Earth has responded to forcings on various timescales, climate simulations and tests of these against observations, detailed study of climate change in recent decades and how the nature of observed change compares with expectations, measurements of changes in atmospheric composition and calculation of implied climate forcings, analysis of ways in which climate response varies among different forcings, quantitative data on different feedback processes and how these compare with expectations, and so on.

Can the broader perspective drawn from various sources of information allow us to ‘see the forest for the trees’, to ‘separate the wheat from the chaff’? That a glacier on Greenland slowed after speeding up, used as ‘proof’ that reticence is appropriate, is little different than the common misconception that a cold weather snap disproves global warming. Spatial and temporal fluctuations are normal. Moreover, short-term expectations for Greenland glaciers are different from long-term expectations for West Antarctica. Integration via the gravity satellite measurements puts individual glacier fluctuations in a proper perspective. The broader picture gives a strong indication that ice sheets will, and are already beginning to, respond in a nonlinear fashion to global warming. There is enough information now, in my opinion, to make it a near certainty that IPCC BAU climate forcing scenarios would lead to a disastrous multi-meter sea level rise on the century timescale.

Almost four decades ago Eipper (1970), in a section of his paper titled ‘The Scientist’s Role’, provided cogent advice and wisdom about the responsibility of scientists to warn the public about the potential consequences of human activities. Eipper recognized sources of scientific reticence, but he concluded that scientists should not shrink from exercising their rights as citizens and responsibilities as scientists. Climate change adds additional imperative to Eipper’s thesis, which was developed with reference to traditional air and water pollution. Positive climate feedbacks and global warming already ‘in the pipeline’ due to climate system inertia together yield the possibility of climate ‘tipping points’ (Hansen *et al* 2006b, 2007), such that large additional climate change and climate impacts are possible with little additional human-made forcing. Such a system demands early warnings and forces the concerned scientist to abandon the comfort of waiting for incontrovertible confirmations.

There is, in my opinion, a huge gap between what is understood about human-made global warming and its consequences, and what is known by the people who most need to know, the public and policy makers. The IPCC is doing a commendable job, but we need something more. Given the reticence that the IPCC necessarily exhibits, there need to be supplementary mechanisms. The onus, it seems to me, falls on us scientists as a community.

Important decisions are being made now and in the near future. An example is the large number of new efforts to make liquid fuels from coal, and a resurgence of plans for energy-intensive ‘cooking’ of tar-shale mountains to squeeze out liquid hydrocarbon fuels. These are just the sort of actions needed to preserve a BAU greenhouse gas path indefinitely. We know enough about the carbon cycle to say that at least of the order of a quarter of the CO₂ emitted in burning fossil fuels under a BAU scenario will stay in the air for an eternity, the latter defined practically as more than 500 years. Readily available conventional oil and gas are enough to take atmospheric CO₂ to a level of the order of 450 ppm.

In this circumstance it seems vital that we provide the best information we can about the threat to the great ice sheets posed by human-made climate change. This information, and appropriate caveats, should be provided publicly, and in plain language. The best suggestion I can think of is for the National Academy of Sciences to carry out a study, in the tradition of the Charney and Cicerone reports on global warming. I would be glad to hear alternative suggestions.

Acknowledgments

I thank Tad Anderson, Mark Bowen, Svend Brandt-Erichsen, Jonathan Gregory, Jost Heintzenberg, John Holdren, Ines Horovitz, Bruce Johansen, Ralph Keeling, John Lyman, Len Ornstein, Maureen Raymo, Christopher Shuman, Richard Somerville, and Bob Thomas for comments on a draft version of this letter.

References

- Automobile Manufacturers 2006 Central Valley Chrysler-Jeep v. Catherine Witherspoon, California Air Resources Board, United States District Court, Fresno, Case 1:04-CV-06663

- Axtell R L and McRae G J 2006 Changing how we discount to make public policy more responsive to citizens' time preferences *Regulatory Analysis 06-01* AEI-Brookings Joint Center for Regulatory Studies. Accessed at <http://www.aei-brookings.org/publications/abstract.php?pid=1049>
- Barber B 1961 Resistance by scientists to scientific discovery *Science* **134** 596–602
- Barrett P J, Adams C J, McIntosh W C, Swisher C C and Wilson G S 1992 Geochronological evidence supporting Antarctic deglaciation three million years ago *Nature* **359** 816–8
- Cazenave A 2006 How fast are the ice sheets melting? *Science* **314** 1250–2
- Chen J L, Wilson C R and Tapley B D 2006 Satellite gravity measurements confirm accelerated melting of Greenland Ice Sheet *Science* **313** 1958–60
- Crowley T J 1996 Pliocene climates: the nature of the problem *Mar. Micropaleontol.* **27** 3–12
- Davis C H, Li Y, McConnell J R, Frey M M and Hanna E 2005 Snowfall-driven growth in East Antarctica ice sheet mitigates recent sea-level rise *Science* **308** 1898–1901
- Dowsett H, Barron J and Poore R 1996 Middle Pliocene sea surface temperatures: a global reconstruction *Mar. Micropaleontol.* **27** 13–26
- Dowsett H J, Thompson R, Barron J, Cronin T, Fleming F, Ishman R, Poore D, Willard D and Holtz T 1994 Joint investigations of the Middle Pliocene climate *Glob. Planet. Change* **9** 169–95
- Eipper A W 1970 Pollution problems, resource policy, and the scientist *Science* **169** 11–15
- Fahnestock M A, Abdalati W and Shuman C A 2002 Long melt seasons on ice shelves of the Antarctic Peninsula: an analysis using satellite-based microwave emission measurements *Ann. Glaciol.* **34** 127–33
- Ghosh P, Garzzone C N and Eiler J M 2006 Rapid uplift of the Altiplano revealed through ^{13}C – ^{18}O bonds in paleosol carbonates *Science* **311** 511–5
- Hansen J 2005 A slippery slope: how much global warming constitutes dangerous anthropogenic interference? *Clim. Change* **68** 269–79
- Hansen J, Johnson D, Lacis A, Lebedeff S, Lee P, Rind D and Russell G 1981 Climate impact of increasing atmospheric carbon dioxide *Science* **213** 957–66
- Hansen J, Sato M, Kharecha P, Russell G, Lea D W and Siddall M 2007 Climate change and trace gases *Phil. Trans. R. Soc. A* at press, doi:10.1098/rsta.2007.2052
- Hansen J, Sato M, Ruedy R, Lo K, Lea D W and Medina-Elizade M 2006a Global temperature change *Proc. Natl Acad. Sci.* **103** 14288–93
- Hansen J *et al* 2005 Earth's energy imbalance: confirmation and implications *Science* **308** 1431–5
- Hansen J *et al* 2006b Dangerous human-made interference with climate: A GISS modelE study *Atmos. Chem. Phys. Discuss.* **6** 12549–610
- Hariri A R, Brown S M, Williamson D E, Flory J D, de Wit H and Manuck S B 2006 Preference for immediate over delayed rewards is associated with magnitude of ventral striatal activity *J. Neurosci.* **26** 13213–7
- Hughes T 1972 Is the West Antarctic ice sheet disintegrating? *ISCAP Bulletin* no. 1 Ohio State University
- IPCC (Intergovernmental Panel on Climate Change) 2001 *Climate Change 2001: The Scientific Basis* ed J T Houghton *et al* (Cambridge: Cambridge University Press)
- IPCC 2007 *Climate Change 2007: The Physical Basis—Summary for Policymakers* Accessed at <http://www.ipcc.ch/SPM2feb07.pdf>
- Johannessen O M, Khvorostovsky K, Miles M W and Bobylev L P 2005 Recent ice-sheet growth in the interior of Greenland *Science* **310** 1013–6
- Kerr R A 1989 Hansen vs. the world on the greenhouse threat *Science* **244** 1041–3
- Kerr R A 2007 Predicting fate of glaciers proves slippery task *ScienceNOW* Accessed at <http://sciencenow.sciencemag.org/cgi/content/full/2007/215/2>
- Klosco S *et al* 2007 private communication
- Lisiecki L E and Raymo M E 2005 A Pliocene-Pleistocene stack of 57 globally distributed benthic $\delta^{18}\text{O}$ records *Paleoceanography* **20** PA1003
- MacCracken M C 1983 Climatic effects of atmospheric carbon dioxide *Science* **220** 873–4
- Mercer J 1978 West Antarctic ice sheet and CO_2 greenhouse effect: a threat of disaster *Nature* **271** 321–5
- Monaghan A J *et al* 2006 Insignificant change in Antarctic snowfall since the International Geophysical Year *Science* **313** 827–31
- Nghiem S V, Steffen K, Neumann G and Huff R 2007 Snow accumulation and snowmelt monitoring in Greenland and Antarctica *Dynamic Planet—Monitoring and Understanding a Dynamic Planet with Geodetic and Oceanographic Tools: Proc. IAG Symp. (Cairns, Aug. 2005) (Intl. Assoc. Geodesy Symposia vol 130)* ed C Rizos and P Tregoning (New York: Springer)
- Payne A J, Vieli A, Shepherd A P, Wingham D J and Rignot E 2004 Recent dramatic thinning of largest West Antarctic ice stream triggered by oceans *Geophys. Res. Lett.* **31** L23401
- Rahmstorf S 2007 A semi-empirical approach to projecting future sea-level rise *Science* **315** 368–70
- Raymo M E, Grant B, Horowitz M and Rau G H 1996 Mid-Pliocene warmth: stronger greenhouse and stronger conveyor *Mar. Micropaleontol.* **27** 313–26
- Raymo M E and Ruddiman W F 1992 Tectonic forcing of late Cenozoic climate *Nature* **359** 117–22
- Rignot E, Casassa G, Gogineni P, Krabill W, Rivera A and Thomas R 2004 Accelerated discharge from the Antarctic Peninsula following collapse of Larsen B ice shelf *Geophys. Res. Lett.* **31** L18401
- Rignot E and Jacobs S S 2002 Rapid bottom melting widespread near Antarctic ice sheet grounding lines *Science* **296** 2020–3
- Rignot E and Thomas R H 2002 Mass balance of polar ice sheets *Science* **297** 1502–6
- Rind D and Chandler M 1991 Increased ocean heat transports and warmer climate *J. Geophys. Res.* **96** 7437–61
- Scambos T A, Bohlander J A, Shuman C A and Skvarca P 2004 Glacier acceleration and thinning after ice shelf collapse in the Larsen B embayment, Antarctica *Geophys. Res. Lett.* **31** L18402
- Shepherd A, Wingham D, Payne T and Skvarca P 2003 Larsen ice shelf has progressively thinned *Science* **302** 856–9
- Shepherd A, Wingham D and Rignot E 2004 Warm ocean is eroding West Antarctic ice sheet *Geophys. Res. Lett.* **31** L23402
- Shindell D T and Schmidt G A 2004 Southern Hemisphere climate response to ozone changes and greenhouse gas increases *Geophys. Res. Lett.* **31** L18209
- Steffen K, Nghiem S V, Huff R and Neumann G 2004 The melt anomaly of 2002 on the Greenland Ice Sheet from active and passive microwave satellite observations *Geophys. Res. Lett.* **31** L20402
- Tedesco M 2007 Snowmelt detection over the Greenland ice sheet from SSM/I brightness temperature daily variations *Geophys. Res. Lett.* **34** L02504
- Thomas R *et al* 2004 Accelerated sea-level rise from West Antarctica *Science* **306** 255–8
- Van den Broeke M 2005 Strong surface melting preceded collapse of Antarctic Peninsula ice shelf *Geophys. Res. Lett.* **32** L12815
- Vaughan D G, Marshall G J, Connolley W M, Parkinson C, Mulvaney R, Hodgson D A, King J C, Pudsey C J and Turner J 2003 Recent rapid regional climate warming on the Antarctic Peninsula *Clim. Change* **60** 243–74
- Velicogna I and Wahr J 2006 Measurements of time-variable gravity show mass loss in Antarctica *Science* **311** 1754–6
- Wardlaw B R and Quinn T M 1991 The record of Pliocene sea-level change at Enewetak atoll *Quat. Sci. Rev.* **10** 247–58
- Wild M, Calanca P, Scherer S C and Ohmura A 2003 Effects of polar ice sheets on global sea level in high-resolution greenhouse scenarios *J. Geophys. Res.* **108(D5)** 4165
- Zwally H J, Abdalati W, Herring T, Larson K, Saba J and Steffen K 2002 Surface melt-induced acceleration of Greenland ice-sheet flow *Science* **297** 218–22

Target Atmospheric CO₂: Where Should Humanity Aim?

James Hansen,^{1,2*} Makiko Sato,^{1,2} Pushker Kharecha,^{1,2} David Beerling,³
Valerie Masson-Delmotte,⁴ Mark Pagani,⁵ Maureen Raymo,⁶ Dana Royer,⁷ James C. Zachos⁸

Paleoclimate data show that climate sensitivity is ~3°C for doubled CO₂, including only fast feedback processes. Equilibrium sensitivity, including slower surface albedo feedbacks, is ~6°C for doubled CO₂ for the range of climate states between glacial conditions and ice-free Antarctica. Decreasing CO₂ was the main cause of a cooling trend that began 50 million years ago, large scale glaciation occurring when CO₂ fell to 425±75 ppm, a level that will be exceeded within decades, barring prompt policy changes. If humanity wishes to preserve a planet similar to that on which civilization developed, paleoclimate evidence and ongoing climate change suggest that CO₂ will need to be reduced from its current 385 ppm to at most 350 ppm. The largest uncertainty in the target arises from possible changes of non-CO₂ forcings. An initial 350 ppm CO₂ target may be achievable by phasing out coal use except where CO₂ is captured and adopting agricultural and forestry practices that sequester carbon. If the present overshoot of this target CO₂ is not brief, there is a possibility of seeding irreversible catastrophic effects.

Human activities are altering Earth's atmospheric composition. Concern about global warming due to long-lived human-made greenhouse gases (GHGs) led to the United Nations Framework Convention on Climate Change (1) with the objective of stabilizing GHGs in the atmosphere at a level preventing "dangerous anthropogenic interference with the climate system."

The Intergovernmental Panel on Climate Change (IPCC, 2) and others (3) used several "reasons for concern" to estimate that global warming of more than 2-3°C may be dangerous. The European Union adopted 2°C above pre-industrial global temperature as a goal to limit human-made warming (4). Hansen et al. (5) argued for a limit of 1°C global warming (relative to 2000, 1.7°C relative to pre-industrial time), aiming to avoid practically irreversible ice sheet and species loss. This 1°C limit, with nominal climate sensitivity of 3/4°C per W/m² and plausible control of other GHGs (22), implies maximum CO₂ ~ 450 ppm (5).

Our current analysis suggests that humanity must aim for an even lower level of GHGs. Paleoclimate data and ongoing global changes indicate that 'slow' climate feedback processes not included in most climate models, such as ice sheet disintegration, vegetation migration, and GHG release from soils, tundra or ocean sediments, may begin to come into play on time scales as short as centuries or less (6). Rapid on-going climate changes and realization that Earth is out of energy balance, implying that more warming is 'in the pipeline' (7), add urgency to investigation of the dangerous level of GHGs.

We use paleoclimate data to evaluate equilibrium or long-term climate sensitivity to climate forcings including GHGs. The time scale of response to rapidly increasing human-made forcings is difficult to assess, but emerging climate changes help us estimate an initial GHG target level.

Climate sensitivity. A global climate forcing, measured in W/m² averaged over the planet, is an imposed perturbation of the planet's energy balance. Increase of solar irradiance (S₀) by 2% and doubling of atmospheric CO₂ are each forcings of about 4 W/m² (8).

Charney (9) defined an idealized climate sensitivity problem, asking how much global surface temperature would increase if atmospheric CO₂ were instantly doubled, assuming that slowly-changing planetary surface conditions, such as ice sheets and forest cover, were fixed.

Long-lived GHGs, except for the specified CO₂ change, were also fixed, not responding to climate change. The Charney problem thus provides a measure of climate sensitivity including only the effect of ‘fast’ feedback processes, such as changes of water vapor, clouds and sea ice.

Classification of climate change mechanisms into fast and slow feedbacks is useful, even though time scales of these changes may overlap. We include as fast feedbacks the aerosol changes, e.g., of desert dust and marine dimethylsulfide, that occur in response to climate change (6).

Charney (9) used climate models to estimate fast-feedback doubled CO₂ sensitivity of $3 \pm 1.5^\circ\text{C}$. Water vapor increase and sea ice decrease in response to global warming were both found to be strong positive feedbacks, amplifying the surface temperature response. Climate models in the current IPCC (2) assessment still agree with Charney’s estimate.

Climate models alone are unable to define climate sensitivity more precisely, because it is difficult to prove that models realistically incorporate all feedback processes. The Earth’s history, however, allows empirical inference of both fast feedback climate sensitivity and long-term sensitivity to specified GHG change including the slow ice sheet feedback.

Pleistocene Epoch.

Atmospheric composition and surface properties in the late Pleistocene are known well enough to allow accurate assessment of the fast-feedback (Charney) climate sensitivity. We first compare the pre-industrial Holocene with the last glacial maximum (LGM, 20 ky BP). The planet was in energy balance in both periods within a small fraction of 1 W/m^2 , as shown by considering the contrary: an imbalance of 1 W/m^2 maintained a few millennia would melt all ice on the planet or change ocean temperature an amount far outside measured variations (Table S1 of 7). The approximate equilibrium in these paleoclimate periods is unlike the current situation, in which GHG levels are rising much faster than the coupled climate system can respond.

Climate forcing in the LGM equilibrium state, relative to the Holocene, due to the slow-feedback ice age surface properties, i.e., increased ice area, different vegetation distribution, and continental shelf exposure, was $-3.5 \pm 1 \text{ W/m}^2$ (10). The forcing due to reduced amounts of long-lived GHGs (CO₂, CH₄, N₂O) was $-3 \pm 0.5 \text{ W/m}^2$, with the indirect effects of CH₄ on tropospheric ozone and stratospheric water vapor included (fig. S1). Global forcing due to slight changes in the Earth’s orbit is a negligible fraction of 1 W/m^2 (fig. S2). The combined 6.5 W/m^2 forcing and global surface temperature change of $5 \pm 1^\circ\text{C}$ relative to the Holocene (10b,c), yields an empirical sensitivity $\sim 3/4 \pm 1/4 \text{ }^\circ\text{C per W/m}^2$ forcing, i.e., a Charney sensitivity of $3 \pm 1 \text{ }^\circ\text{C}$ for the 4 W/m^2 forcing of doubled CO₂. This empirical fast-feedback climate sensitivity allows water vapor, clouds, aerosols, sea ice, and all other fast feedbacks that exist in the real world to respond naturally to global climate change.

Climate sensitivity varies as Earth becomes warmer or cooler. Toward colder extremes, as the area of sea ice grows, the planet approaches runaway snowball-Earth conditions, and at high temperatures it can approach a runaway greenhouse effect (8). At its present temperature Earth is on a flat portion of its fast-feedback climate sensitivity curve (fig. S3). Thus our empirical sensitivity, although strictly the mean fast-feedback sensitivity for climate states ranging from the ice age to the current interglacial period, is valid as today’s fast-feedback climate sensitivity.

Verification. Our empirical fast-feedback climate sensitivity, derived by comparing conditions at two points in time, can be checked over the longer period of ice core data. Fig. 1A shows CO₂ and CH₄ data from the Antarctic Vostok ice core (11) and sea level based on Red Sea sediment cores (12). Gases are from the same ice core and have a consistent time scale, but dating with respect to sea level may have errors up to several thousand years.

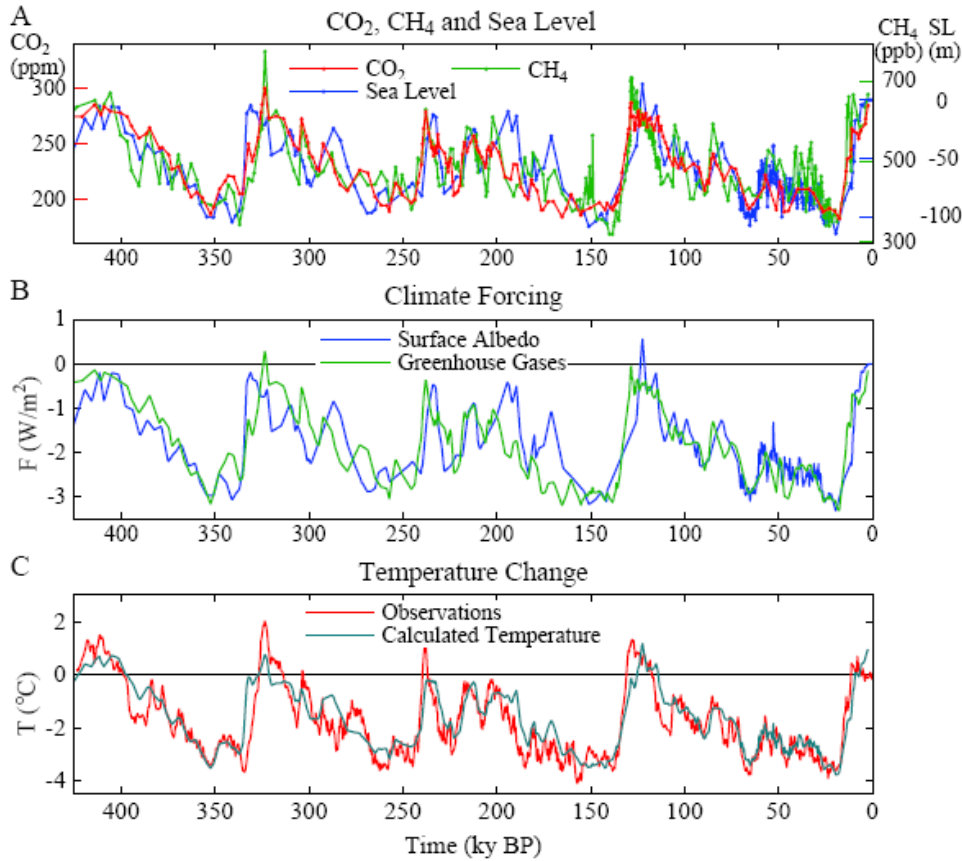


Fig. 1. (A) CO₂, CH₄ (11) and sea level (12) for past 425 ky. (B) Climate forcings due to changes of GHGs and ice sheet area, the latter inferred from sea level change. (C) Calculated global temperature change based on climate sensitivity of 3/4°C per W/m². Observations are Antarctic temperature change (11) divided by two.

We use the GHG and sea level data to calculate climate forcing by GHGs and surface albedo change, with two refinements relative to prior calculations (6). First, the climate forcing by N₂O is only about 12 percent of the sum of the CO₂ and CH₄ forcings for the GHG changes between the LGM and late Holocene (see tabulation in fig. S1), rather than 15 percent estimated earlier (6). Because N₂O data are not available for the entire record, its forcing is small, and its variations have high coherence with CO₂ and CH₄, we take the effective forcing as

$$F_e (\text{GHGs}) = 1.12 [F_a(\text{CO}_2) + 1.4 F_a(\text{CH}_4)], \quad (1)$$

using published formulae for F_a of each gas (13). The factor 1.4 accounts for the higher efficacy of CH₄ relative to CO₂, which is due mainly to the indirect effect of CH₄ on tropospheric ozone and stratospheric water vapor (8). The resulting GHG forcing between the LGM and late Holocene is 3 W/m², divided as CO₂ (75%), CH₄ (14%), N₂O (11%).

The second refinement is to the surface albedo. Based on models of ice sheet shape, we take the horizontal area of the ice sheet as proportional to the 4/5 power of volume. Fig. S4 compares our present albedo forcing with prior use (6) of exponent 2/3, showing that this choice and division of the ice into multiple ice sheets has only a minor effect.

Multiplying the sum of GHG and surface albedo forcings by climate sensitivity 3/4°C per W/m² yields the blue curve in Fig. 1(C), which is compared with observed Vostok temperature change (11) divided by two (red curve). Antarctic temperature change divided by two is a crude measure of global temperature change, as typical glacial-interglacial temperature change is ~5°C

on global average and $\sim 10^\circ\text{C}$ in Antarctica (14). Figure 1C shows that fast-feedback climate sensitivity $\frac{3}{4}^\circ\text{C}$ per W/m^2 (3°C for doubled CO_2) is a good approximation for the entire period.

Slow feedbacks. Let us consider climate change averaged over a few thousand years, long enough to assure energy balance and minimize effects of ocean thermal response time and climate change leads and lags between hemispheres (16). At such temporal resolution the temperature variations in Fig.1 are global, with high latitude amplification, being present in sea surface temperature derived from ocean sediment cores and polar ice cores (fig S3).

GHG and surface albedo changes are the mechanisms causing the large global climate changes in Fig. 1, but they do not instigate the climate swings. GHG changes lag temperature change by typically several hundred years (17, fig.1 of 6). Sea level, a measure of ice sheet size, also lags temperature change (18).

GHG and surface albedo changes are positive climate feedbacks. Major glacial-interglacial climate swings are instigated by slow changes of Earth's orbit, especially the tilt of Earth's spin-axis relative to the orbital plane (19, 20). Global radiative forcing due to orbital changes is small, but geographical and seasonal changes of insolation affect ice sheet size, e.g., ice melts at both poles when the spin-axis tilt increases. Also a warming climate causes net release of GHGs. The most direct GHG feedback is release of CO_2 by the ocean due to temperature dependence of CO_2 solubility and increased ocean mixing in a warmer climate that flushes the deep ocean of CO_2 that accumulated through biologic and physical processes (21).

GHG and surface albedo feedbacks operate, given sufficient time, in response to temperature change caused by any climate forcing, including added human-made GHGs. The GHG feedback is nearly linear in global temperature during the late Pleistocene (Fig. 7 of 22, 22b). Surface albedo feedback increases as Earth becomes colder and the area of ice increases. Climate sensitivity including slow feedbacks is larger than the Charney climate sensitivity, at least on the Pleistocene time scale, because the dominant slow feedbacks are positive. Other feedbacks, some negative, may become important on longer geologic time scales.

Paleoclimate data permit evaluation of long-term sensitivity to specified GHG change. We assume only that the amount of ice on the planet over the long run is a function of global temperature, plotting GHG forcing (6), from ice core data (15), against temperature. Fig. 2 shows that global climate sensitivity including the slow surface albedo feedback is 1.5°C per W/m^2 or 6°C for doubled CO_2 , twice as large as the Charney sensitivity for fast feedbacks.

This long-term climate sensitivity is relevant to GHGs that remain airborne for centuries-to-millennia. Human-made GHGs will decline if emissions decrease enough, but the GHG amount also is affected by climate feedbacks. Empirical data (22, 22b) and carbon cycle models (2) both find a positive GHG feedback as the globe warms. Empirical amplification of GHGs is moderate if warming is kept within the range of recent interglacial periods (22), but greater warming risks release of CH_4 and CO_2 from methane hydrates in tundra and ocean sediments (23) that could elevate GHG amount over centuries to millennia.

Time scales. How long does it take to approach equilibrium temperature? Response is slowed by ocean thermal inertia and the time needed for ice sheets to disintegrate.

Ocean-caused delay is estimated in fig. S5 using a coupled atmosphere-ocean model. One-third of the response occurs in the first few years, in part because of rapid response over land, one-half in ~ 25 years, three-quarters in 250 years, and nearly full response in a millennium. The ocean-caused delay is a strong (quadratic) function of climate sensitivity and it depends on the rate of mixing of surface water and deep water (24), as discussed in the Supplementary material.

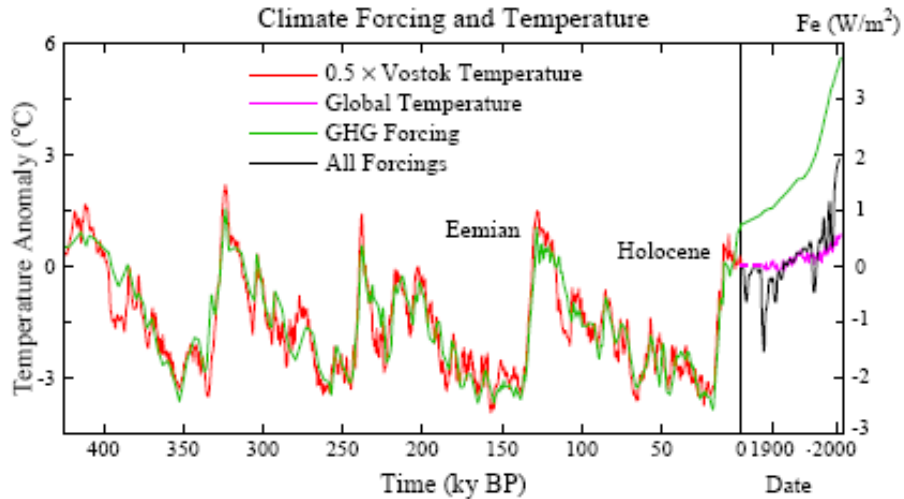


Fig. 2. Global temperature (left scale) and GHG forcing (right scale) due to CO₂, CH₄ and N₂O from the Vostok ice core (11, 15). Ratio of temperature and forcing scales is 1.5°C per W/m². The time scale is expanded for the industrial era. Modern forcings include human-made aerosols, volcanic aerosols and solar irradiance (5). GHG forcing zero point is the mean for 10-8 ky before present. Net climate forcing and modern temperature zero points are at 1850.

Ice sheet response time is often assumed to be several millennia, based on the broad sweep of past sea level change (Fig. 1A) and primitive ice sheet models designed to capture that change. However, this long time scale may reflect the slowly changing orbital forcing, rather than inherent inertia, as there is no discernable lag between maximum ice sheet melt rate and local insolation that favors melt (6). Paleo sea level data with high time resolution (25, 26) reveal frequent ‘suborbital’ sea level changes at rates of 1 m/century or more.

Present-day observations of Greenland and Antarctica show increasing surface melt (27), loss of buttressing ice shelves (28), accelerating ice streams (29), and increasing overall mass loss (30). Critical physics of ice sheet disintegration is absent in existing ice sheet models (31). Sea level changes of several meters per century occur in the paleoclimate record (25, 26), in response to forcings slower and weaker than the present human-made forcing. It seems likely that large ice sheet response will occur within centuries, if human-made forcings continue to increase. Once ice sheet disintegration is underway, decadal changes of sea level may be substantial.

Warming “in the pipeling”. The expanded time scale for the industrial era (Fig. 2) reveals a growing gap between actual global temperature (purple curve) and equilibrium (long-term) temperature based on the net estimated forcing (black curve). Ocean and ice sheet response times together account for this gap, which is now 2.0°C.

The forcing in Fig. 2 (black curve, Fe scale), when used to drive a global climate model (5), yields global temperature change that agrees closely (fig. 3 in 5) with observations (purple curve, Fig. 2). That climate model, which includes only fast feedbacks, has additional warming of ~0.6°C in the pipeline today because of ocean thermal inertia (5, 7).

The remaining gap between equilibrium temperature for current atmospheric composition and actual global temperature is ~1.4°C. This further 1.4°C warming in the pipeline is due to the slow surface albedo feedback.

The time needed for slow feedbacks to ‘kick in’ is uncertain. Current models are inadequate and no paleoclimate analogue to the rapid human-made GHG increase exists. Pleistocene ice

sheet disintegrations occurred over millennia (11b, 12, 18), but response time may be due in part to the slow pace of the forcing (6). It has been argued that ice sheet response time could be only centuries, with substantial response expected this century (31).

One may ask whether the climate system, as the Earth warms from its present ‘interglacial’ state, still has the capacity to supply slow feedbacks that double the fast-feedback sensitivity. This issue can be addressed by considering longer time scales including times with no ice.

Cenozoic Era.

Pleistocene atmospheric CO₂ variations occur as a climate feedback, carbon being exchanged among the ocean, atmosphere, soils and biosphere. On longer time scales CO₂ is exchanged between these surface reservoirs and the solid earth, making CO₂ an instigator of long-term climate change and orbital effects a ‘noise’ on larger climate swings.

The Cenozoic era, the past 65.5 My, provides a valuable complement to the Pleistocene for exploring climate sensitivity. Cenozoic data on climate and atmospheric composition are not as precise, but larger climate variations include an ice-free planet, putting glacial-interglacial changes in a wider perspective.

Oxygen isotopic composition of benthic (deep ocean dwelling) foraminifera shells in a global compilation of ocean sediment cores (20) provides a starting point for analyzing Cenozoic climate change (Fig. 3A). At times with negligible ice sheets, oxygen isotope change, $\delta^{18}\text{O}$, provides a direct measure of deep ocean temperature (T_{do}). Thus $T_{\text{do}} (\text{°C}) \sim -4 \delta^{18}\text{O} + 12$ between 65.5 and 34 My BP.

Rapid increase of $\delta^{18}\text{O}$ at about 34 My is associated with glaciation of Antarctica (20, 31a) and global cooling, as evidenced by data from North America (31b) and Asia (31c). From then until the present, $\delta^{18}\text{O}$ is affected by both ice volume and T_{do} , lighter $\delta^{16}\text{O}$ evaporating preferentially from the ocean and accumulating in ice sheets. Between 34 My and the last ice age (20 ky) the change of $\delta^{18}\text{O}$ was ~ 3 , with T_{do} change $\sim 6^\circ\text{C}$ (from $+5$ to -1°C) and ice volume change ~ 180 msl (meters of sea level). As $\delta^{18}\text{O} \sim 1.5$ is associated with the T_{do} change of $\sim 6^\circ\text{C}$, we assign the remaining $\delta^{18}\text{O}$ change to ice volume linearly at the rate 60 msl per mil $\delta^{18}\text{O}$ change (thus 180 msl for $\delta^{18}\text{O}$ between 1.75 and 4.75). Equal division of $\delta^{18}\text{O}$ between temperature and sea level yields sea level change in the late Pleistocene in reasonable accord with available sea level data (fig. S7). Subtracting the ice volume portion of $\delta^{18}\text{O}$ makes the deep ocean temperature after 34 My, $T_{\text{do}} (\text{°C}) = -2 (\delta^{18}\text{O} - 4.25)$, as in Fig. 3B.

The large Cenozoic temperature change, $\sim 14^\circ\text{C}$ between 50 My and the ice age at 20 ky, must have been driven by changes of atmospheric composition. Alternative drives could come from outside (solar irradiance) or the Earth’s surface (continental locations). But solar brightness increased $\sim 0.4\%$ in the Cenozoic (32), a linear forcing change of only $+1 \text{ W/m}^2$ and of the wrong sign to contribute to the cooling trend. Climate forcing due to continental locations was $< 1 \text{ W/m}^2$, because continents 65 My ago were already close to present latitudes (Fig. S8). Opening or closing of oceanic gateways might affect the timing of glaciation, but it would not provide the climate forcing needed for global cooling.

CO₂ concentration, in contrast, varied from ~ 180 ppm in glacial times to 1500 ± 500 ppm in the early Cenozoic (33). This change is a forcing of more than 10 W/m^2 (Table 1 in 13), an order of magnitude larger than other known forcings. CH₄ and N₂O, positively correlated with CO₂ and global temperature in the period with accurate data (ice cores), likely increase the total GHG forcing, but their forcings are much smaller than that of CO₂ (33b, c).

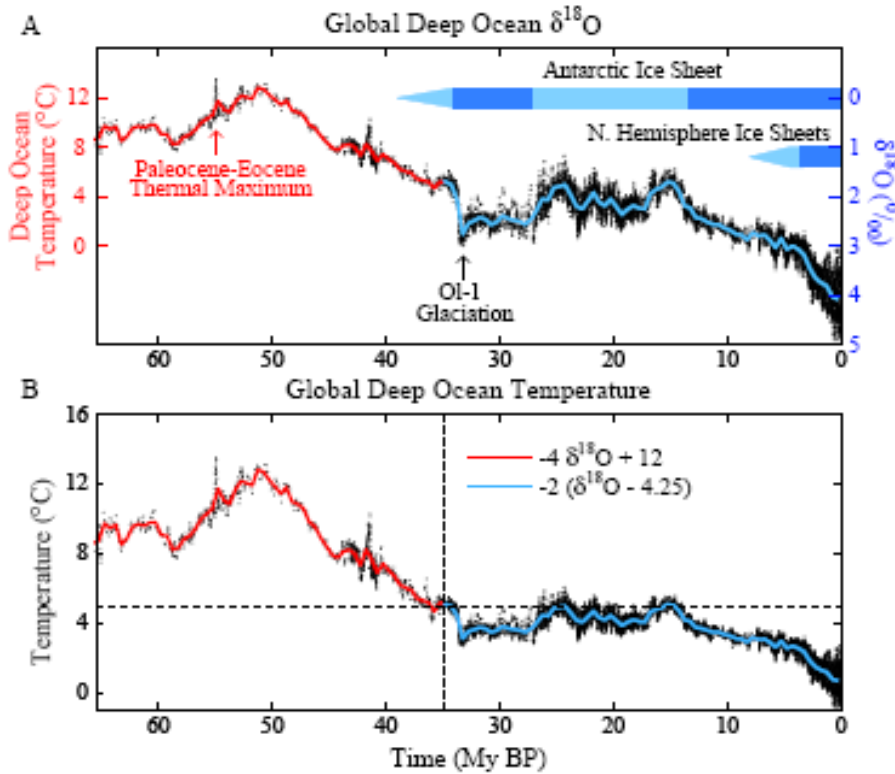


Fig. 3. Global deep ocean (A) $\delta^{18}\text{O}$ (20) and (B) temperature. Black curve is 5-point running mean of $\delta^{18}\text{O}$ original temporal resolution, while red and blue curves have 0.5 my resolution.

Cenozoic carbon cycle. Solid Earth sources and sinks of CO_2 are generally not balanced (34). CO_2 is removed from surface reservoirs by: (1) chemical weathering of silicate rocks, which deposits carbonates on the ocean floor, and (2) burial of organic matter; weathering is the dominant process (35). CO_2 returns via metamorphism and volcanic outgassing where carbonate-rich oceanic crust is subducted beneath moving continental plates.

Burial and outgassing of CO_2 are each typically $2\text{-}4 \times 10^{12}$ mol C/year (35, 36). An imbalance of 2×10^{12} mol C/year, confined to the atmosphere, is ~ 0.01 ppm/year, but as the CO_2 is spread among surface reservoirs, it is only ~ 0.0001 ppm/year in the air. This is negligible compared to the present human-made atmospheric CO_2 increase of ~ 2 ppm/year, yet in a million years such a crustal imbalance alters atmospheric CO_2 by 100 ppm.

Between 60 and 50 My ago India moved north rapidly, 18-20 cm/year (37), through a region that long had been a depocenter for carbonate sediments. Subduction of carbonate-rich crust was surely a source of CO_2 outgassing and a prime cause of global warming, which peaked 50 My ago (Fig. 3b) with the Indo-Asian collision that initiated uplift of the Himalayas and Tibetan Plateau and drawdown of atmospheric CO_2 by weathering (38). Since then the Indian and Atlantic Oceans have been the major depocenters for carbon, with subduction of carbonate-rich crust limited largely to regions near Indonesia and Central America (35).

Thus atmospheric CO_2 declined in the past 50 My (33) and climate cooled (Fig. 3B) to the point of Antarctic glaciation at ~ 34 My. Antarctica has remained glaciated ever since, although glaciation may have reversed temporarily, e.g., ~ 26 My ago, perhaps due to negative feedback of reduced weathering (39).

Knowledge of Cenozoic CO_2 is limited to imprecise proxy measures, except for recent ice core data. Proxies suggest that CO_2 was $\sim 1000\text{-}2000$ ppm in the early Cenozoic but < 500 ppm in the last 20 My (2, 33).

Cenozoic forcing and CO₂. The entire Cenozoic climate forcing history (Fig. 4A) is implied by the temperature reconstruction (Fig. 3B), assuming a fast-feedback sensitivity of $\frac{3}{4}^{\circ}\text{C}$ per W/m^2 . Subtracting the solar and surface albedo forcings (Fig. 4B), the latter from Eq. S2 with ice sheet area vs time from $\delta^{18}\text{O}$, we obtain the GHG forcing history Fig. 4C).

We hinge our calculations 35 My ago for several reasons. Between 65 and 35 My ago there was little ice on the planet, so climate sensitivity is defined by fast feedbacks alone. We want to estimate the CO₂ amount that precipitated Antarctic glaciation. Finally, the relation between global surface air temperature change (ΔT_s) and deep ocean temperature change (ΔT_{do}) differs for ice-free and glaciated worlds.

In the ice-free world (65-35 My ago) we take $\Delta T_s \sim \Delta T_{do}$, but with generous (50%) uncertainty, as climate models show that global temperature change is tied closely to ocean temperature change.(40). In the glaciated world ΔT_{do} is limited by the freezing point in the deep ocean. ΔT_s between the last ice age (20 ky) and the present interglacial period ($\sim 5^{\circ}\text{C}$) was ~ 1.5 times larger than ΔT_{do} . In fig. S5 we show that this relationship fits well throughout the period of ice core data.

If we specify CO₂ at 35 My, the GHG forcing defines CO₂ at other times, assuming CO₂ provides 75% of the GHG forcing, as in the late Pleistocene. CO₂ ~ 400 -450 ppm at 35 My keeps CO₂ in the range of early Cenozoic proxies (Fig. 5A) and yields a good fit to the amplitude and mean CO₂ amount in the late Pleistocene (Fig. 5B). A ~ 500 ppm CO₂ threshold for Antarctic glaciation was previously inferred from proxy CO₂ data and a carbon cycle model (41a).

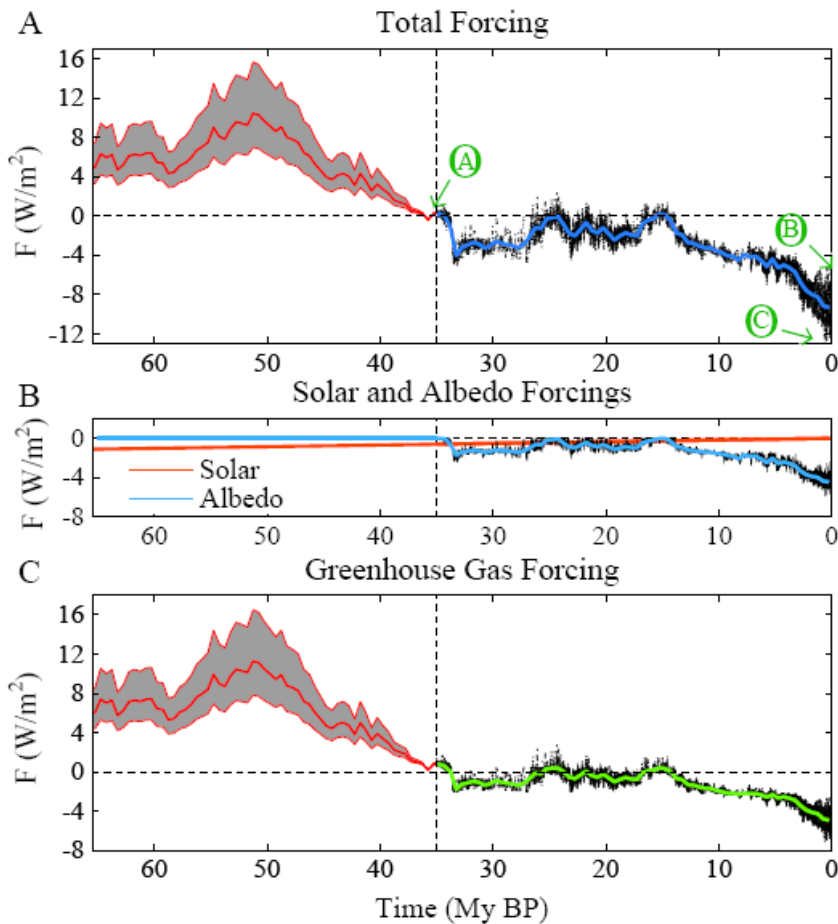


Fig. 4. (A) Total climate forcing, (B) solar and surface albedo forcings, and (C) GHG forcing in the Cenozoic, based on T_{do} history of Fig. 3B and assumed fast-feedback climate sensitivity $\frac{3}{4}^{\circ}\text{C}$ per W/m^2 . Ratio of T_s change and T_{do} change is assumed to be near unity in the minimal ice world between 65 and 35 My, but the gray area allows for 50% uncertainty in the ratio. In the later era with large ice sheets we take $T_s/T_{do} = 1.5$, in accord with Pleistocene data.

Individual CO₂ proxies (Fig. S9) clarify limitations due to scatter among the measurements. Early Cenozoic low CO₂ of some proxies may suggest higher climate sensitivity. However, in general the sensitivities inferred from the Cenozoic and Phanerozoic (41x, 41y, 41z) agree well with our analysis, if we account for the ways in which sensitivity is defined and the periods emphasized in each empirical derivation (Table S1).

Figure 5 with the “best fit” CO₂ ~425 ppm at 35 My serves as a prediction to compare with new data on CO₂ amount. Model uncertainties (Fig. S9) include possible changes of non-CO₂ GHGs and the relation of ΔT_s to ΔT_{do} . The model fails to account for cooling in the past 15 My if CO₂ increased, as most proxies suggest (Fig. S9). Changing ocean currents, as by closing of the Isthmus of Panama, may have contributed, but models find little effect on temperature (39b). Non-CO₂ GHGs may have played an added role, because little forcing is needed to cause cooling due to the magnitude of late Cenozoic albedo feedback.

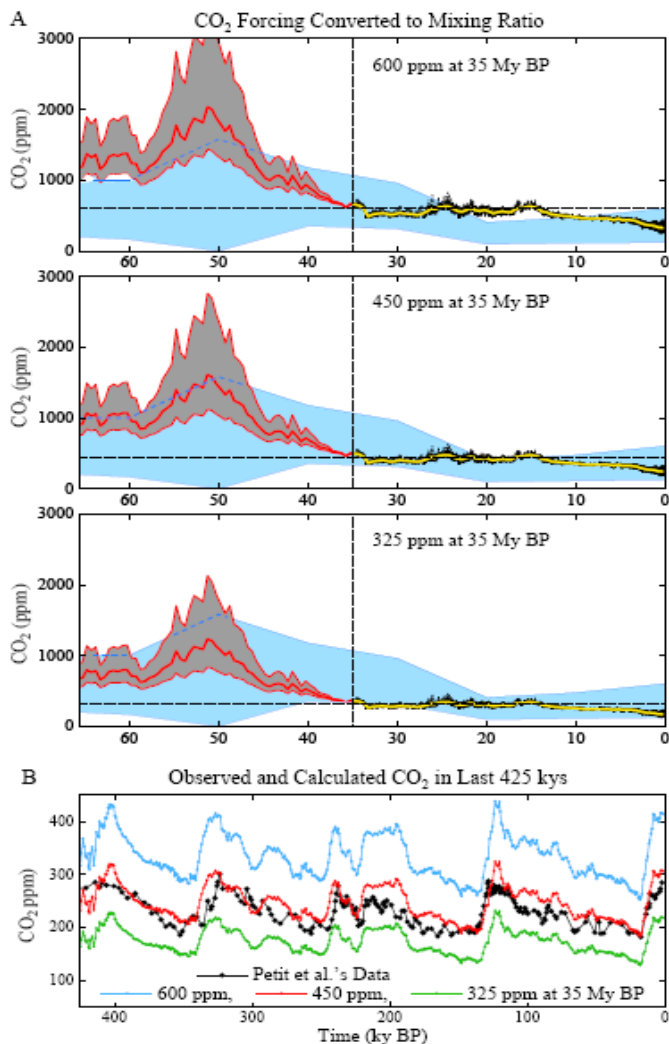


Fig. 5. (A) Simulated CO₂ amounts in the Cenozoic for three choices of CO₂ amount at 35 My (temporal resolution of black and colored curves as in Fig. 3; blue region: multiple CO₂ proxy data; gray region allows 50 percent uncertainty in ratio of global surface and deep ocean temperatures). (B) Expanded view of late Pleistocene, including precise ice core CO₂ measurements (black curve).

Implications. We infer from the Cenozoic data that CO₂ was the dominant Cenozoic forcing, that CO₂ was only ~450 ppm when Antarctica glaciated, and that glaciation is reversible. Together these inferences have profound implications.

Consider three points marked in Fig. 4: point A at 35 My, just before Antarctica glaciated; point B at recent interglacial periods; point C at the depth of recent ice ages. Point B is half way between points A and C in global temperature (Fig. 3) and climate forcings (Fig. 4). For example, the climate forcing for CO₂ change from 180 to 285 ppm is 2.6 W/m² and further change from 285 to 450 ppm is 2.7 W/m².

Thus equilibrium climate sensitivity, including slow feedbacks, between today and an ice-free world, is about 1.5°C per W/m² or 6°C for doubled CO₂, the same as between today and the last ice age. Evidently amplification provided by loss of Greenland and Antarctic ice and spread of vegetation over the vast high-latitude land area in the Northern Hemisphere, in response to positive forcing, is comparable to amplification provided by the Laurentide and other ice sheets, in response to negative forcing.

Anthropocene Era.

Human-made global climate forcings now dominate over natural forcings (Fig. 2). Earth may have entered the Anthropocene era (41b, c) 6-8 ky ago (41d), but the net human-made forcing was small, perhaps slightly negative (6), prior to the industrial era. GHG forcing overwhelmed natural and negative human-made forcings only in the past quarter century (Fig. 2).

Human-made climate change is delayed by ocean (fig. S6) and ice sheet response times. Warming ‘in the pipeline’, most due to slow feedbacks, is now about 2°C (Fig. 2). No additional forcing is required to raise global temperature to at least the level of the Pliocene, 2-3 million years ago, a degree of warming that would surely yield ‘dangerous’ climate impacts (5).

Tipping points. Realization that today’s climate is far out of equilibrium with current climate forcings raises the specter of ‘tipping points’, the concept that climate can reach a point such that, without additional forcing, rapid changes proceed practically out of our control (2, 6, 41e). Arctic sea ice and the West Antarctic Ice Sheet are examples of potential tipping points. Arctic sea ice loss is magnified by the positive feedback of increased absorption of sunlight as global warming initiates sea ice retreat (42). West Antarctic ice loss can be accelerated by several feedbacks, once ice loss is substantial (31).

We define: (1) the *tipping level*, the global climate forcing that, if long maintained, gives rise to a specific consequence, and (2) the *point of no return*, a climate state beyond which the consequence is inevitable, even if climate forcings are reduced. A point of no return can be avoided, even if the tipping level is temporarily exceeded. Ocean and ice sheet inertia permit overshoot, provided the climate forcing is returned below the tipping level before initiating irreversible dynamic change.

Points of no return are inherently difficult to define, because the dynamical problems are nonlinear. Existing models are more lethargic than the real world for phenomena now unfolding, including changes of sea ice (44), ice streams (45), ice shelves (46), and expansion of the subtropics (47).

The tipping level is easier to assess, because the paleoclimate equilibrium response to known climate forcing is relevant. The tipping level is a measure of the long-term climate forcing that humanity must aim to stay beneath to avoid large climate impacts, but the tipping level does not define the magnitude or period of tolerable overshoot.

Target CO₂. GHGs other than CO₂ cause climate forcing comparable to that of CO₂ (2, 22), but growth of non-CO₂ GHGs is falling below IPCC (2) scenarios (fig. S10). Thus the GHG

climate forcing change is determined mainly by CO₂ (fig. S11). Net human-made forcing is comparable to the CO₂ forcing, as non-CO₂ GHGs tend to offset negative aerosol forcing (2, 5).

Thus we take future CO₂ change as approximating the net human-made forcing change, with two caveats. First, special effort to reduce non-CO₂ GHGs could alleviate the CO₂ requirement, allowing up to about +25 ppm CO₂ for the same climate effect, while resurgent growth of non-CO₂ GHGs could reduce allowed CO₂ a similar amount (22). Second, reduction of human-made aerosols, which have a net cooling effect, could force stricter GHG requirements. However, an emphasis on reducing black soot could largely off-set reductions of high albedo aerosols (13).

We define a target CO₂ level by considering several specific climate impacts:

Stabilization of Arctic sea ice cover requires, to first approximation, restoration of planetary energy balance. Climate models driven by known forcings yield a present planetary energy imbalance of +0.5-1 W/m² (5), a result supported by observed increasing ocean heat content (48). CO₂ amount must be reduced to 325-355 ppm to increase outgoing flux 0.5-1 W/m², if other forcings are unchanged. A further reduced flux, by ~0.5 W/m², and thus CO₂ ~300-325 ppm, may be needed to restore sea ice to its area of 25 years ago.

Equilibrium sea level rise for today's 385 ppm CO₂ is at least several meters, judging from paleoclimate history (11b, 12, 25). Accelerating mass losses from Greenland (49) and West Antarctica (50) heighten concerns about ice sheet stability. An initial CO₂ target of 350 ppm, to be reassessed as the effect on ice sheet mass balance is observed, is suggested.

Coral reefs are suffering from multiple stresses, with ocean acidification and ocean warming principal among them (51). Given additional warming 'in-the-pipeline', 385 ppm CO₂ is already deleterious. A 300-350 ppm CO₂ target would significantly relieve both of these stresses.

Alpine glaciers are in near-global retreat (54, 55). After a flush of fresh water, glacier loss foretells long summers of frequently dry rivers, including rivers originating in the Himalayas, Andes and Rocky Mountains that now supply water to hundreds of millions of people. Present glacier retreat, and warming in the pipeline, indicate that 385 ppm CO₂ is already a threat.

Civilization is adapted to climate zones of the Holocene. Theory and models indicate that subtropical regions expand poleward with global warming (2, 52). Data reveal a 4-degree latitudinal shift already (53), larger than model predictions, yielding increased aridity in southern United States, the Mediterranean region, Australia and parts of Africa. Impacts of this climate shift (54) support the conclusion that 385 ppm CO₂ is already deleterious.

CO₂ scenarios. A large fraction of fossil fuel CO₂ emissions stays in the air a long time, one-quarter remaining airborne for several centuries (56, 57). Thus moderate delay of fossil fuel use will not appreciably reduce long-term human-made climate change. Preservation of climate requires that most remaining fossil fuel carbon is never emitted to the atmosphere.

Coal is the largest reservoir of conventional fossil fuels (fig. S12), exceeding combined reserves of oil and gas (2, 58). The only realistic way to sharply curtail CO₂ emissions is to phase out coal use except where CO₂ is captured and sequestered.

Phase-out of coal emissions by 2030 (Fig. 6) keeps maximum CO₂ close to 400 ppm, depending on oil and gas reserves and reserve growth. IPCC reserves (figs. 6, S11) assume that half of readily minable oil has already been used (fig. S12). EIA (58b) estimates (fig. S12) have larger reserves and reserve growth. Even if EIA estimates are accurate, the IPCC case remains valid if the most difficult to extract oil and gas is left in the ground, via a rising price on carbon emissions that discourages remote exploration and environmental regulations that place some areas off-limit. If IPCC gas reserves (fig. S12) are underestimated, the IPCC case in Fig. 6 remains valid if added gas reserves are used at facilities where CO₂ is captured.

However, even with phase-out of coal emissions and IPCC oil and gas reserves, CO₂ remains above 350 ppm for more than two centuries. Ongoing Arctic and ice sheet changes, examples of rapid paleoclimate change, and other criteria cited above all drive us to consider scenarios that bring CO₂ back to 350 ppm or less more rapidly.

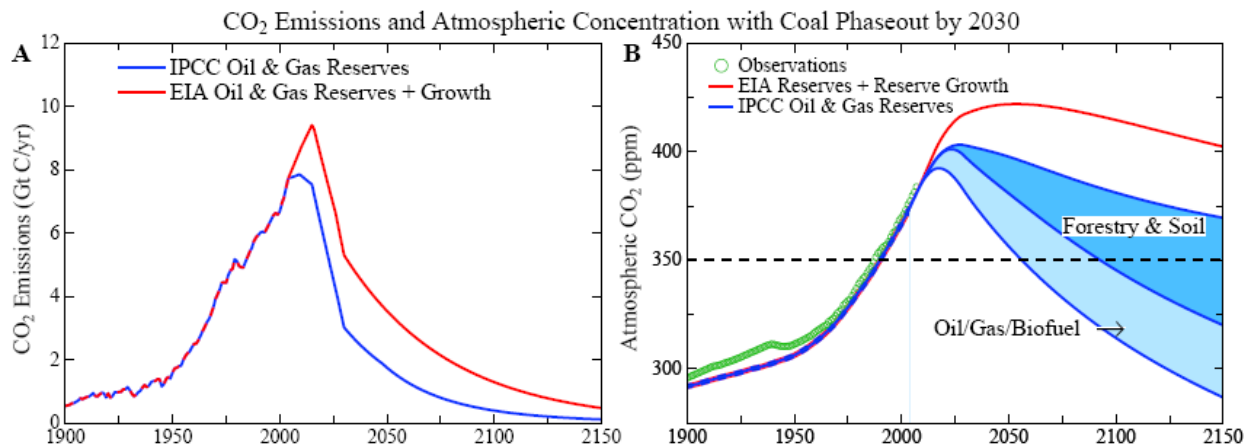


Fig. 6. (A) Fossil fuel CO₂ emissions with coal phase-out by 2030 based on IPCC (2) and EIA (58b) estimated fossil fuel reserves. (B) Resulting atmospheric CO₂ based on use of a dynamic-sink pulse response function representation of the Bern carbon cycle model (57, 58).

Policy relevance. Desire to reduce airborne CO₂ raises the question of whether CO₂ could be drawn from the air artificially. There are no large-scale technologies for CO₂ air capture now, but with strong research and development support and industrial-scale pilot projects sustained over decades it may be possible to achieve costs ~\$200/tC (59) or perhaps less (60). At \$100/tC, the cost of removing 50 ppm of CO₂ is ~\$10 trillion.

Improved agricultural and forestry practices offer a more natural way to draw down CO₂. Deforestation contributed a net emission of 60±30 ppm over the past few hundred years, of which ~20 ppm CO₂ remains in the air today (2, 58a, figs S11, S13). Reforestation could absorb a significant fraction of the 60±30 ppm net deforestation emission.

Carbon sequestration in soil also has significant potential. Biochar, produced in pyrolysis of residues from crops, forestry, and animal wastes, can be used to restore soil fertility while storing carbon for centuries to millennia (61). Biochar helps soil retain nutrients and fertilizers, reducing emissions of GHGs such as N₂O (61b). Replacing slash-and-burn agriculture with slash-and-char and use of agricultural and forestry wastes for biochar production could provide a CO₂ drawdown of ~8 ppm in half a century (61b).

In Supplementary Material we define a forest/soil drawdown scenario that reaches 50 ppm by 2150 (Fig. 6B). This scenario returns CO₂ below 350 ppm late this century, after about 100 years above that level.

More rapid drawdown could be provided by CO₂ capture at power plants fueled by gas and biofuels (62). Low-input high-diversity biofuels grown on degraded or marginal lands, with associated biochar production, could accelerate CO₂ drawdown, but the nature of a biofuel approach must be carefully designed (61b, 61c).

A rising price on carbon emissions and payment for carbon sequestration is surely needed to make drawdown of airborne CO₂ a reality. A 50 ppm drawdown via agricultural and forestry practices seems plausible. But if most of the CO₂ in coal is put into the air, no such “natural” drawdown of CO₂ to 350 ppm is feasible. Indeed, if the world continues on a business-as-usual

path for even another decade without initiating phase-out of unconstrained coal use, prospects for avoiding a dangerously large, extended overshoot of the 350 ppm level will be dim.

Summary.

Humanity today, collectively, must face the uncomfortable fact that industrial civilization itself has become the principal driver of global climate. If we stay our present course, using fossil fuels to feed a growing appetite for energy-intensive life styles, we will soon leave the climate of the Holocene, the world of human history. The eventual response to doubling pre-industrial atmospheric CO₂ likely would be a nearly ice-free planet.

Humanity's task of moderating human-caused global climate change is urgent. Ocean and ice sheet inertias provide a buffer delaying full response by centuries, but there is a danger that human-made forcings could drive the climate system beyond tipping points such that change proceeds out of our control. The time available to reduce the human-made forcing is uncertain, because models of the global system and critical components such as ice sheets are inadequate. However, climate response time is surely less than the atmospheric lifetime of the human-caused perturbation of CO₂. Thus remaining fossil fuel reserves should not be exploited without a plan for retrieval and disposal of resulting atmospheric CO₂.

Paleoclimate evidence and ongoing global changes imply that today's CO₂, about 385 ppm, is already too high to maintain the climate to which humanity, wildlife, and the rest of the biosphere are adapted. Realization that we must reduce the current CO₂ amount has a bright side: effects that had begun to seem inevitable, including impacts of ocean acidification, loss of fresh water supplies, and shifting of climatic zones, may be averted by the necessity of finding an energy course beyond fossil fuels sooner than would otherwise have occurred.

We suggest an initial objective of reducing atmospheric CO₂ to 350 ppm, with the target to be adjusted as scientific understanding and empirical evidence of climate effects accumulate. Limited opportunities for reduction of non-CO₂ human-caused forcings are important to pursue but do not alter the initial 350 ppm CO₂ target. This target must be pursued on a timescale of decades, as paleoclimate and ongoing changes, and the ocean response time, suggest that it would be foolhardy to allow CO₂ to stay in the dangerous zone for centuries.

A practical global strategy almost surely requires a rising global price on CO₂ emissions and phase-out of coal use except for cases where the CO₂ is captured and sequestered. The carbon price should eliminate use of unconventional fossil fuels, unless, as is unlikely, the CO₂ can be captured. A reward system for improved agricultural and forestry practices that sequester carbon could remove the current CO₂ overshoot. With simultaneous policies to reduce non-CO₂ greenhouse gases, it appears still feasible to avert catastrophic climate change.

Present policies, with continued construction of coal-fired power plants without CO₂ capture, suggest that decision-makers do not appreciate the gravity of the situation. We must begin to move now toward the era beyond fossil fuels. Continued growth of greenhouse gas emissions, for just another decade, practically eliminates the possibility of near-term return of atmospheric composition beneath the tipping level for catastrophic effects.

The most difficult task, phase-out over the next 20-25 years of coal use that does not capture CO₂, is herculean, yet feasible when compared with the efforts that went into World War II. The stakes, for all life on the planet, surpass those of any previous crisis. The greatest danger is continued ignorance and denial, which could make tragic consequences unavoidable.

References and Notes

1. Framework Convention on Climate Change, United Nations, <http://www.unfccc.int/>, (1992).

2. Intergovernmental Panel on Climate Change (IPCC), *Climate Change 2007*, S. Solomon et al., Eds. (Cambridge Univ. Press, New York, 2007).
3. M.D. Mastrandrea, S.H. Schneider, *Science* **304**, 571 (2004).
4. http://ec.europa.eu/news/energy/070110_1_en.htm (Is there a better reference for European Union 2°C goal?)
5. J. Hansen et al., *Atmos. Chem. Phys.* **7**, 2287 (2007).
6. J. Hansen et al., *Phil. Trans. Roy. Soc. A* **365**, 1925 (2007).
7. J. Hansen et al., *Science* **308**, 1431 (2005).
8. J. Hansen et al., *J. Geophys. Res.* **110**, D18104 (2005).
9. J. Charney, *Carbon Dioxide and Climate: A Scientific Assessment* (Natl. Acad. Sci. Press, Washington, D.C., 1979).
10. J. Hansen et al., *Am. Geophys. Union Geophys. Mono. Ser.* **29**, 130 (1984).
- 10b P. Braconnot et al., *Clim. Past* **3**, 261 (2007).
- 10c I. Farrera et al., *Clim. Dyn.* **15**, 823 (1999).
11. J.R. Petit et al., *Nature* **399**, 429 (1999).
- 11b P.J. Hearty et al., *Quat. Sci. Rev.* **26**, 2090 (2007). = reference 26
12. M. Siddall et al., *Nature* **423**, 853 (2003).
13. J. Hansen et al., *Proc. Natl. Acad. Sci.* **97**, 9875 (2000).
14. V. Masson-Delmotte et al., *Clim. Dyn.* **XX**, yyy (2006).
15. F. Vimeux, K.M. Cuffey, J. Jouzel, *Earth Planet. Sci. Lett.* **203**, 829 (2002).
16. EPICA community, *Nature* **444**, 195 (2006).
17. N. Caillon et al., *Science* **299**, 1728 (2003).
18. M. Mudelsee, *Quat. Sci. Rev.* **20**, 583 (2001).
19. J.D. Hays, et al., *Science* **194**, 1121 (1976).
20. J. Zachos, *Science* **292**, 686 (2001).
21. P. Kohler, H. Fischer, *Clim. Past* **2**, 57-78 (2006).
22. J. Hansen, M. Sato, *Proc. Natl. Acad. Sci.* **101**, 16109 (2004).
- 22b U. Siegenthaler et al., *Science* **310**, 1313 (2005).
23. D. Archer, *Biogeosci.* **4**, 521 (2007).
24. J. Hansen et al., *Science* **229**, 857 (1985).
25. W.G. Thompson, S.L. Goldstein, *Science* **308**, 401 (2005).
26. P.J. Hearty et al., *Quat. Sci. Rev.* **26**, 2090 (2007).
27. M. Tedesco, *Geophys. Res. Lett.* **34**, L02504 (2007).
28. E. Rignot, S.S. Jacobs, *Science* **296**, 2020 (2002).
29. H.J. Zwally et al., *Science* **297**, 218 (2002).
30. J.L. Chen, et al., *Science* **313**, 1958 (2006).
31. J. Hansen, *Clim. Change* **68**, 269 (2005).
- 31a R.M.DeConto, D. Pollard, *Nature* **421**, 245 (2003).
- 31b A. Zanazzi et al., *Nature* **445**, 639 (2007).
- 31c G. Dupont-Nivet et al., *Nature* **445**, 635 (2007).
32. L.J. Sackmann et al., *Astrophys. J.* **418**, 457 (1993).
33. M. Pagani et al., *Science* **309**, 600 (2005).
- 33b O. Bartdorff et al., *Global Biogeochem. Cycles* **22**, GB1008 (2008).
- 33c D. Beerling et al., *Am. J. Sci.*, in press (2008).
34. J.M. Edmond, Y. Huh, *Earth Planet. Sci. Lett.* **216**, 125 (2003).
35. R.A. Berner, *The Phanerozoic Carbon Cycle: CO₂ and O₂* (Oxford Univ. Press, New York, 2004).
36. H. Staudigel et al., *Geochim. Cosmochim. Acta* **53**, 3091 (1989).
37. P. Kumar et al., *Nature* **449**, 894 (2007).
38. M.E. Raymo and W.F. Ruddiman, *Nature* **359**, 117 (1992).
39. C.H. Lear et al., *Paleocean.* **19**, PA4015 (2004).
- 39b D.J. Lunt et al. *Clim. Dyn.* **30**, 1 (2008).

40. M.M. Joshi, *et al.*, *Clim. Dyn.* **30**, 455 (2008).
- 41a D.L. Royer, *Geochim. Cosmochim. Acta* **70**, 5665 (2006).
- 41b P.J. Crutzen, *Global Change Newsletter* **41**, 12 (2000).
- 41c J. Zalasiewicz *et al.*, *GSA Today* **18**, 4 (2008).
- 41d W.F. Ruddiman, *Clim. Change* **61**, 261 (2003).
- 41e T.M. Lenton *et al.*, *Proc. Natl. Acad. Sci.* **105**, 1786 (2008).
- 41x. D.L. Royer *et al.*, *Nature* **446**, 530 (2007).
- 41y. J.A. Higgins, D.P. Schrag, *Earth Plan. Sci. Lett.* **245**, 523 (2006).
- 41z. M. Pagani, *et al.*, *Science* **314**, 1556 (2006).
42. R.W. Lindsay, J. Zhang, *J. Climate* **18**, 4879 (2005).
43. reference deleted – number available
44. J. Stroeve *et al.*, *EOS Trans. Amer. Geophys. Union* **89**, 13 (2008).
45. I.M. Howat *et al.*, *Science* **315**, 1559 (2007).
46. E. Rignot, S.S. Jacobs, *Science* **296**, 2020 (2002).
47. D.J. Seidel, W.J. Randel, *J. Geophys. Res.* **111**, D21101 (2006).
48. S. Levitus *et al.*, *Geophys. Res. Lett.* **32**, L02604 (2005).
49. K. Steffen, *et al.*, Chap. 2 in *Abrupt Climate Change*, U.S. Climate Change Science Program, SAP 3.4 (in press).
50. E. Rignot *et al.*, *Nature Geoscience*, doi:10.1038/ngeo102 (2008).
51. R. Stone, *Science* **316**, 678 (2007).
52. I.M. Held, B.J. Soden, *J. Climate* **19**, 5686 (2006).
53. D.J. Seidel, W.J. Randel, *J. Geophys. Res.* **111**, D21101 (2006)=47
54. IPCC Impacts volume
55. T.P. Barnett *et al.*, *Nature* **438**, 303 (2005).
56. D. Archer, *J. Geophys. Res.* **110**, C09S05 (2005).
57. F. Joos, *et al.*, *Tellus* **48B**, 397 (1996).
58. P.A. Kharecha, J.E. Hansen, *Global Biogeo. Cycles* (in review).
- 58a R.A. Houghton, *Tellus* **55B**, 378 (2003).
- 58b. Energy Information Administration (EIA), U.S. DOE, *International Energy Outlook 2006*, <http://www.eia.doe.gov/oiaf/archive/ieo06/index.html> (2006).
59. D.W. Keith, *et al.*, *Clim. Change* **74**, 17 (2006).
60. F.S. Zeman, K.S. Lackner, *World Res. Rev.* **16**, 62 (2004).
61. J. Lehmann, *Nature* **447**, 143 (2007).
- 61b J. Lehmann, *et al.*, *Mitiga. Adap. Strat. Glob. Chan.* **11**, 403 (2006).
- 61c Tilman *et al.* (2006).
62. J. Hansen, Congressional Testimony, <http://arxiv.org/abs/0706.3720v1> (2007).
63. O. Morton, *Nature* **447**, 132 (2007).
- X. We thank H. Harvey, G. Lenfest, and NASA program managers D. Anderson and J. Kaye for research support, J. Romm and S. Weart for comments on a draft manuscript, and NOAA Earth System Research Laboratory for data.

Supporting Online Material

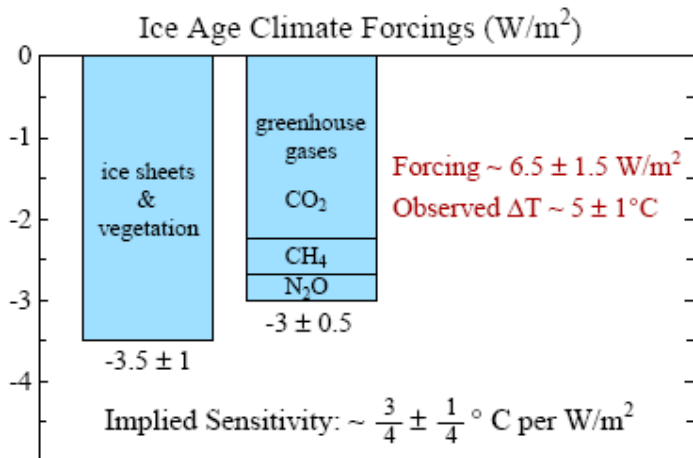


Fig. S1. Climate forcings during ice age 20 ky BP, relative to the present (pre-industrial) interglacial period.

Ice age climate forcings. Figure S1 shows the climate forcings during the depth of the last ice age, 20 ky BP, relative to the Holocene (10). The largest contribution to the uncertainty in the calculated 3.5 W/m^2 forcing due to surface changes (ice sheet area, vegetation distribution, shoreline movements) is due to uncertainty in the ice sheet sizes (10, S1). Formulae (13) for the GHG forcings yield 2.25 W/m^2 for CO₂ (185 ppm \rightarrow 275 ppm), 0.43 W/m^2 for CH₄ (350 \rightarrow 675 ppb) and 0.32 W/m^2 for N₂O (200 \rightarrow 270 ppb). The CH₄ forcing includes a factor 1.4 to account for indirect effects of CH₄ on tropospheric ozone and stratospheric water vapor (8).

The climate sensitivity inferred from the ice age climate change ($\sim \frac{3}{4} \text{ °C per W/m}^2$) includes only fast feedbacks, such as water vapor, clouds, aerosols (including dust) and sea ice. Ice sheet size and greenhouse gas amounts are specified boundary conditions in this derivation of the fast-feedback climate sensitivity.

It is permissible to, alternatively, specify aerosol changes as part of the forcing and thus derive a climate sensitivity that excludes the effect of aerosol feedbacks. That approach was used in the initial empirical derivation of climate sensitivity from Pleistocene climate change (10). The difficulty with that approach is that, unlike long-lived GHGs, aerosols are distributed inhomogeneously, so it is difficult to specify aerosol changes accurately. Also the forcing is a sensitive function of aerosol single scatter albedo, which is also not well measured, and the vertical distribution of aerosols in the atmosphere. Further, the aerosol indirect effect on clouds also depends upon all of these poorly known aerosol properties.

One recent study (S2) specified an arbitrary glacial-interglacial aerosol forcing slightly larger than the GHG glacial-interglacial forcing. As a result, because temperature, GHGs, and aerosol amount, overall, are positively correlated in glacial-interglacial changes, this study inferred a climate sensitivity of only $\sim 2 \text{ °C}$ for doubled CO₂. This study used the correlation of aerosol and temperature in the Vostok ice core at two specific times to infer an aerosol forcing for a given aerosol amount. The conclusions of the study are immediately falsified by considering the full Vostok aerosol record (Fig. 2, 11), which reveals numerous large aerosol fluctuations without any corresponding temperature change. In contrast, the role of GHGs in climate change is confirmed when this same check is made for GHGs (Fig. 2), and the fast-feedback climate sensitivity of 3 °C for doubled CO₂ is confirmed (Fig. 1).

All the problems associated with imprecise knowledge of aerosol properties become moot if, as is appropriate, aerosols are included in the fast feedback category. Indeed, soil dust, sea salt,

dimethylsulfide, and other aerosols are expected to vary (in regional, inhomogeneous ways) as climate changes. The effect of these aerosol changes is fully included in the observed global temperature change. The climate sensitivity that we derive in Fig. S1 includes the aerosol effect accurately, because both the climate forcings and the global climate response are known. The indirect effect of aerosol change on clouds is, of course, also included precisely.

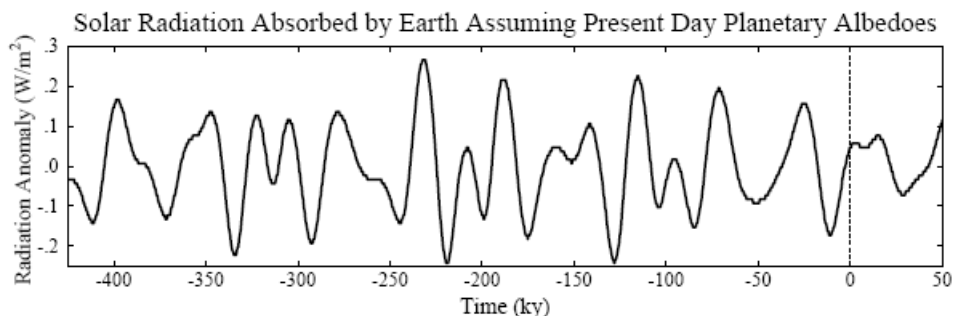


Fig. S2. Annual-mean global-mean perturbation of the amount of solar radiation absorbed by the Earth, calculated by assuming present-day seasonal and geographical distribution of albedo.

Earth orbital (Milankovitch) climate forcing. Figure S2 shows the perturbation of solar radiation absorbed by the Earth due to changes in Earth orbital elements, i.e., the tilt of the Earth's spin axis relative to the orbital plane, the eccentricity of the Earth's orbit, and the time of year at which the Earth is closest to the sun (precession of equinoxes). This perturbation is calculated assuming fixed (present day) seasonal and geographical distribution of planetary albedo. It measures the global forcing that instigates the glacial-interglacial climate changes.

This weak forcing is negligible, per se, on global-mean annual-mean basis. However, regional seasonal insolation perturbations are as much as several tens of W/m². These insolation perturbations instigate ice sheet and GHG changes, slow feedbacks, which amplify the global annual-mean orbital forcing.

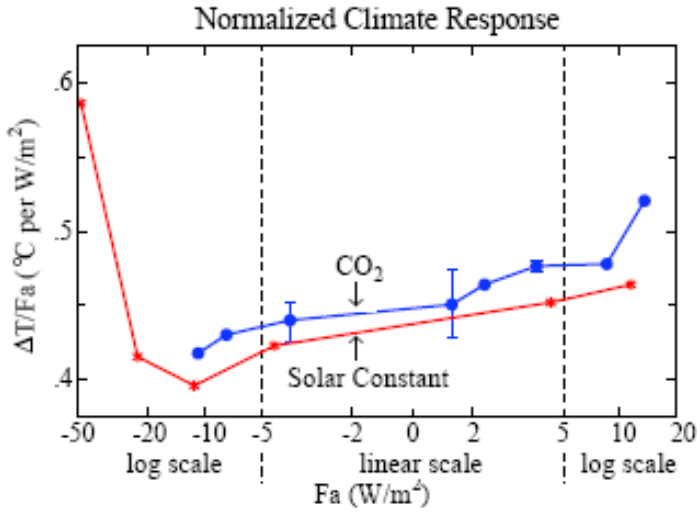


Fig. S3. Global surface air temperature change (8) after 100 years (mean of years 81-120) in simulations with the Goddard Institute for Space Studies (GISS) modelE (S3, 5) as a function of climate forcing for changes of solar irradiance and atmospheric CO₂. Fa is the standard adjusted climate forcing (8). Results here are extracted from Fig. 25(a) of (8).

Climate response function. Figure S3 shows that climate forcings of the order of 20-50 W/m² are needed to approach either the runaway snowball-Earth feedback or the runaway greenhouse effect, if only the Charney fast feedbacks are included. However, the negative forcing required to approach snowball-Earth is reduced by amplifying slow feedbacks, especially increasing ice sheet area. Indeed, the real-world Earth has experienced snowball conditions (S4), or at least a ‘slushball’ state (S5), on at least two occasions, the most recent ~640 My BP, aided by reduced solar irradiance (32) and favorable continental locations. The mechanism that allowed Earth to escape from the snowball state was probably the reduced weathering in a glaciated world, which allowed volcanic CO₂ to accumulate in the atmosphere (S4).

It would, of course, be interesting to extend the simulations of Fig. S3 to both smaller and larger forcings. The reason that the curves in Fig. 2 terminate is that the climate model “bombed” at the next increment of forcing due to failure of one or more of the parameterizations of physical processes in the model when extreme conditions are approached. The accuracy of the representations at extreme temperatures must be improved before the model can be used to simulate well transitions to snowball Earth or the runaway greenhouse effect.

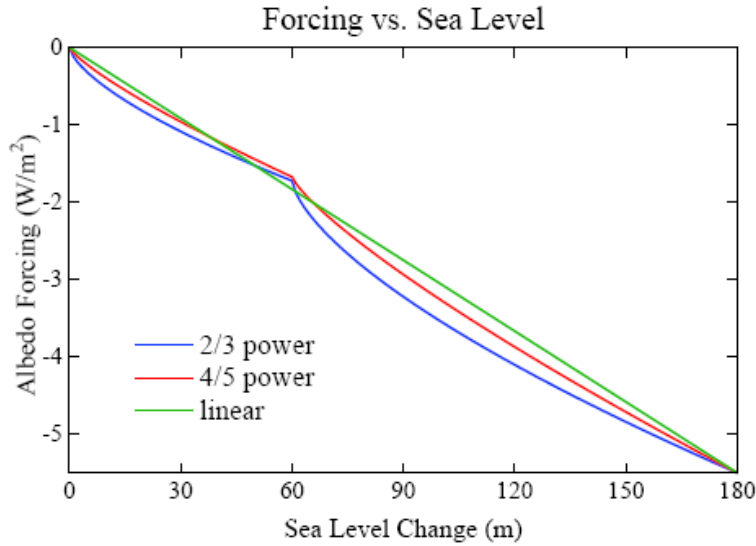


Fig. S4. Surface albedo climate forcing as a function of sea level for three approximations of the ice sheet area as a function of sea level change, from an ice free planet to the last glacial maximum. For sea level between 0 and 60 m only Antarctica contributes to the albedo change. At the last glacial maximum Antarctica contains 75 m of sea level and the Northern Hemisphere contains 105 m.

Ice sheet albedo. In the present paper we take the surface area covered by an ice sheet to be proportional to the 4/5 power of the volume of the ice sheet, based on ice sheet modeling of one of us (VM-D). We extend the formulation all the way to zero ice on the planet, with separate terms for each hemisphere. At 20 ky ago, when the ice sheets were at or near their maximum size in the Cenozoic era, the forcing by the Northern Hemisphere ice sheet was -3.5 W/m^2 and the forcing by the Southern Hemisphere ice sheet was -2 W/m^2 , relative to the ice-free planet (10). It is assumed that the first 60 m of sea level fall went entirely into growth of the Southern Hemisphere ice sheet. The water from further sea level fall is divided proportionately between hemispheres such that when sea level fall reaches -180 m there is 75 m in the ice sheet of the Southern Hemisphere and 105 m in the Northern Hemisphere.

The climate forcing due to sea level changes in the two hemispheres, SL_S and SL_N , is

$$F_{\text{Albedo}} (\text{W/m}^2) = -2 (SL_S/75 \text{ m})^{4/5} - 3.5 (SL_N/105 \text{ m})^{4/5}, \quad (\text{S2})$$

where the climate forcings due to fully glaciated Antarctica (-2 W/m^2) and Northern Hemisphere glaciation during the last glacial maximum (-3.5 W/m^2) were derived from global climate model simulations (10).

Figure S4 compares results from the present approach with results from the same approach using exponent 2/3 rather than 4/5, and with a simple linear relationship between the total forcing and sea level change. Use of exponent 4/5 brings the results close to the linear case, suggesting that the simple linear relationship is a reasonably good approximation. The similarity of Fig. 1c in our present paper and Fig. 2c in (6) indicates that change of exponent from 2/3 to 4/5 did not have a large effect.

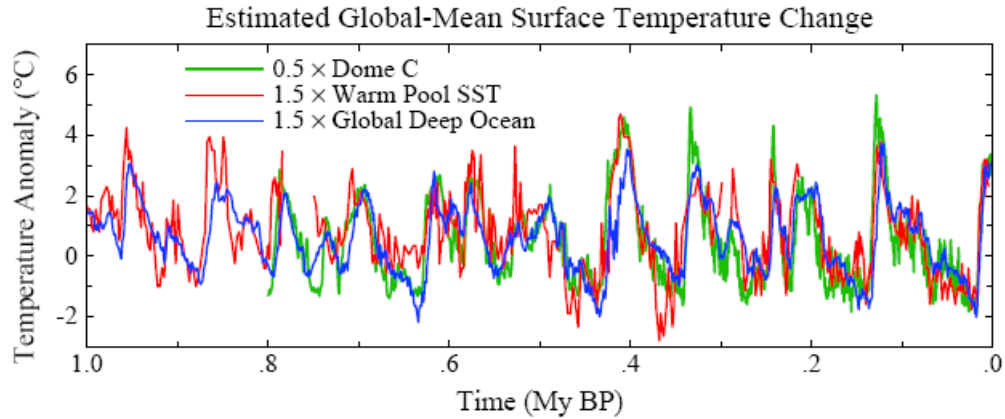


Fig. S5. Estimated global temperature change based on measurements at a single point or, in the case of the deep ocean, a near-global stack of ocean drilling sites: Antarctica Dome C (S6), Warm Pool (S7), deep ocean (20).

Global nature of major climate changes. Climate changes often begin in a specific hemisphere, but the large climate changes are invariably global, in part because of the global GHG feedback. Even without the GHG feedback, forcings that are located predominately in one hemisphere, such as ice sheet changes or human-made aerosols, still evoke a global response (8), albeit with the response being larger in the hemisphere of the forcing. Both the atmosphere and ocean transmit climate response between hemispheres. The deep ocean can carry a temperature change between hemispheres with little loss, but because of the ocean’s thermal inertia there can be a hemispheric lag of up to a millennium (see Ocean Response Time, below).

Figure S5 compares temperature change in Antarctica (S6), the tropical sea surface (S7), and the global deep ocean (20). Temperature records are multiplied by specific factors intended to convert the temperature record to an estimate of global temperature change. Based on paleoclimate records, polar temperature change is typically twice the global average temperature change, and tropical temperature change is about two-thirds of the global mean change. This polar amplification of the temperature change is an expected consequence of feedbacks (10), especially the snow-ice albedo feedback. The empirical result that deep ocean temperature changes are only about two-thirds as large as global temperature change is obtained from data for the Pleistocene epoch, when deep ocean temperature change is limited by its approach to the freezing point.

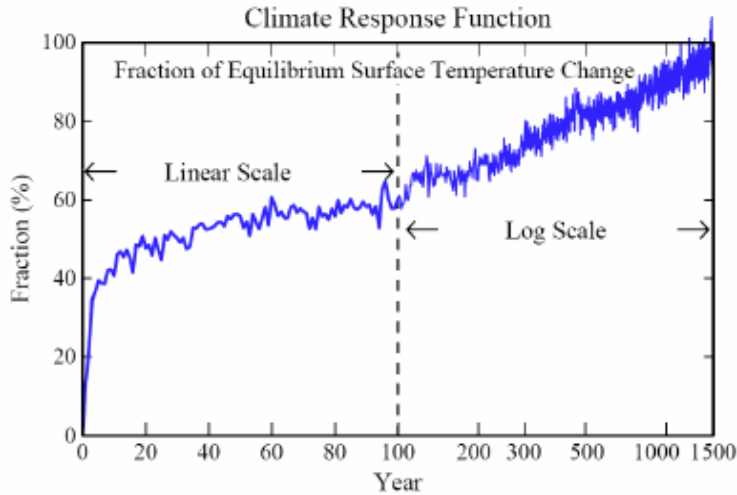


Fig. S6. Fraction of equilibrium surface temperature response versus time in the GISS climate model (6, 8, S3) with the Russell (S8) ocean. The forcing was doubled atmospheric CO₂. The ice sheets, vegetation distribution and other long-lived GHGs were fixed.

Ocean response time. Figure S6 shows the climate response function, defined as the fraction of equilibrium global warming that is obtained as a function of time. This response function was obtained (6) from a 3000-year simulation after instant doubling of atmospheric CO₂, using GISS modelE (S3, 8) coupled to the Russell ocean model (S8). Note that although 40% of the equilibrium solution is obtained within several years, only 60% is achieved after a century, and nearly full response requires a millennium. The long response time is caused by slow uptake of heat by the deep ocean, which occurs primarily in the Southern Ocean.

This delay of the surface temperature response to a forcing, caused by ocean thermal inertia, is a strong (quadratic) function of climate sensitivity and it depends on the rate of mixing of water into the deep ocean (24). The ocean model used for Fig. S6 may mix somewhat too rapidly in the waters around Antarctica, as judged by transient tracers (S8), reducing the simulated surface response on the century time scale. However, this uncertainty does not qualitatively alter the shape of the response function (Fig. S6).

When the climate model used to produce Fig. S6 is driven by observed changes of GHGs and other forcings it yields good agreement with observed global temperature and ocean heat storage (5). The model has climate sensitivity $\sim 3^{\circ}\text{C}$ for doubled CO₂, in good agreement with the fast-feedback sensitivity inferred from paleoclimate data.

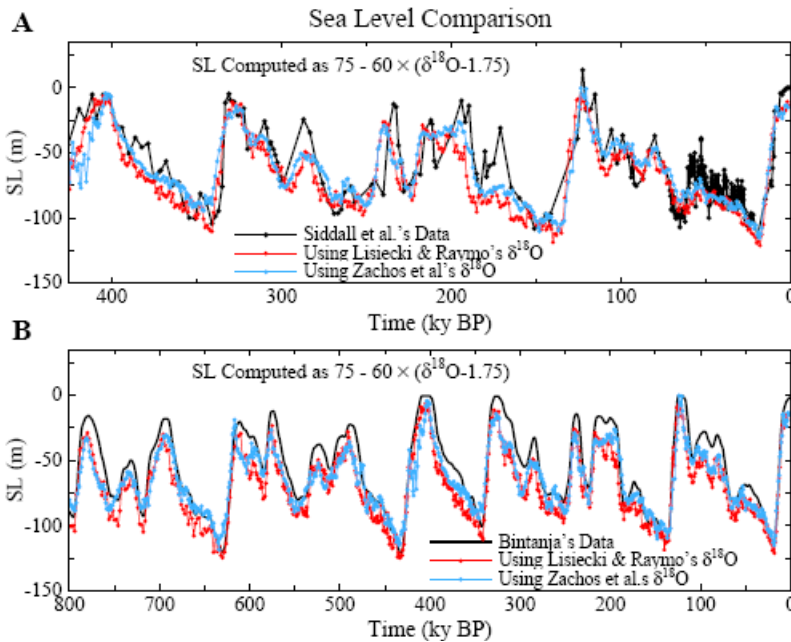


Fig. S7. (A) Comparison of Siddall *et al.* (12) sea level record with sea level computed from $\delta^{18}\text{O}$ via Eq. S1 using two alternative global benthic stacks (20, S9). (B) Comparison of Bintanja *et al.* (S10) sea level reconstruction with the same global benthic stacks as in (A).

Separation of $\delta^{18}\text{O}$ into ice volume and temperature. $\delta^{18}\text{O}$ of benthic (deep ocean dwelling) foraminifera is affected by both deep ocean temperature and continental ice volume. Between 34 My and the last ice age (20 ky) the change of $\delta^{18}\text{O}$ was ~ 3 , with T_{do} change $\sim 6^\circ\text{C}$ (from $+5$ to -1°C) and ice volume change ~ 180 msl (meters of sea level). Based on the rate of change of $\delta^{18}\text{O}$ with deep ocean temperature in the prior period without land ice, ~ 1.5 of $\delta^{18}\text{O}$ is associated with the T_{do} change of $\sim 6^\circ\text{C}$, and we assign the remaining $\delta^{18}\text{O}$ change to ice volume linearly at the rate 60 msl per mil $\delta^{18}\text{O}$ change (thus 180 msl for $\delta^{18}\text{O}$ between 1.75 and 4.75).

Thus we assume that ice sheets were absent when $\delta^{18}\text{O} < 1.75$ with sea level 75 msl higher than today. Sea level at smaller values of $\delta^{18}\text{O}$ is given by

$$\text{SL (m)} = 75 - 60 \times (\delta^{18}\text{O} - 1.75). \quad (\text{S1})$$

Figure S7 shows that the division of $\delta^{18}\text{O}$ equally into sea level change and deep ocean temperature captures well the magnitude of the major glacial to interglacial changes.

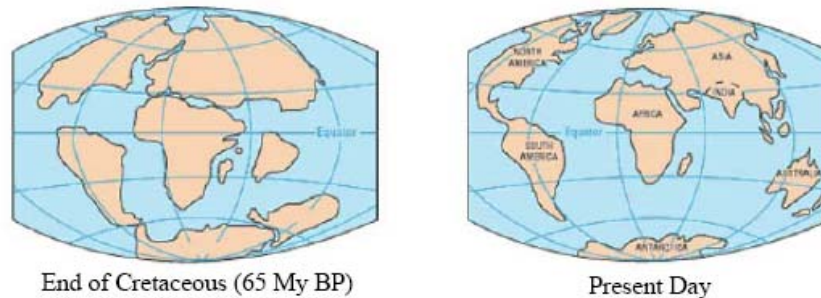


Fig. S8. Continental locations at the beginning and end of the Cenozoic era (S11).

Continental drift and atmospheric CO_2 . At the beginning of the Cenozoic era 65 My ago the continents were already close to their present latitudes, so the effect of continental location per se did not have a large effect on the planet's energy balance (Fig. S8). However, continental

drift has a major effect on the balance, or imbalance, of uptake and out-gassing of CO₂ by the solid Earth. Out-gassing, which occurs in regions of volcanic activity, depends upon the rate at which carbonate-rich oceanic crust is subducted beneath moving continental plates (34). Drawdown of atmospheric CO₂ occurs with weathering of rocks exposed by uplift, with weathering products carried by rivers to the ocean and eventually deposited as carbonates on the ocean floor (35).

At the beginning of the Cenozoic the African plate was already in collision with Eurasia, pushing up the Alps. India was still south of the equator, but moving north rapidly through a region with fresh carbonate deposits. It is likely that subduction of carbonate rich crust of the Tethys Ocean, long a depocenter for sediments, caused an increase of atmospheric CO₂ and the early Cenozoic warming that peaked ~50 My ago. The period of rapid subduction terminated with the collision of India with Eurasia, whereupon uplift of the Himalayas and the Tibetan Plateau greatly increased weathering rates and drawdown of atmospheric CO₂ (38).

Since 50 My ago the major rivers of the world have emptied into the Indian and Atlantic Oceans. But there is little subduction of oceanic crust associated with the ocean basins in which these sediments are accumulating (34). Thus the present continental geography is the presumed cause of CO₂ drawdown and cooling over the past 50 My.

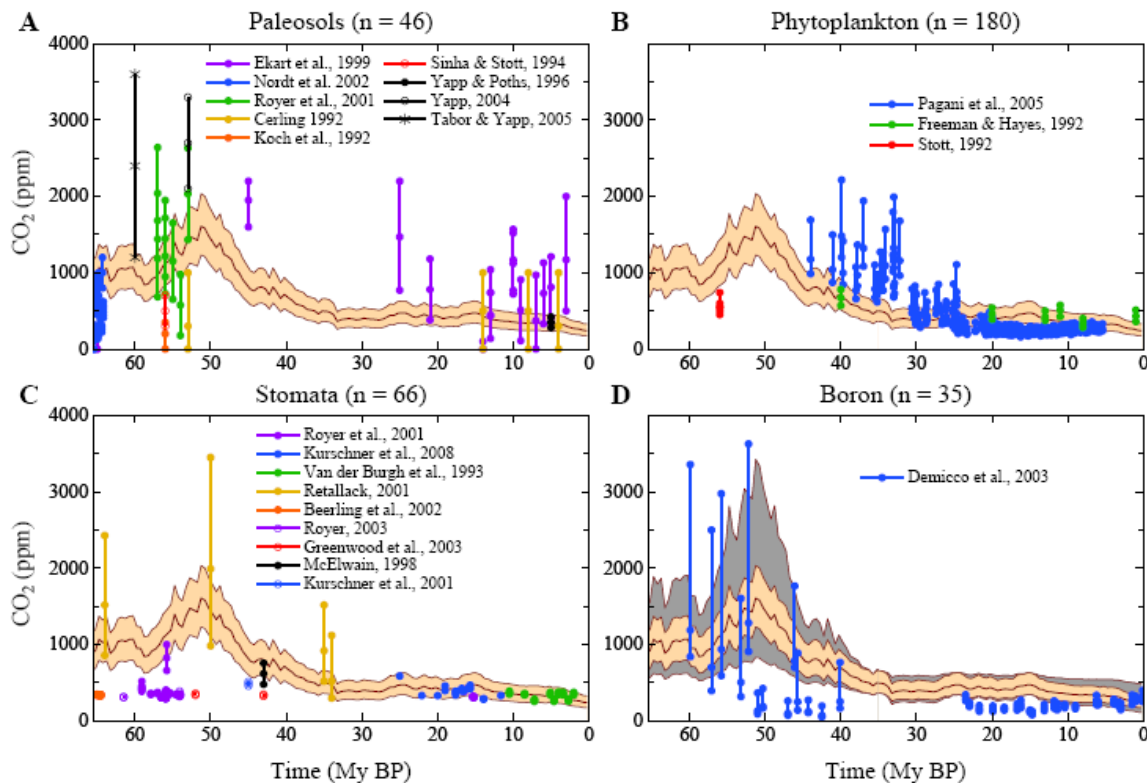


Fig. S9. Comparison of proxy CO₂ measurements with CO₂ predictions based on deep-ocean temperature, the latter inferred from benthic $\delta^{18}\text{O}$. The beige range of model results, intended only to guide the eye in comparing different proxies, is for the case $T_s = T_{do}$, the dark central line for the case $\text{CO}_2 = 450$ ppm at 34 My ago and the borders of the beige area being 325 and 600 ppm. Part D shows the additional range in the model prediction for a 50% uncertainty in the relationship of T_s and T_{do} . Our assumption that CO₂ provides 75% of the GHG throughout the Cenozoic adds additional uncertainty to the predicted CO₂ amount.

Proxy CO₂ data. Strengths and weaknesses of the four paleo-CO₂ reconstruction methods reported in Fig S9, discussed in detail elsewhere (S12), constrain their utility for rigorously evaluating the CO₂ predictions. In brief, the paleosol method is based on the $\delta^{13}\text{C}$ of pedogenic carbonate nodules, whose formation can be represented by a two end-member mixing model between atmospheric CO₂ and soil-derived carbon (S13). Variables that need to be constrained or assumed include an estimation of nodule depth from the surface of the original soil, the respiration rate of the ecosystem that inhabits the soil, the porosity/diffusivity of the original soil, and the isotopic composition the vegetation contribution respired CO₂. The uncertainties in CO₂ estimates with this proxy are substantial at high CO₂ (± 500 -1000 ppm when CO₂ > 1000 ppm) and somewhat less in the lower CO₂ range (± 400 -500 ppm when CO₂ < 1000 ppm).

The stomatal method is based on the genetically-controlled relationship (S14) between the proportion of leaf surface cells that are stomata and atmospheric CO₂ concentrations (S15). The error terms with this method are comparatively small at low CO₂ (< ± 50 ppm), but the method rapidly loses sensitivity at high CO₂ (> 500-1000 ppm). Because stomatal-CO₂ relationships are often species-specific, only extant taxa with long fossil records can be used (S16). Also, because the fundamental response of stomata is to the partial pressure of CO₂ (S17), constraints on paleoelevation are required.

The phytoplankton method is based on the Rayleigh distillation process of fractionating stable carbon isotopes during photosynthesis (S18). In a high CO₂ environment, for example, there is a higher diffusion rate of CO₂ through phytoplankton cell membranes, leading to a larger available intercellular pool of CO_{2[aq]}} and more depleted $\delta^{13}\text{C}$ values in photosynthate. Cellular growth rate and cell size also impact the fractionation of carbon isotopes in phytoplankton and thus fossil studies must take these factors into account (S19). This approach to reconstructing CO₂ assumes that the diffusional transport of CO₂ into the cell dominates, and that any portion of carbon actively transported into the cell remains constant with time. Error terms are typically small at low CO₂ (< ± 50 ppm) and increase substantially under higher CO₂ concentrations (S19).

The boron-isotope approach is based on the pH-dependency of the $\delta^{11}\text{B}$ of marine carbonate (S20). This current method assumes that only borate is incorporated in the carbonate lattice and that the fractionation factor for isotope exchange between boric acid and borate in solution is well-constrained. Additional factors that must be taken into account include test dissolution and size, species-specific physiological effects on carbonate $\delta^{11}\text{B}$, and ocean alkalinity (S21-23). As with the stomatal and phytoplankton methods, error terms are comparatively small at low CO₂ (< ± 50 ppm) and the method loses sensitivity at higher CO₂ (> 1000 ppm). Uncertainty is unconstrained for extinct foraminiferal species.

Climate sensitivity comparisons. Other empirical or semi-empirical derivations of climate sensitivity from paleoclimate data (Table S1) are in reasonable accord with our results, when account is taken of differences in definitions of sensitivity and the periods considered.

Royer et al. (41x) use a carbon cycle model, including temperature dependence of weathering rates, to find a best-fit doubled CO₂ sensitivity of 2.8°C based on comparison with Phanerozoic CO₂ proxy amounts. Best-fit in their comparison of model and proxy CO₂ data is dominated by the times of large CO₂ in the Phanerozoic, when ice sheets would be absent, not by the times of small CO₂ in the late Cenozoic. Their inferred sensitivity is consistent with our inference of ~3°C for doubled CO₂ at times of little or no ice on the planet.

Higgins and Schrag (41y) infer climate sensitivity of ~4°C for doubled CO₂ from the temperature change during the Paleocene-Eocene Thermal Maximum (PETM) ~55 My ago Fig. 3), based on the magnitude of the carbon isotope excursion at that time. Their climate sensitivity for an ice-free planet is consistent with ours within uncertainty ranges. Furthermore, recalling that we assume non-CO₂ to provide 25% of the GHG forcing, if one assumes that part of the PETM warming was a direct effect of methane, then their inferred climate sensitivity is even more closely coincident with ours.

Pagani et al. (41z) also use the magnitude of the PETM warming and the associated carbon isotopic excursion to discuss implications of climate sensitivity, providing a graphical relationship to help assess alternative assumptions about the origin and magnitude of carbon release. They conclude that the observed PETM warming of about 5°C implies a high climate sensitivity, but with large uncertainty due to imprecise knowledge of the carbon release.

Table S1. Climate sensitivities inferred semi-empirically from Cenozoic or Phanerozoic climate change.

Reference	Period	Doubled CO ₂ Sensitivity
Royer et al. (41x)	0-420 My	~ 2.8°C
Higgins and Schrag (41y)	PETM	~4°C
Pagani et al. (41z)	PETM	high

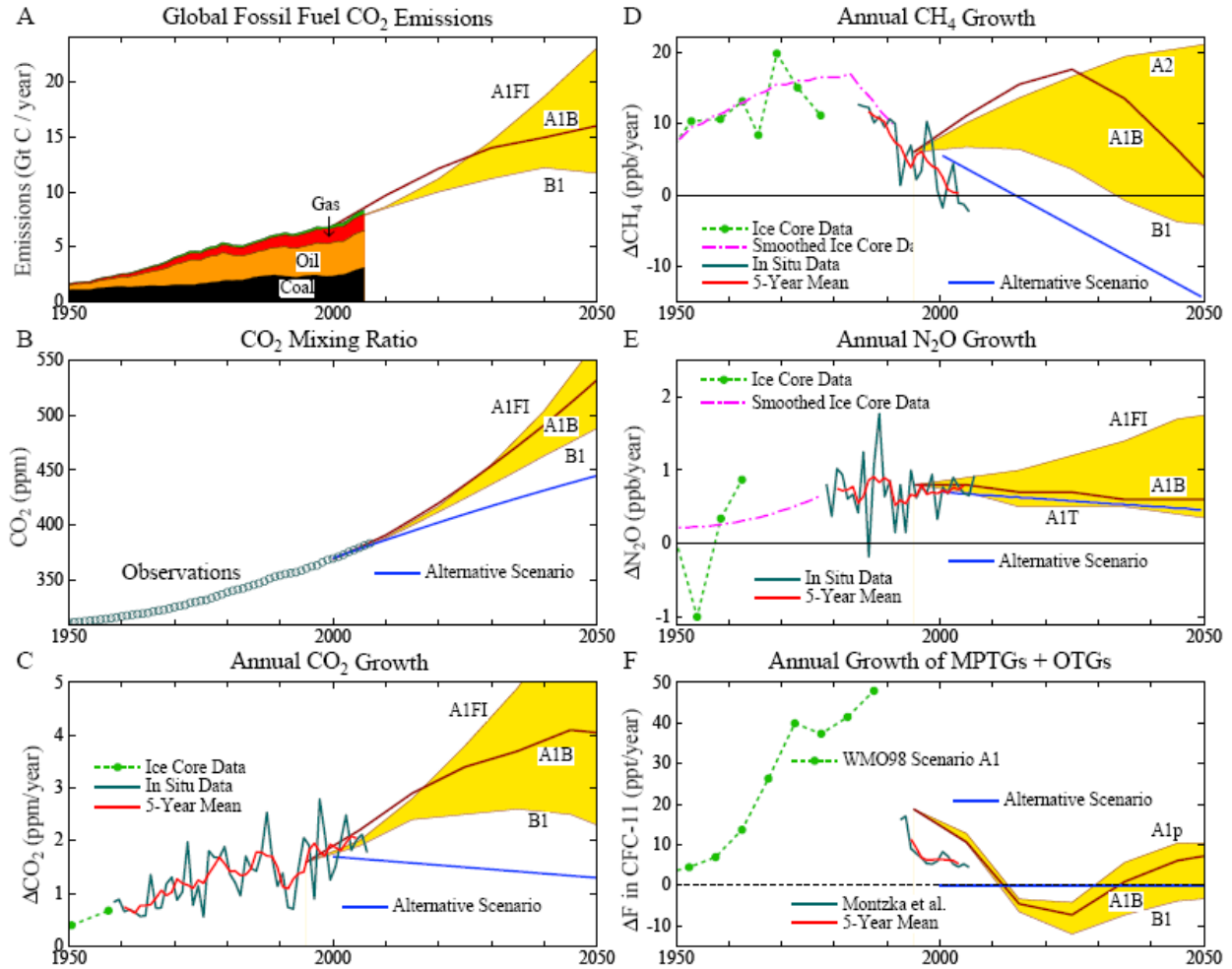


Fig. S10. (A) Fossil fuel CO₂ emissions by fuel type (the thin green sliver is gas flaring plus cement production) and IPCC fossil fuel emissions scenarios, (B) observed atmospheric CO₂ amount and IPCC and “alternative” scenarios for the future, (C) annual atmospheric CO₂ growth rates, (D, E, F) annual growth rates of atmospheric CH₄, N₂O, and the sum of MPTGs (Montreal Protocol Trace Gases) and OTGs (Other Trace Gases). Data here is an update of data sources defined in (6).

Greenhouse gas growth rates. Fossil fuel CO₂ emissions have been increasing at a rate close to the highest IPCC (S17) scenario (Fig. S10A). Increase of CO₂ in the air, however, appears to be in the middle of the IPCC scenarios (Fig. S10B, C), but as yet the scenarios are too close and interannual variability too large, for assessment. CO₂ growth is well above the “alternative scenario”, which was defined with the objective of keeping added GHG forcing in the 21st century at about 1.5 W/m² and 21st century global warming less than 1°C (13).

Atmospheric methane growth is below all IPCC scenarios, and even below the “alternative scenario” growth rate. Nitrous oxide (N₂O) is increasing at a rate within the range of IPCC scenarios. Climate forcing by the sum of all Montreal Protocol trace gases (MPTGs) and other trace gases (OTGs) is increasing at a rate below all IPCC scenarios, but above the “alternative scenario”. Recent international agreement to phase out hydrochlorofluorocarbons (HCFCs, S18) makes it likely that the future growth of MPTGs + OTGs will fall below even the “alternative scenario”.

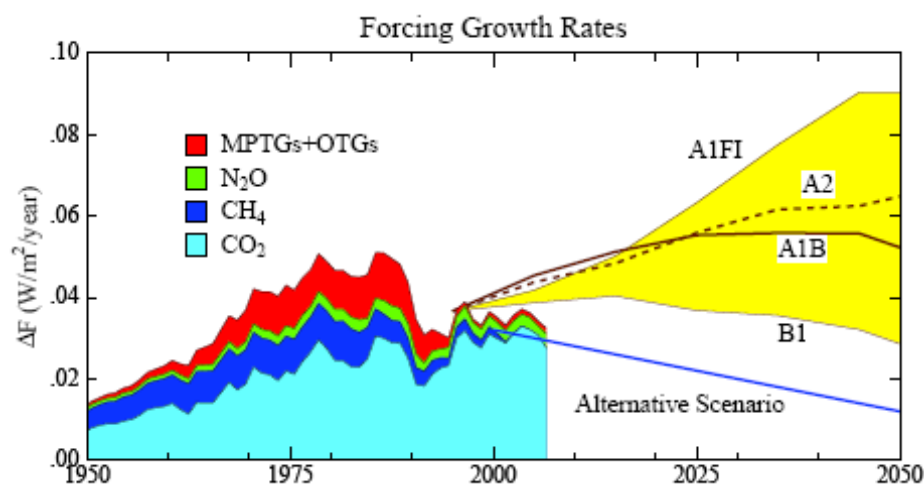


Fig. S11. Five-year running mean of GHG climate forcing annual growth rate, with the 2005 point being a 3-year mean and the 2006 point a 1-year mean (22). Scenarios are defined by IPCC (2) except the ‘alternative scenario’ (13).

Greenhouse gas climate forcing. Figure S11 shows that the net growth rate of the climate forcing by all long-lived GHGs is falling below all IPCC (S17) scenarios. This is in part due to the slower than projected growth of CH₄, MPTGs, and OTGs, but also because the increase of airborne CO₂ (see below) has not quite matched the rapid growth of fossil fuel CO₂ emissions. However, inter-annual and inter-decadal variability of CO₂ uptake by the ocean and biosphere are too variable for firm conclusions to be drawn from these short-term trends.

If fossil fuel CO₂ emissions would begin to decrease, as opposed to their actual resurgent growth this decade, Figure S11 suggests that it is still feasible to get onto a path that keeps GHG climate forcing close to the “alternative scenario”. Unfortunately, the basic conclusion of our present paper is that the limit of 1°C additional global warming (above that in 2000), which the “alternative scenario” was designed to stay within, is well into the “dangerous” range.

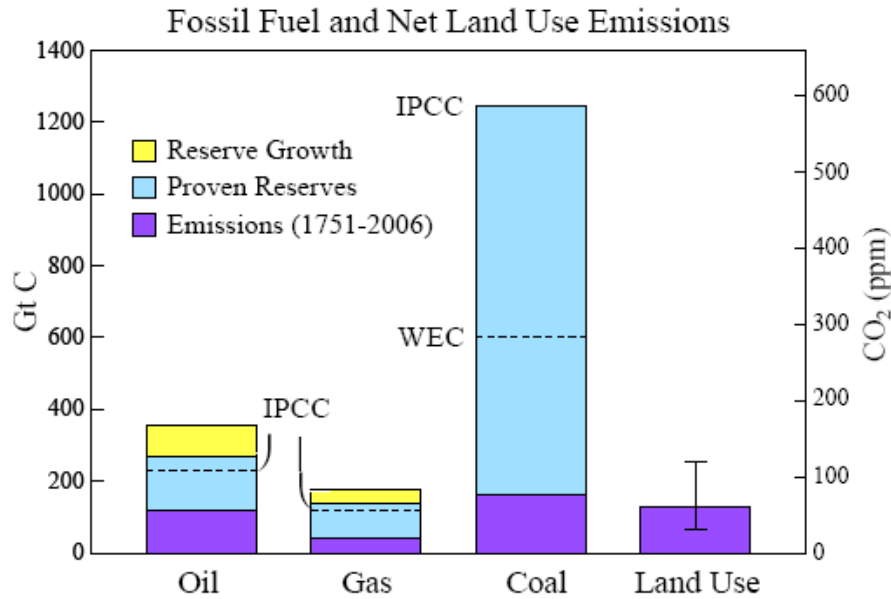


Fig. S12. Fossil fuel and land-use CO₂ emissions, and potential fossil fuel emissions. Historical fossil fuel emissions are from the Carbon Dioxide Information Analysis Center (CDIAC, S25) and British Petroleum (BP, S26). Lower limits on oil and gas reserves are from IPCC (S24) and higher limits are from the United States Energy Information Administration (EIA, 58b). Lower limit for coal reserves is from the World Energy Council (WEC, S27) and upper limit from IPCC (S24). Land use estimate from integrated emissions of Houghton/2 (Fig. S14) supplemented to include pre-1850 and post-2000 emissions; uncertainty bar is subjective.

Fossil fuel and land-use CO₂ emissions. Figure S12 shows estimates of anthropogenic CO₂ emissions to the atmosphere. Although fossil emissions through 2006 are known with good accuracy, probably better than 10%, reserves and potential reserve growth are highly uncertain. IPCC (S24) estimates for oil and gas proven reserves are probably a lower limit for future oil and gas emissions, but they are perhaps a feasible goal that could be achieved via a substantial growing carbon price that discourages fossil fuel exploration in extreme environments together with national and international policies that accelerate transition to carbon-free energy sources and limit fossil fuel extraction in extreme environments and on government controlled property.

Coal reserves are highly uncertain, but the reserves are surely enough to take atmospheric CO₂ amount far into the region that we assess as being “dangerous”. Thus we only consider scenarios in which coal use is phased out as rapidly as possible, except for uses in which the CO₂ is captured and stored so that it cannot escape to the atmosphere. Thus the magnitude of coal reserves does not appreciably affect our simulations of future atmospheric CO₂ amount.

Integrated 1850–2008 net land-use emissions based on the full Houghton et al. (58a) historical emissions (fig. S14), extended with constant emissions for the past several years, are 79 ppm CO₂. Although this could be an overestimate by up to a factor of two (see below), substantial pre-1850 deforestation must be added in. Our subjective estimate of uncertainty in the total land-use CO₂ emission is a factor of two.

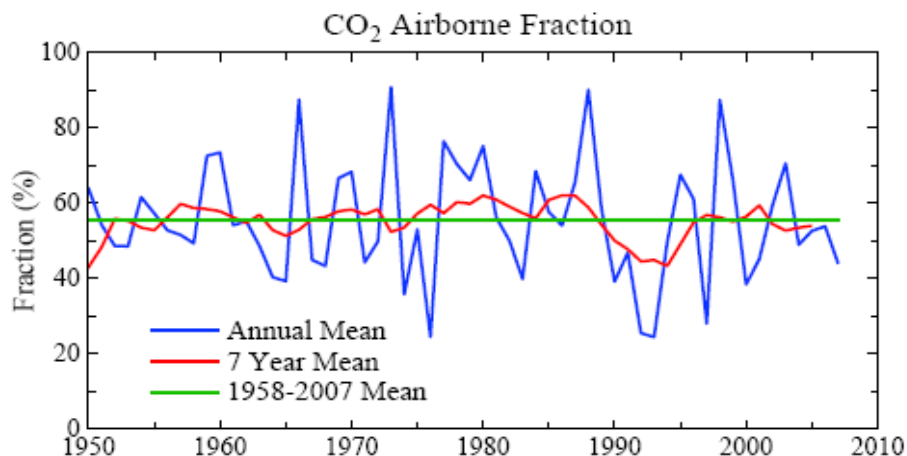


Fig. S13. CO₂ airborne fraction, AF, the ratio of annual observed atmospheric CO₂ increase to annual fossil fuel CO₂ emissions.

The modern carbon cycle. Atmospheric CO₂ amount is affected significantly not only by fossil fuel emissions, but also by agricultural and forestry practices. Quantification of the role of land-use in the uptake and release of CO₂ is needed to assess strategies to minimize human-made climate effects.

Figure S13 shows the CO₂ airborne fraction, AF, the annual increase of atmospheric CO₂ divided by annual fossil fuel use. AF is a critical metric of the modern carbon cycle, because it is based on the two numbers characterizing the global carbon cycle that are well known. AF averages 56% over the period of accurate data, which began with the CO₂ measurements of Keeling in 1957, with no discernable trend. The fact that 44% of fossil fuel emissions seemingly “disappears” immediately provides a hint of optimism with regard to the possibility of stabilizing, or reducing, atmospheric CO₂ amount

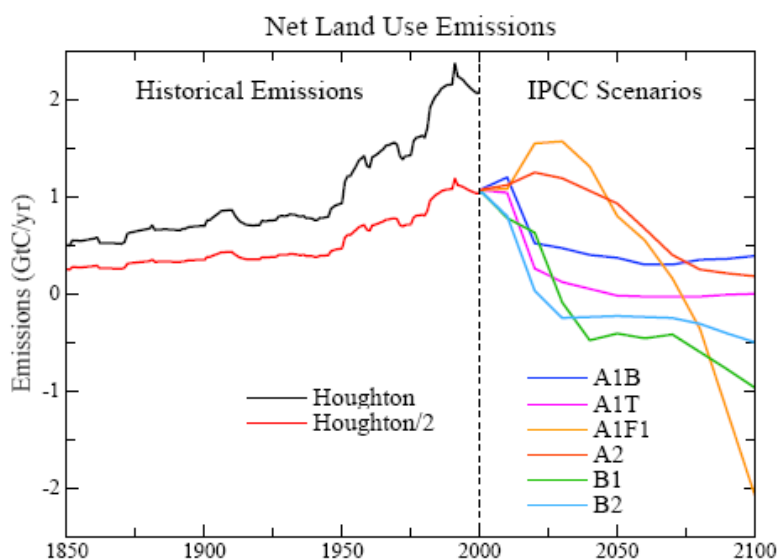


Fig. S14. Left side: estimate by Houghton et al. (58a) of historical net land-use CO₂ emissions, and a 50 percent reduction of that estimate. Right side: IPCC (2) scenarios for land-use CO₂ emissions.

That optimism needs to be tempered, as we will see, by realization of the magnitude of the actions required to halt and reverse CO₂ growth. However, it is equally important to realize that assertions that fossil fuel emissions must be reduced close to 100% on an implausibly fast schedule are not necessarily valid.

A second definition of the airborne fraction, AF₂, is also useful. In AF₂ includes the net anthropogenic land-use emission of CO₂ in the denominator. This AF₂ definition of airborne fraction has become common in recent carbon cycle literature. However, AF₂ is not an observed or accurately known quantity; it involves estimates of net land-use CO₂ emissions, which vary among investigators by a factor of two or more (2).

Figure S14 shows an estimate of net land-use CO₂ emissions commonly used in carbon cycle studies, labeled “Houghton” (58a), as well as “Houghton/2”, a 50% reduction of these land-use emissions. An over-estimate of land-use emissions is one possible solution of the long-standing “missing sink” problem that emerges when the full “Houghton” land-use emissions are employed in carbon cycle models (2, S24, 58).

Principal competing solutions of the “missing sink” paradox are (1) land-use CO₂ emissions are over-estimated by about a factor of two, or (2) the biosphere is being “fertilized” by anthropogenic emissions, via some combination of increasing atmospheric CO₂, nitrogen deposition, and global warming, to a greater degree than included in typical carbon cycle models. Reality may include contributions from both candidate explanations. There is also a possibility that imprecision in the ocean uptake of CO₂, or existence of other sinks such as clay formation, could contribute increased CO₂ uptake, but these uncertainties are believed to be small.

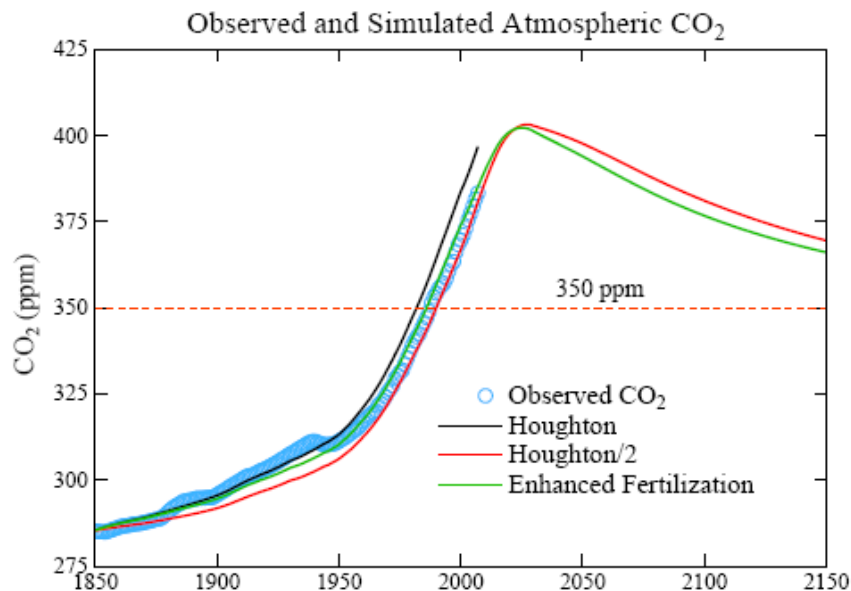


Fig. S15. Computed and observed time evolution of atmospheric CO₂. “Enhanced Fertilization” uses the full “Houghton” land use emissions for 1850–2000. “Houghton/2” and “Enhanced Fertilization” simulations are extended to 2100 assuming coal phase-out by 2030 and the IPCC (2) A1T land-use scenario. Observations are from Law Dome ice core data and flask and in-situ measurements (22, S30, <http://www.esrl.noaa.gov/gmd/ccgg/trends/>).

Figure S15 shows resulting atmospheric CO₂, and Figure S16 shows AF and AF2, for two extreme assumptions: “Houghton/2” and “Enhanced Fertilization”, as computed with a dynamic-sink pulse response function (PRF) representation of the Bern carbon cycle model (57, 58). Fertilization is implemented via a parameterization (57) that can be adjusted to achieve an improved match between observed and simulated CO₂ amount. In the “Houghton/2” simulation the original value (57) of the fertilization parameter is employed while in the “Enhanced Fertilization” simulation the full Houghton emissions are used with a larger fertilization parameter (58). Both “Houghton/2” and “Enhanced Fertilization” yield good agreement with the observed CO₂ history, but Houghton/2 does a better job of matching the time dependence of observed AF.

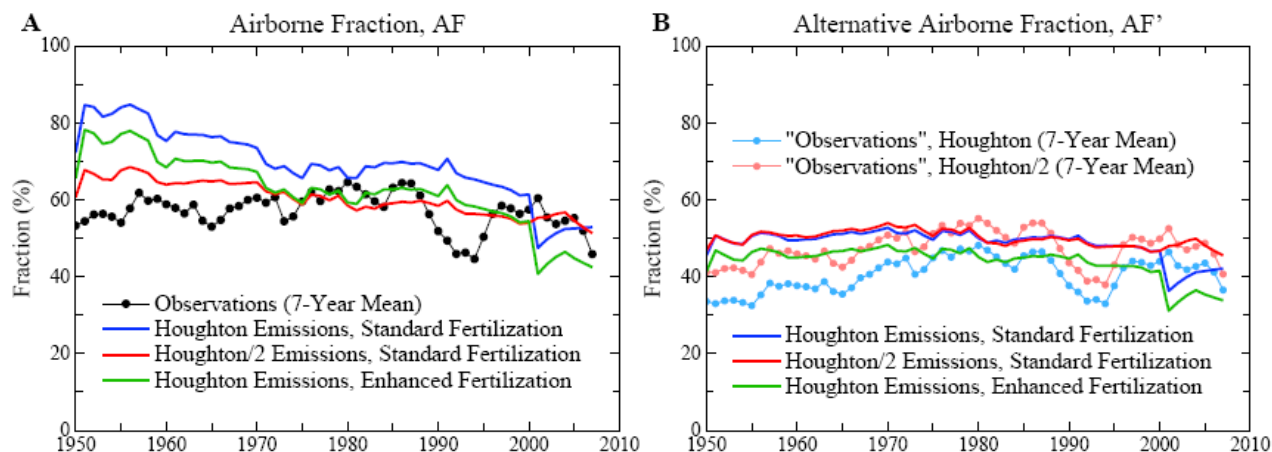


Fig. S16. (A) Observed and simulated airborne fraction (AF), the ratio of annual CO₂ increase in the air over annual fossil fuel CO₂ emissions, (B) AF2 includes the sum of land use and fossil fuel emissions in the denominator in defining airborne fraction; thus AF2 is not accurately known because of the large uncertainty in land use emissions.

It would be possible to match observed CO₂ to an arbitrary precision if we allowed the adjustment to “Houghton” land-use to vary with time, but there is little point or need for that. Fig. S15 shows that projections of future CO₂ do not differ much even for the extremes of Houghton/2 and Enhanced Fertilization. Thus in Figure 6 we show results for only the case Houghton/2, which is in better agreement with the airborne fraction and also is continuous with IPCC scenarios for land use.

Implications of Figure 6: CO₂ Emissions and Atmospheric Concentration with Coal Phaseout by 2030. Figure 6 provides an indication of the magnitude of actions that are needed to return atmospheric CO₂ to a level of 350 ppm or lower. Figure 6 allows for the fact that there is disagreement about the magnitude of fossil fuel reserves, and that the magnitude of useable reserves depends upon policies.

A basic assumption underlying Figure 6 is that, within the next several years, there will be a moratorium on construction of coal-fired power plants that do not capture and store CO₂, and that CO₂ emissions from existing power plants will be phased out by 2030. This coal emissions phase out is the sine qua non for stabilizing and reducing atmospheric CO₂. If the sine qua non of coal emissions phase-out is achieved, atmospheric CO₂ can be kept to a peak amount ~400-425 ppm, depending upon the magnitude of oil and gas reserves.

Figure 6 illustrates two widely different assumptions about the magnitude of oil and gas reserves (illustrated in fig. S12). The smaller oil and gas reserves, those labeled “IPCC”, are realistic if “peak oil” advocates are more-or-less right, i.e., if the world has already exploited about half of readily accessible oil and gas deposits, so that production of oil and gas will begin to decline within the next several years.

There are also “resource optimists” who dispute the “peakists”, arguing that there is much more oil (and gas) to be found. It is possible that both the “peakists” and “resource optimists” are right, it being a matter of how hard we work to extract maximum fossil fuel resources. From the standpoint of controlling human-made climate change, it does not matter much which of these parties is closer to the truth.

Figure 6 shows that, if peak CO₂ is to be kept close to 400 ppm, the oil and gas reserves actually exploited need to be close to the “IPCC” reserve values. In other words, if we phase out coal emissions we can use remaining oil and gas amounts equal to those which have already been used, and still keep peak CO₂ at about 400 ppm. Such a limit is probably necessary if we are to retain the possibility of a drawdown of CO₂ beneath the 350 ppm level by methods that are more-or-less “natural”. If, on the other hand, reserve growth of the magnitude that EIA estimates (Figs. 6 and S12) occurs, and if these reserves are burned with the CO₂ emitted to the atmosphere, then the forest and soil sequestration that we discuss would be inadequate to achieve drawdown below the 350 ppm level in less than several centuries.

Even if the greater resources estimated by EIA are potentially available, it does not mean that the world necessarily must follow the course implied by EIA estimates for reserve growth. If a sufficient price is applied to carbon emissions it will discourage extraction of fossil fuels in the most extreme environments. Other actions that would help keep effective reserves close to the IPCC estimates would include prohibition of drilling in environmentally sensitive areas, including the Arctic and Antarctic.

National policies, in most countries, have generally pushed to expand fossil fuel reserves as much as possible. This might partially account for the fact that energy information agencies, such as the EIA in the United States, which are government agencies, tend to forecast strong growth of fossil fuel reserves. On the other hand, state, local, and citizen organizations can influence imposition of limits on fossil fuel extraction, so there is no guarantee that fossil resources will be fully exploited. Once the successors to fossil energy begin to take hold, there may be a shifting away from fossil fuels that leaves some of the resources in the ground. Thus a scenario with oil and gas emissions similar to that for IPCC reserves may be plausible.

Assumptions yielding the Forestry & Soil wedge in Figure 6B are as follows. It is assumed that current net deforestation will decline linearly to zero between 2010 and 2015. It is assumed that uptake of carbon via reforestation will increase linearly until 2030, by which time reforestation will achieve a maximum potential sequestration rate of 1.6 GtC per year (S28). Waste-derived biochar application will be phased in linearly over the period 2010-2020, by which time it will reach a maximum uptake rate of 0.16 GtC/yr (77). Thus after 2030 there will be an annual uptake of $1.6 + 0.16 = 1.76$ GtC per year, based on the two processes described.

Thus Figure 6 shows that the combination of (1) moratorium and phase-out of coal emissions by 2030, (2) policies that effectively keep fossil fuel reserves from significantly exceeding the IPCC reserve estimates, and (3) major programs to achieve carbon sequestration in forests and soil, together can return atmospheric CO₂ below the 350 ppm level before the end of the century.

The final wedge in Figure 6 is designed to provide an indication of the degree of actions that would be required to bring atmospheric CO₂ back to the level of 350 ppm by a time close to the

middle of this century, rather than the end of the century. This case also provides an indication of how difficult it would be to compensate for excessive coal emissions, if the world should fail to achieve a moratorium and phase-out of coal as assumed as our “sine qua non”.

Assumptions yielding the Oil-Gas-Biofuels wedge in Figure 6B are as follows: energy efficiency, conservation, carbon pricing, and government standards and regulations will lead to decline of oil and gas emissions at 4% per year beginning when 50% of the estimated resource (oil or gas) has been exploited, rather than the 2% per year baseline decline rate (58). Also capture of CO₂ at gas-fired power plants will be phased in over the period 2010-2020, and beyond 2020 gas-fired power plants (with CO₂ capture) will use 50% of remaining gas supplies. It is also assumed that there will be a linear phase-in of liquid biofuels between 2015 and 2025 leading to a maximum global bioenergy from “low-input/high-diversity” biofuels (~23 EJ/yr, inferred from 61c) that is used as a substitute for oil; this is equivalent to ~0.5 GtC/yr, based on energy conversion of 50 EJ/GtC for oil. Finally, from 2025 onward, twice this number (i.e., 1 GtC/yr) is subtracted from annual oil emissions, assuming root/soil carbon sequestration via this biofuel-for-oil substitution is at least as substantial as in Tilman et al. (61c). An additional option that could contribute to this wedge is burning of biofuels in powerplants with CO₂ capture and sequestration (62).

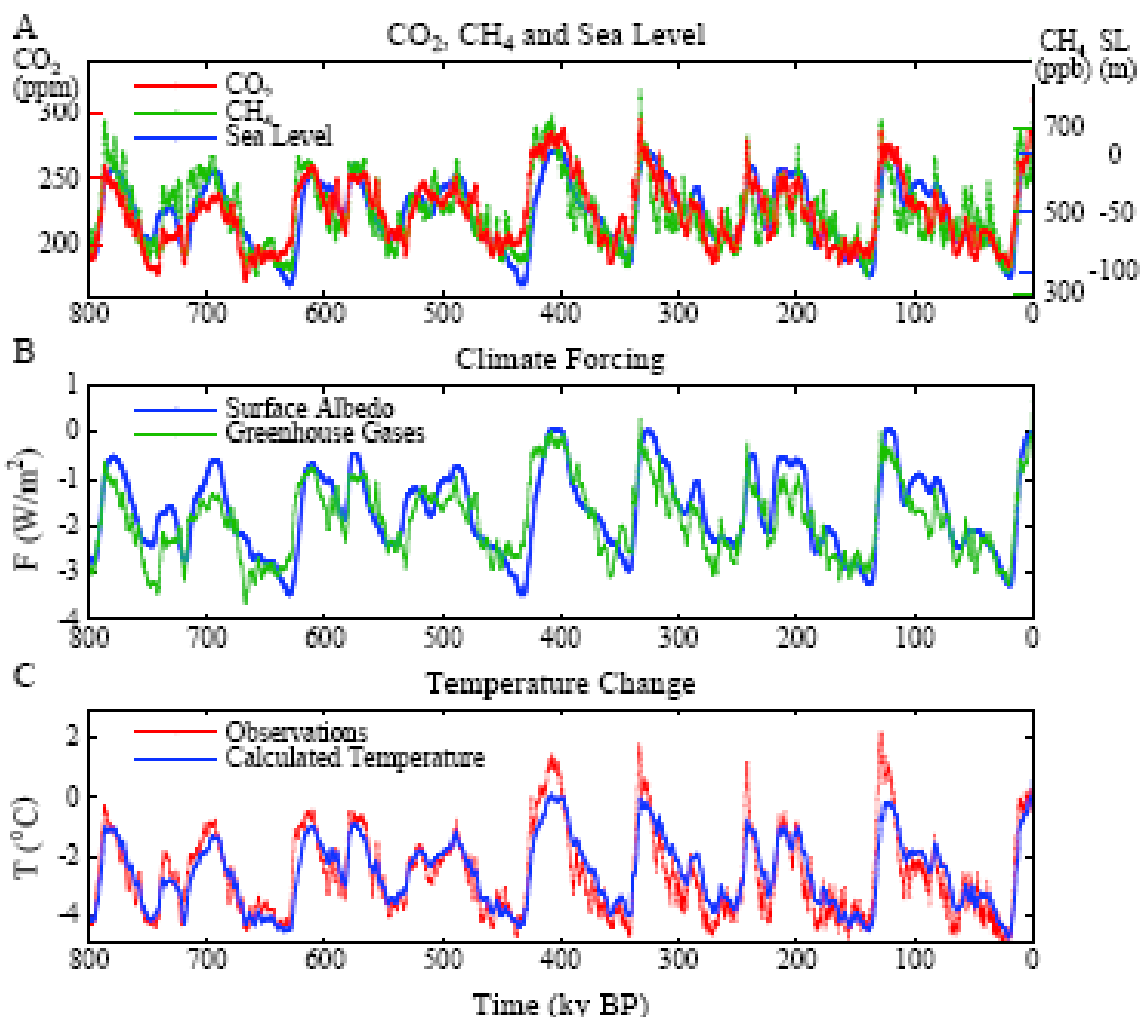


Fig. S17. (A) CO₂ (S34), CH₄ (S35) and sea level (S10) for past 800 ky. (B) Climate forcings due to changes of GHGs and ice sheet area, the latter inferred from the sea level history of Bintanja et al. (S10). (C) Calculated global temperature change based on the above forcings and climate sensitivity $\frac{3}{4}^{\circ}\text{C}$ per W/m^2 . Observations are Antarctic temperature change from the Dome C ice core (S6) divided by two.

EPICA 800 ky data. Antarctic Dome C ice core data acquired by EPICA (European Project for Ice Coring in Antarctica) provide a record of atmospheric composition and temperature spanning 800 ky (S6), almost double the time covered by the Vostok data (11) of Figs. 1 and 2. This extended record allows us to examine the relationship of climate forcing mechanisms and temperature change over a period that includes a substantial change in the nature of glacial-interglacial climate swings. During the first half of the EPICA record, the period 800-400 ky BP, the climate swings were smaller, sea level did not rise as high as the present level, and the GHGs did not increase to amounts as high as those of recent interglacial periods.

Figure S17 shows that the temperature change calculated exactly as described for the Vostok data of Fig. 1, i.e., multiplying a fast-feedback climate sensitivity of $\frac{3}{4}^{\circ}\text{C}$ per W/m^2 by the sum of the GHG and surface albedo forcings (Fig. S17B), yields a remarkably close fit in the first half of the Dome C record to one-half of the temperature inferred from the isotopic composition of

the ice. In the more recent half of the record slightly larger than $\frac{3}{4}^{\circ}\text{C}$ per W/m^2 would yield a noticeably better fit to the observed Dome C temperature divided by two (Figure S18). However, there is no good reason to change our approximate estimate of $\frac{3}{4}^{\circ}\text{C}$ per W/m^2 , because the assumed polar amplification by a factor of two is only approximate.

The sharper spikes in recent observed interglacial temperature, relative to the calculated temperature, must be in part an artifact of differing temporal resolutions. Temperature is from the isotopic composition of the ice, being a function of the temperature at which the snowflakes formed, and thus inherently has a very high temporal resolution. GHG amounts, in contrast, are smoothed over a few ky by mixing of air in the snow that occurs up until the snow is deep enough to compress the snow into ice. In the central Antarctic, where both Vostok and Dome C are located, it requires a few thousand years for bubble closure (11).

Sea level records used to compute the surface albedo forcing in Fig. S17B, generally, are smoother even more than the GHG forcing. This is in part because the sea level change is inferred from $\delta^{18}\text{O}$ in ocean sediment cores. The sediments are stirred by bioturbation, resulting in a smoothing of at least several thousand years. In addition, the sea level record used for the albedo forcings in Figs. S17 and S18 (S10) was based in part on an ice sheet model, which was used to separate the ice volume and ocean temperature components of $\delta^{18}\text{O}$. The ice sheet model employed did not allow the possibility of rapid ice sheet collapse. Some sea level reconstructions based on evidence of shoreline changes suggest the existence of rapid sea level changes within interglacial periods (25), with the possibility of brief sea level high-stands as much as 9 m above present sea level (26).

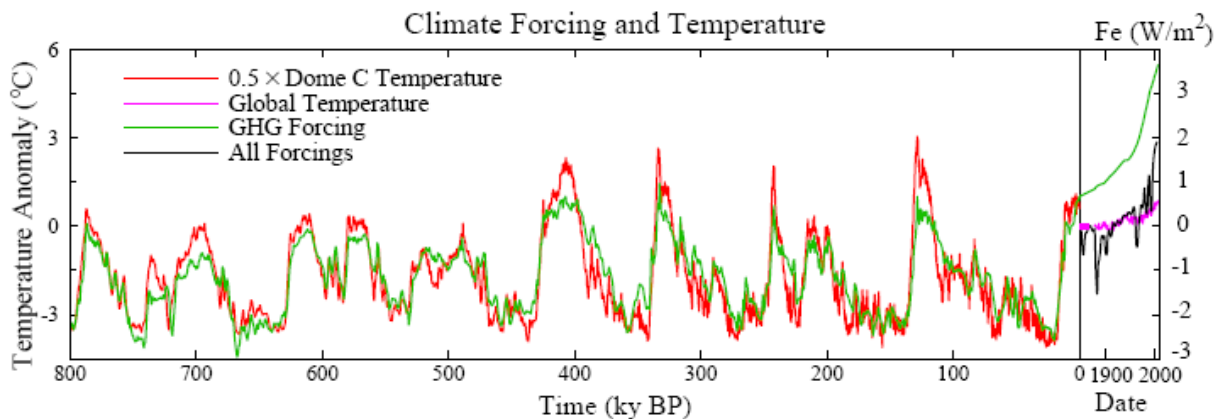


Fig. S18. Global temperature (left scale) and GHG forcing (right scale) due to CO_2 , CH_4 and N_2O from Vostok ice core (11, 15). Ratio of temperature and forcing scales is 1.5°C per W/m^2 . Time scale is expanded in the extension to recent years. Modern forcings include human-made aerosols, volcanic aerosols and solar irradiance (5). GHG forcing zero point is the mean for 10-8 ky before present. Net climate forcing and modern temperature zero points are at 1850. The implicit presumption that the positive GHG forcing at 1850 is largely offset by negative human-made forcings (6) is supported by the lack of rapid climate change at that time.

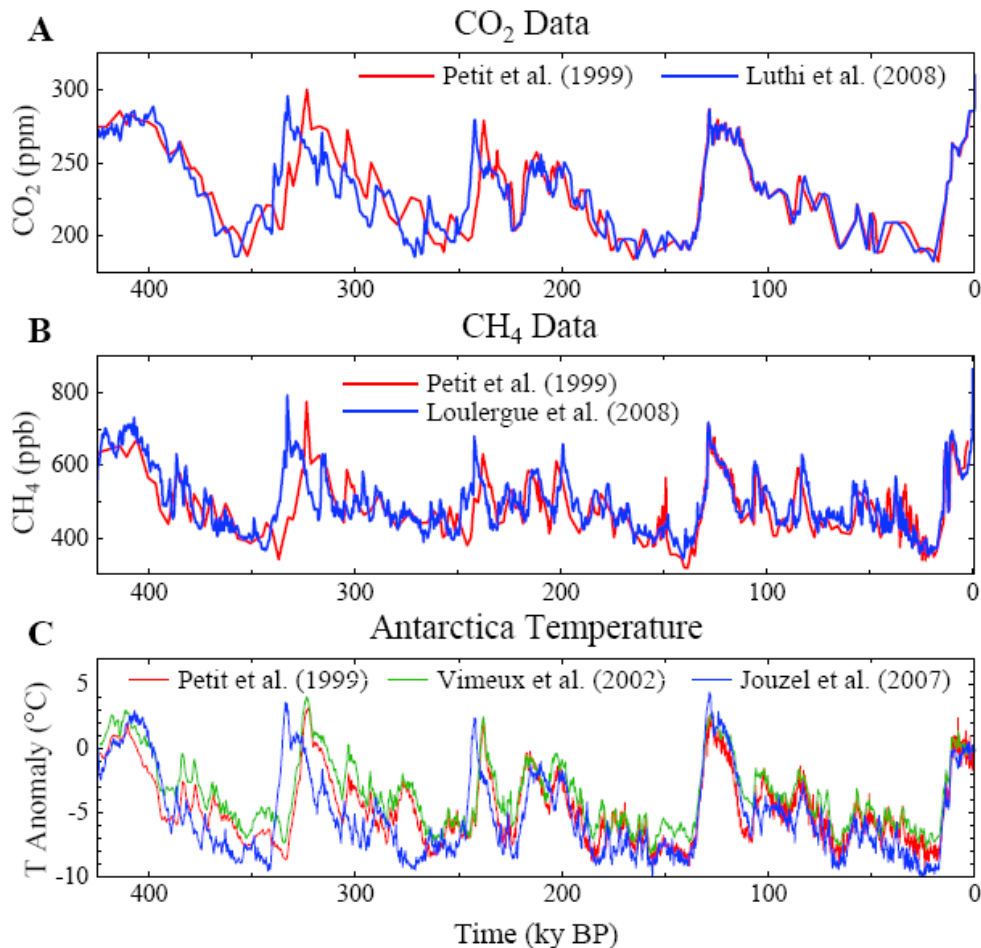


Fig. S19. Comparison of Antarctic CO₂, CH₄, and temperature records in several analyses of Antarctic ice core data.

Comparison of Antarctic data sets. Figure S19 compares Antarctic data sets used in this supplementary section and in our parent paper. This comparison is also relevant to interpretations of the ice core data in prior papers using the original Vostok data.

The temperature records of Petit et al. (11) and Vimeux et al. (15) are from the same Vostok ice core, but Vimeux et al. (15) have adjusted the temperatures with a procedure designed to correct for climate variations in the water vapor source regions. The isotopic composition of the ice is affected by the climate conditions in the water vapor source region as well as by the temperature in the air above Vostok where the snowflakes formed; thus the adjustment is intended to yield a record that more accurately reflects the air temperature at Vostok. The green temperature curve in Fig. S19C, which includes the adjustment, reduces the amplitude of glacial-interglacial temperature swings from those in the original (red curve) Petit et al. (11) data. Thus it seems likely that there will be some reduction of the amplitude and spikiness of the Dome C temperature record when a similar adjustment is made to the Dome C data set.

The temporal shift of the Dome C temperature data (S6), relative to the Vostok records, is a result of the improved EDC3 (S31, S32) time scale. With this new time scale, which has a 1σ uncertainty of ~ 3 ky for times earlier than ~ 130 ky BP, the rapid temperature increases of Termination IV (~ 335 ky BP) and Termination III (~ 245 ky BP) are in close agreement with the

contention (6) that rapid ice sheet disintegration and global temperature rise should be nearly coincident with late spring (April-May-June) insolation maxima at 60N latitude., as was already the case for Terminations II and I, whose timings are not significantly affected by the improved time scale.

The CO₂ data (Fig. S19A) used for Fig.S17 and Fig. S18 are a combined stack of Vostok (11) and Dome C (S33, S34) data on the EDC3 time scale, as presented by Luthi et al. (S35). The addition of Dome C data does not noticeably affect the amplitude of CO₂ glacial-interglacial changes. The CH₄ data (Fig. S19B) used for Figs. S17 and S18 are from the Vostok ice core (S36), but on the EDC3 time scale (S31, S32).

Supplementary References

- S1. C. Hewitt, J. Mitchell, *Clim. Dyn.* **13**, 834 (1997).
- S2. P. Chylek, U. Lohmann, *Geophys. Res. Lett.* **15**, L04804, doi:10.1029/2007GL032759 (2008).
- S3. W. Ehrmann, *Palaeogeogr. Palaeoclimatol. Palaeoecol* **150**, 247 (1998).
- S3. G.A. Schmidt *et al.*, *J. Clim.* **19**, 153 (2006).
- S4. P.F. Hoffman, D.P. Schrag, *Terra Nova* **14**, 129 (2002).
- S5. M.A. Chandler, L.E. Sohl, *J. Geophys. Res.* **105**, 20737 (2000).
- S6. J. Jouzel *et al.*, *Science* **317**, 793 (2007).
- S7. M. Medina-Elizade, D.W. Lea, *Science* **310**, 1009 (2005).
- S8. G.L. Russell, *et al.*, *Dyn. Atmos. Oceans* **9**, 253 (1995).
- S9. L.E. Lisiecki, M.E. Raymo, *Paleocean.* **20**, PA1003 (2005).
- S10. R. Bintaja *et al.*, *Nature* **437**, 125 (2005).
- S11. E.A. Keller, N. Pinter, in *This Dynamic Earth: The Story of Plate Tectonics*, eds. J. Kious, R.I. Tilling, Prentice-Hall, New York, (1996).
- S12. D. L. Royer, R. A. Berner, D. J. Beerling, *Earth-Science Reviews* **54**, 349 (2001).
- S13. T. E. Cerling, *Am. J. Sci.* **291**, 377 (1991).
- S14. J. E. Gray *et al.*, *Nature* **408**, 713 (2000).
- S15. F. I. Woodward, *Nature* **327**, 617 (1987).
- S16. D. L. Royer, *Rev. Palaeobot. Palynol.* **114**, 1 (2001).
- S17. F. I. Woodward, F. A. Bazzaz, *J. Exper. Bot.* **39**, 1771 (1988).
- S18. B. N. Popp, *et al.*, *Amer. J. Sci.* **289**, 436 (1989).
- S19. M. Pagani, *Philosophical Transactions of the Royal Society London A* **360**, 609 (2002).
- S20. A. J. Spivack, *et al.*, *Nature* **363**, 149 (1993).
- S21. D. Blamart *et al.*, *Geochem., Geophys., Geosys.* **8**, Q12001, doi:10.1029/2007GC001686 (2007).
- S22. D. Lemarchand, *et al.*, *Nature* **408**, 951 (2000).
- S23. M. Pagani, *et al.*, *Geochimica et Cosmochimica Acta* **69**, 953 (2005).
- S24. Intergovernmental Panel on Climate Change (IPCC), *Climate Change 2001*, J.T. Houghton et al., Eds. (Cambridge Univ. Press, New York, 2001).
- S25. G. Marland, *et al.*, *Trends*, Carbon Dioxide Information Analysis Center, Oak Ridge Nat. Lab., U.S. DOE, Oak Ridge, TN (2006).
- S26. British Petroleum, *Stat. Rev. World Energy*, www.bp.com/pdf/statistical_review_of_world_energy_full_report2006.pdf (2006).
- S27. World Energy Council (2007), *Survey of Energy Resources*, http://www.worldenergy.org/publications/survey_of_energy_resources_2007/default.asp (2007).
- S28. Intergovernmental Panel on Climate Change (IPCC), *Land Use, Land-Use Change, and Forestry*, R.T. Watson et al., Eds. (Cambridge Univ. Press, Cambridge, UK, 2000).
- S29. E. Kintisch, *Science* **317**, 1843 (2007).
- S30. C.D. Keeling, T.P. Whorf, *Trends: A Compendium on Global Change*, Carbon Dioxide Information Analysis Center, Oak Ridge Nat. Lab., U.S. DOE, Oak Ridge, TN (2005).

- S31. Parrenin, *et al.*, *Clim. Past* **3**, 243 (2007).
- S32. G. Dreyfus *et al.*, *Clim. Past* **3**, 341 (2007).
- S33. U. Siegenthaler, *et al.*, *Science* **310**, 1313 (2005).
- S34. D. Luthi *et al.*, *Nature* (in press).
- S35. L. Louergue, *et al.*, *Nature* (cond. accepted, 2008).
- S36. R. Spahni *et al.*, *Science* **310**, 1317 (2005).



Passenger Vehicle Greenhouse Gas and Fuel Economy Standards: A Global Update



The goal of the International Council on Clean Transportation (ICCT) is to dramatically reduce conventional pollution and greenhouse gas emissions from personal, public, and goods transportation in order to improve air quality and human health, and mitigate climate change. The Council is made up of leading government officials and experts from around the world that participate as individuals based on their experience with air quality and transportation issues. The ICCT promotes best practices and comprehensive solutions to improve vehicle emissions and efficiency, increase fuel quality and sustainability of alternative fuels, reduce pollution from the in-use fleet, and curtail emissions from international goods movement.

www.theicct.org

Published by The International Council on Clean Transportation

© July 2007 The International Council on Clean Transportation

Designed by Big Think Studios

Printed on 100% recycled paper with soy-based ink

This document does not necessarily represent the views of organizations or government agencies represented by ICCT reviewers or participants.



Authors:

Feng An

Innovation Center for Energy and Transportation

Deborah Gordon

Transportation Policy Consultant

Hui He, Drew Kodjak, and Daniel Rutherford

International Council on Clean Transportation

Acknowledgments

The authors would like to thank our many colleagues around the world that have generously contributed their time and insight in reviewing and commenting on the draft version of this report. We would like to thank the Hewlett and Energy Foundations for making this report possible through their vision, energy and resources. We are particularly grateful to the following International Council on Clean Transportation participants who have reviewed this report and support its findings and recommendations.

Dr. Axel Friedrich

Head, Environment, Transport, and Noise Division
Federal Environment Agency, Germany

Mr. Hal Harvey

Environment Program Director
William and Flora Hewlett Foundation, USA

Dr. Dongquan He

China Transportation Program Officer
Energy Foundation, China

Dr. Youngil Jeong

Director
Korean Institute for Machinery and Materials, Korea

Dr. Alan Lloyd

President
The International Council on Clean Transportation, USA

Ms. Charlotte Pera

Senior Program Officer
Energy Foundation, USA

Dr. Leonora Rojas-Bracho

Director General, Research on Urban and Regional Pollution
National Institute of Ecology, Mexico

Ms. Anumita Roychowdhury

Associate Director, Policy Research and Advocacy
Centre for Science and Environment, India

Mr. Michael Walsh

Chairman, Board of Directors
The International Council on Clean Transportation, USA

Dr. Michael Wang

Manager, Systems Assessment Section
Center for Transportation Research, Argonne National Laboratory,
USA

Dr. Martin Williams

Head, Air and Environment Quality Division
UK Department for Environment, Food and Rural Affairs, UK

Table of contents

ACKNOWLEDGMENTS	3
EXECUTIVE SUMMARY	6
1. THE STATE OF VEHICLE GHG EMISSION AND FUEL ECONOMY REGULATIONS AROUND THE WORLD	10
1.1 JAPAN	11
1.2 THE EUROPEAN UNION	12
1.3 CHINA	14
1.4 CANADA	24
1.5 CALIFORNIA	16
1.6 THE UNITED STATES	18
1.7 SOUTH KOREA	20
1.8 OTHER REGIONS	20
2. COMPARING VEHICLE STANDARDS AROUND THE WORLD	21
2.1 OVERVIEW OF GLOBAL GHG EMISSION AND FUEL ECONOMY STANDARDS	21
2.2 COMPARISON OF PASSENGER VEHICLE STANDARDS	23
3. FINDINGS AND CONCLUSIONS	27
APPENDIX: METHODOLOGY FOR ADJUSTING STANDARDS	28
REFERENCES	34




Figures

Figure ES-1.	Actual and Projected GHG Emissions for New Passenger Vehicles by Country, 2002-2018	8
Figure ES-2.	Actual and Projected Fuel Economy for New Vehicles by Country, 2002 to 2018	9
Figure 1.	New (2015) Japanese Standards Compared to Previous (2010) Standards.	11
Figure 2.	New Versus Old Japanese Vehicle Emission Test Cycles	12
Figure 3.	Average CO ₂ Emission Rates (g/km) by Automakers, EU Market, 2006	13
Figure 4.	California Motor Vehicle Greenhouse Gas Emission Projections	17
Figure 5.	Actual and Projected GHG Emissions for New Passenger Vehicles by Country, 2002-2018	23
Figure 6.	Actual and Projected Fuel Economy for New Vehicles by Country, 2002 to 2018	24
Figure 7.	GHG Emission Reduction Associated with the Most Recent Regulations By Country	26
Figure A-1.	Study Methodology	28
Figure A-2.	Modeled Fuel Economy, CAFE-JC08 Multiplier, and CAFE Adjusted 2015 Japanese Fuel Economy Standard	32
Figure A-3.	CAFE Adjusted Projected New Vehicle Average Fuel Economy in Japan, 2005-2015	33

Tables

Table 1.	Estimates of U.S. Light-Duty Truck Fuel Economy Targets and Projected Percentage Gains	19
Table 2.	Number of Registered Passenger Vehicles (by engine size) and Fleet Average Fuel Economy Levels in S. Korea	20
Table 3.	Fuel Economy and GHG Emissions Standards Around the World	22
Table A-1.	Important Unit Conversions	29
Table A-2.	Summary of International Test Cycles	29
Table A-3.	Simulation Results for Gasoline Vehicle Fuel Economy Ratings Under Various Test Cycles	31
Table A-4.	Driving Test Cycle Multiplier Equations	33





Governments around the world are currently grappling with two distinct but interconnected issues—how to reduce emissions of climate-changing greenhouse gases (GHG) and how to reduce dependence on finite, and often imported, supplies of petroleum.

Vehicle standards, either designed to reduce fuel consumption or GHG emissions, can play an important role in addressing both of these policy goals. There is a great deal of policy activity around these issues today: the European Union is working out the specific regulatory policy to reduce carbon dioxide (CO₂) emissions from passenger vehicles; Canada is expected to propose new fuel economy standards in the fall; the U.S. Congress and a group of federal agencies are developing separate proposals to address fuel economy and climate change respectively; China recently revised its vehicle tax policy to diminish demand for larger, inefficient passenger vehicles; and the State of California is awaiting news on a waiver from the U.S. government to regulate GHG emissions and facing litigation from automakers for trying to do so.

This report compares on an equal basis the vehicle standards that have recently been put in place, updated or proposed by governments around the world to address these two policy goals. Japan and Europe currently lead, and will continue to lead, the world in controlling GHG

emissions and fuel consumption from passenger vehicles, partly due to fuel and vehicle taxation policies that favor more efficient vehicles. In terms of absolute improvement, California and Canada are posed to make the largest gains in the next decade, provided that legal and technical barriers to implementing and enforcing their standards can be overcome.

Other countries could make meaningful strides in the coming years, depending on how policy actions play out. The U.S. and China are both poised to make important decisions in coming years on the next stages of their fuel economy regulations. The most prominent U.S. proposal will bring fuel economy close to current Chinese levels, but considering these two countries together account for close to 40 percent of global sales, each will have a great deal more to do to reduce petroleum consumption in coming years (Automotive News 2007). A few countries with significant and growing vehicle sales, such as India and Mexico, are notably absent from this report and others, such as Brazil and South Korea, could enact stronger vehicle standards to support

their policy goals. Decisions on how to meet and enforce fuel economy or GHG emission goals will not only affect their own domestic affairs, but worldwide conditions for generations to come.

In 2004, the Pew Center on Global Climate Change published a groundbreaking report that compiled and compared GHG emission standards and passenger vehicle fuel economy from seven governments around the world. The report, *Comparison of Passenger Vehicle Fuel Economy and Greenhouse Gas Emission Standards Around the World* (An and Sauer 2004), developed a methodology for directly comparing vehicle standards in terms of European-style grams of CO₂ per kilometer and U.S.-style miles per gallon (mpg). Such a methodology is needed since different parts of the world use different test procedures to determine fuel consumption and GHG emissions. Since the report's publication in 2004, sustained high oil prices and the growing scientific evidence and real world consequences of global climate change have added urgency to these important vehicle performance policies, increasing the need for accessible and reliable benchmarking across jurisdictions.

This report presents a significant update to the 2004 Pew Report. Major changes in vehicle standards have occurred in Japan, Europe and the United States. In addition, the methodology of how standards are converted—in order to compare them on an equal basis—was updated to reflect a broader mix of vehicles sold in the European and Japanese markets and a new Japanese vehicle test cycle. This report identifies new fiscal policies enacted in China and Canada that are

designed to promote fuel-efficient vehicles and to discourage larger, inefficient vehicles. While these fiscal policies are not reflected in our comparisons of regulatory vehicle standards, their importance should not be overlooked or underestimated.

Important findings from this report include:

- While Japan and Europe continue to lead the world with the most stringent passenger vehicle greenhouse gas and fuel economy standards, recent regulatory actions have moved these two important governments in opposite directions.
- In 2006, Japan increased the stringency of its fuel economy standards, while Europe is in the process of weakening its CO₂ standards. As a result, Japan's standards are expected to lead to the lowest fleet average greenhouse gas emissions for new passenger vehicles in the world (125 g CO₂/km) in 2015.
- California's GHG emission standards for passenger vehicles are expected to achieve the greatest absolute emission reductions from any policy in the world.
- U.S. passenger vehicle standards continue to lag behind other industrialized nations, both in absolute terms as well as in the relative improvements required under current regulations to 2011. If targets under discussion in the U.S. Congress are enacted, the U.S. could move ahead of Canada, Australia, South Korean and California by 2020.





- Canada has established the world's only active feebate program with significant incentives and levies for vehicles based on fuel consumption. At the same time, Canada plans to issue an attribute-based fuel economy regulation this fall to take effect in 2011, while it continues to implement its voluntary agreement with automakers.
- The Chinese government warrants significant notice for reforming the passenger vehicle excise tax to encourage the production and purchase of smaller-engine vehicles, and to

eliminate the preferential tax rate that applied to sport utility vehicles (SUVs).

- South Korea is the only nation in the world with fuel economy standards for new passenger vehicles where fleet average fuel economy is projected to decline over the next five years. The South Korean government is considering policy options to address this negative trend.

A comparison of the relative stringency and implementation schedules of GHG emissions and fuel economy standards around the world

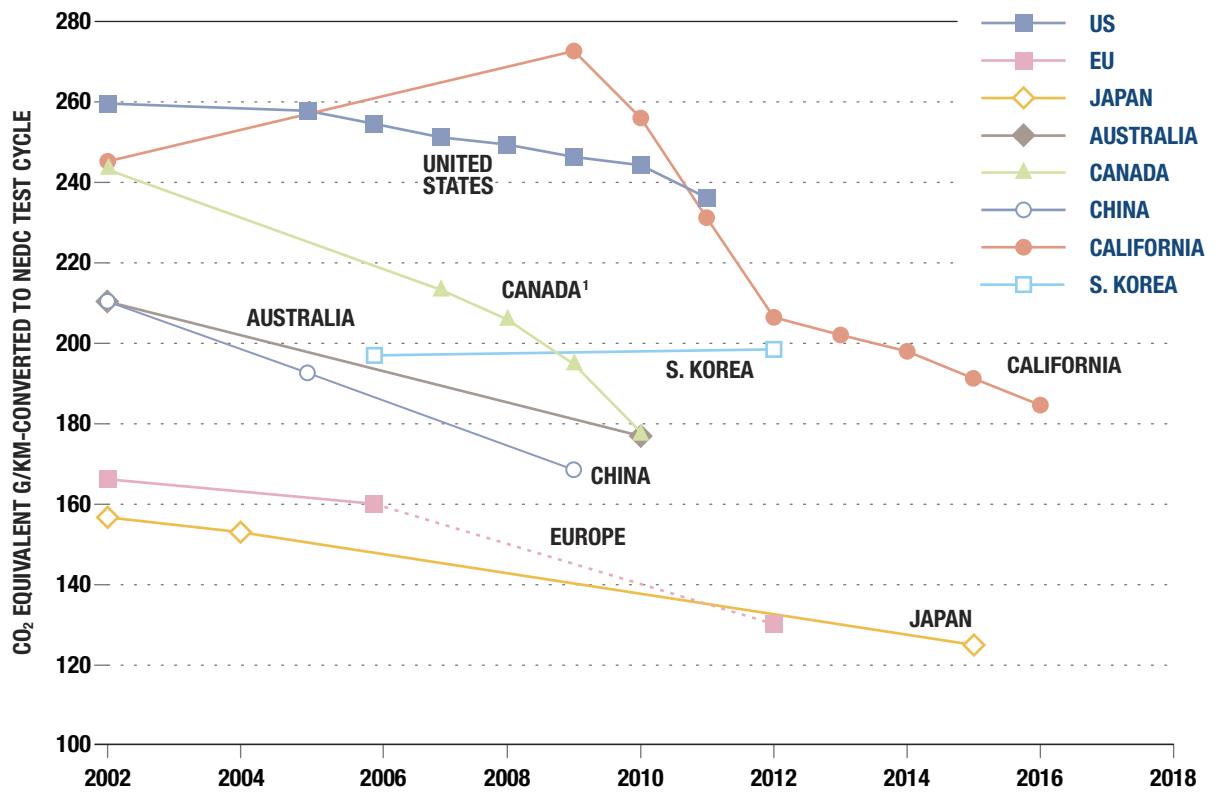


FIGURE ES-1. Actual and Projected GHG Emissions for New Passenger Vehicles by Country, 2002-2018.

Note: Solid lines denote actual performance or projected performance due to adopted regulations; dotted lines denote proposed standards; Values normalized to NEDC test cycle in grams of CO₂-equivalent per km.

[1] For Canada, the program includes in-use vehicles. The resulting uncertainty on new vehicle fuel economy was not quantified.

can be found in Figure ES-1 and Figure ES-2. In order to fairly compare across standards, each country's standard has been converted to units of grams of carbon dioxide equivalent per kilometer traveled on the New European Drive Cycle (NEDC) and miles per gallon on the U.S. Corporate Average Fuel Economy (CAFE) test procedure.

Achieving the maximum feasible standard is a careful regulatory balance that is strengthened by robust benchmarking. This benchmarking exercise proves that there is substantial room for improvement by many governments' policies. Building on this work, future analyses will examine the significant role that regulatory design issues can play in ameliorating competitiveness concerns while achieving ambitious targets.

Vehicle performance standards serve multiple priorities—simultaneously mitigating petroleum dependency, reducing greenhouse gas emissions and increasing consumer welfare.

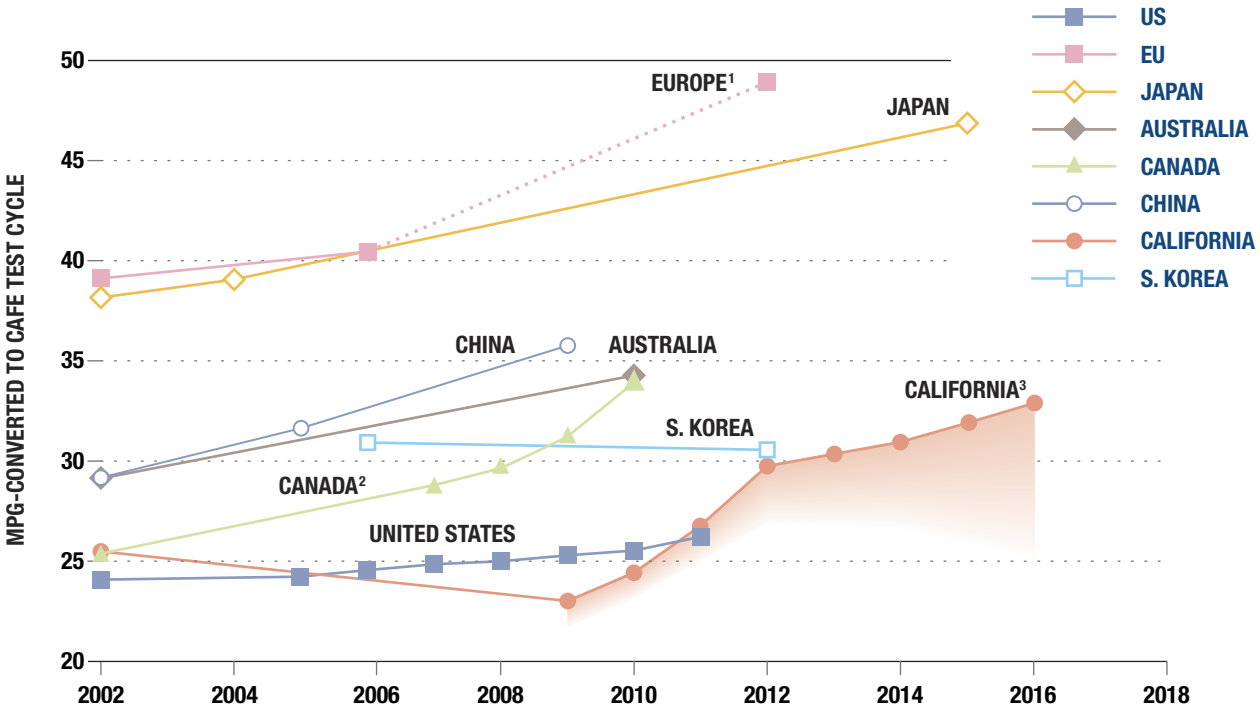


FIGURE ES-2. Actual and Projected Fuel Economy for New Passenger Vehicles by Country, 2002-2018.

[1] The relative stringency of Europe's CO₂-based standards is enhanced under a fuel economy standard because diesel vehicles achieve a boost in fuel economy ratings due to the higher energy content of diesel fuel.

[2] For Canada, the program includes in-use vehicles. The resulting uncertainty of this impact on new vehicle emissions was not quantified.

[3] Shaded area under the California trend line represents the uncertain amount of non-fuel economy related GHG reductions (N₂O, CH₄, HFCs, and upstream emissions related to fuel production) that manufacturers will generate from measures such as low-leak, high efficiency air conditioners, alternative fuel vehicles, and plug-in hybrid electric vehicles.

1. THE STATE OF VEHICLE GHG EMISSION AND FUEL ECONOMY REGULATIONS AROUND THE WORLD

Nine government entities worldwide—Japan, the European Union, United States, California, Canada, China, Australia, South Korea, and Taiwan, China—have proposed, established, or are in the process of revising light-duty vehicle fuel economy or GHG emission standards. Of the 30 Organization for Economic Cooperation and Development (OECD) nations, only five—Iceland, Mexico, Norway, Switzerland, and Turkey—do not currently have programs to reduce GHG emissions or petroleum use from passenger vehicles.

A number of different test procedures, formulas, baselines, and approaches to regulating fuel economy and GHG emissions have evolved over the last several decades. The policy objectives of these regulations vary depending on the priorities of the regulating body, but most standards are applied to new vehicles in order to reduce either fuel consumption or GHG emissions. There are important differences between these two approaches. Fuel economy standards seek to reduce the amount of fuel used by the vehicle per distance driven. Methods to do so may include more efficient engine and transmission technologies, improved aerodynamics, hybridization, or improved tires. GHG emission standards, on the other hand, may target either CO₂ or the whole suite of GHG emissions from the vehicle, such as refrigerants from the air conditioning system or

nitrous oxide (N₂O) from the catalytic converter. GHG emissions standards may even extend beyond the vehicle to encompass the GHG emissions generated from the production of fuels.

The four largest automobile markets—

North America, the European Union, China, and Japan—approach these new vehicle standards quite differently. Within North America alone, a wide variety of approaches have been taken: the U.S. federal government has relied on CAFE standards requiring each manufacturer to meet specified fleet average fuel economy levels for cars and light trucks¹; the state of California has passed fleet average GHG emission standards for new vehicles sold in the state; and Canada's voluntary agreement with automakers is intended to reduce GHG emissions from new and in-use vehicles. The European Union recently announced that it would replace a voluntary agreement with automakers with an enforceable regulatory program because automakers were not on track to meet their voluntary targets. China and Japan have set tiered, weight-based fuel economy standards. Japan's standards allow for credits and trading between weight classes, while China sets minimum standards that every vehicle must achieve or exceed.

Certification of GHG emission and fuel economy performance for new vehicles is based on test procedures intended to reflect real world driving conditions and behavior in each country. The European

Union, Japan, and the U.S. have each established their own test procedures. China and Australia use the European Union’s test procedures. California, Canada, and Taiwan, China follow the U.S. CAFE test procedures, while South Korea adopts the U.S. City test procedure.”

1.1 JAPAN

The Japanese government first established fuel economy standards for gasoline and diesel powered light-duty passenger and commercial vehicles in 1999 under its “Top Runner” energy efficiency program. Fuel economy targets are based on weight class, with automakers allowed to accumulate credits in one weight class for use in another, subject to certain limitations. Penalties apply if the targets are not met, but they are minimal. The effectiveness of the

standards is enhanced by highly progressive taxes levied on the gross vehicle weight and engine displacement of automobiles when purchased and registered. These financial incentives promote the purchase of lighter vehicles with smaller engines. For example, the Japan Automobile Manufacturers Association estimates that the owner of a subcompact car (750 kg curb weight) will pay \$4,000 less in taxes relative to a heavier passenger car (1,100 kg curb weight) over the lifetime of the vehicle (JAMA 2007).

In December 2006, Japan revised its fuel economy targets upward, and expanded the number of weight bins from nine to sixteen (Figure 1). This revision took place before the full implementation of the previous standards because the majority of vehicles sold in Japan in 2002 already met or exceeded the 2010 standards. This new standard is

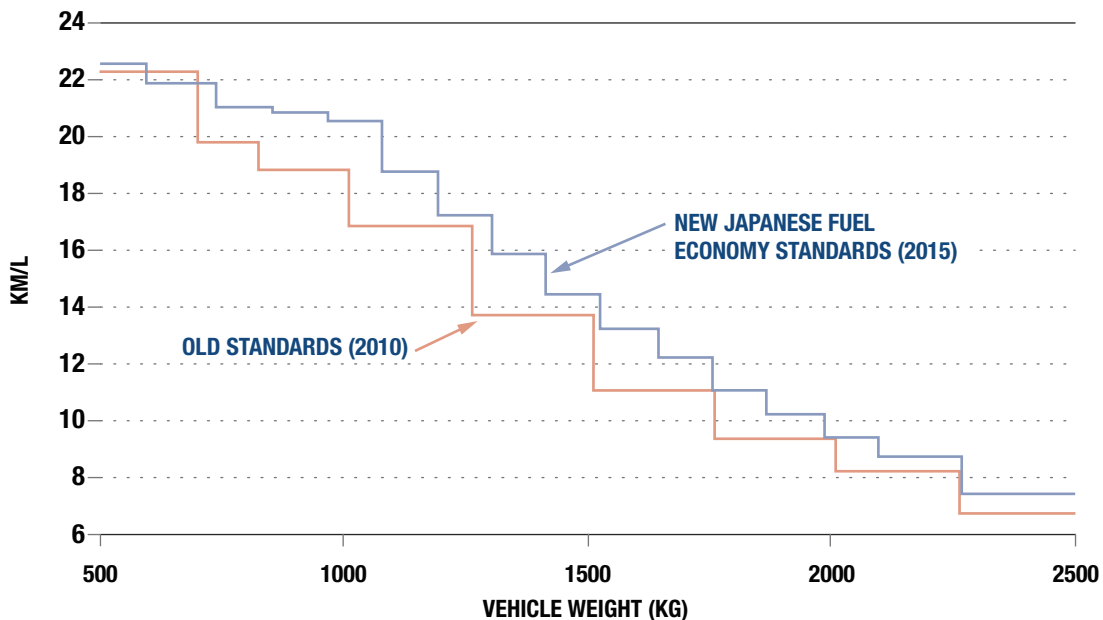


FIGURE 1. New (2015) Japanese Standards Compared to Previous (2010) Standards.

projected to improve the fleet average fuel economy of new passenger vehicles from 13.6 km/L in 2004 to 16.8 km/L in 2015, an increase of 24 percent. Based on our analysis, the new target reaches an average of 125 g/km for CO₂ emissions on the NEDC test cycle (see Figure 5).

In 2010 Japan will introduce a new test cycle, the JC08, to measure progress toward meeting the revised 2015 targets. Relative to the previous 10-15 test cycle, the JC08 test cycle is longer, has higher average and maximum speeds and requires more aggressive acceleration. These differences are illustrated in Figure 2.

According to the Japanese government, the JC08 cycle's higher average speed², quicker acceleration, and new cold start increased the stringency of the test by 9 percent. The

government determined the relative stringency by measuring fuel economy of 2004 model year vehicles under each test cycle. The fleet average fuel economy for MY2004 vehicles was 15.0 km/L under the 10-15 test cycle (MLIT 2006) and 13.6 km/L under the JC08 test cycle (ANRE/MLIT 2006). The more-rigorous JC08 test cycle serves to further increase the stringency of the 2015 standards beyond the difference seen in Figure 1.

1.2 THE EUROPEAN UNION

A decade ago, the European Union entered into a series of voluntary agreements with the associations of automobile manufacturers that sell vehicles in the European market to reduce CO₂ tailpipe emissions. These agreements apply to each manufacturer's new vehicle fleet, and set an industry-wide target of 140 grams CO₂ per kilometer. (Other GHGs were not included in the agree-

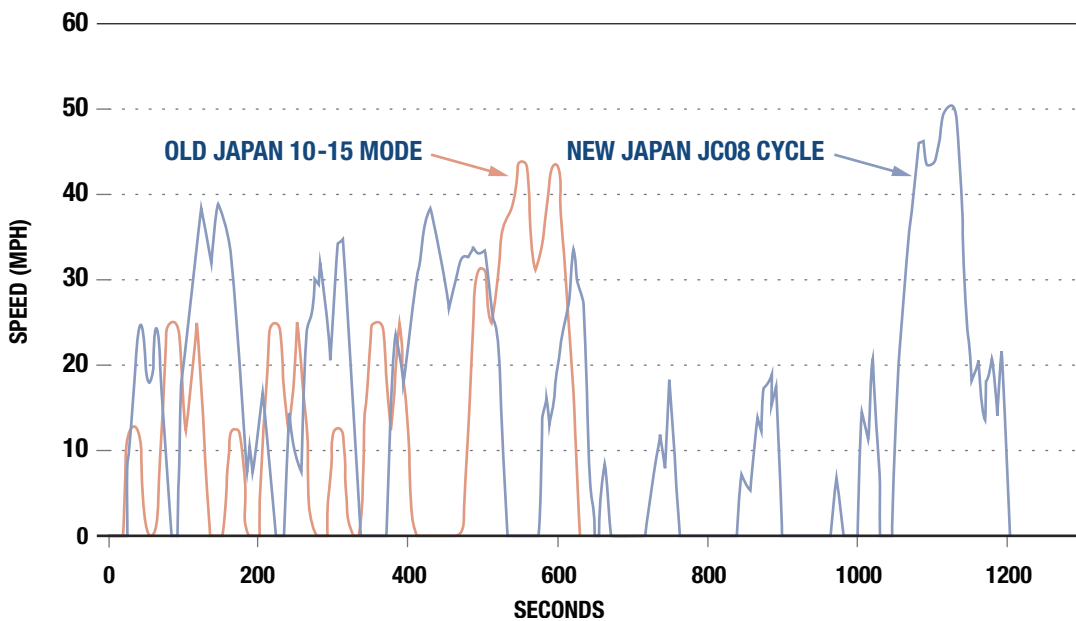


FIGURE 2. New Versus Old Japanese Vehicle Emission Test Cycles

ment.) This target was designed to achieve a 25 percent reduction in CO₂ emissions from passenger cars from 1995. The original agreement with the European Car Manufacturers Association (ACEA) had an initial compliance date of 2008, while the Asian manufacturers (represented by South Korean and Japanese associations, KAMA and JAMA) were given until 2009 to comply³.

Current trends strongly suggest that the automakers will not comply with the 2008 target. In 2006, manufacturer-fleet average CO₂ emissions ranged from 142–238 g/km, with an industry-wide average of 160 g/km (Figure 3). By 2008, the passenger vehicle fleet average CO₂ emissions are projected to reach 155 g/km instead of the 140 g/km target.

In its 2007 review of the EU CO₂ and cars strategy, the European Commission announced that the EU objective of 120 g CO₂/km by 2012 would be met through an “integrated approach”. In June 2007, the Council of Environment Ministers formally adopted a resolution to approve the shift to mandatory standards and an integrated approach to achieve 120 g/km, with carmakers achieving 130 g/km through technical improvements and the remaining 10 g/km coming from complementary measures. Those measures could include efficient tires and air conditioners, tire pressure monitoring systems, gear shift indicators, improvements in light-commercial vehicles, and increased use of biofuels. The Commission

has announced that it will propose a legislative framework for vehicle standards and complementary policies if possible in 2007 and, at the latest, by 2008. The Council expressed a desire to include a longer-term vehicle emissions target for 2020 within the context of an overall strategy to address climate change.

The Council of Environment Ministers insisted that the regulatory framework should be as competitively neutral as possible. A review of 2006 data on European passenger vehicles and CO₂ emissions reveals a wide range of fleet averages from 142 to 238

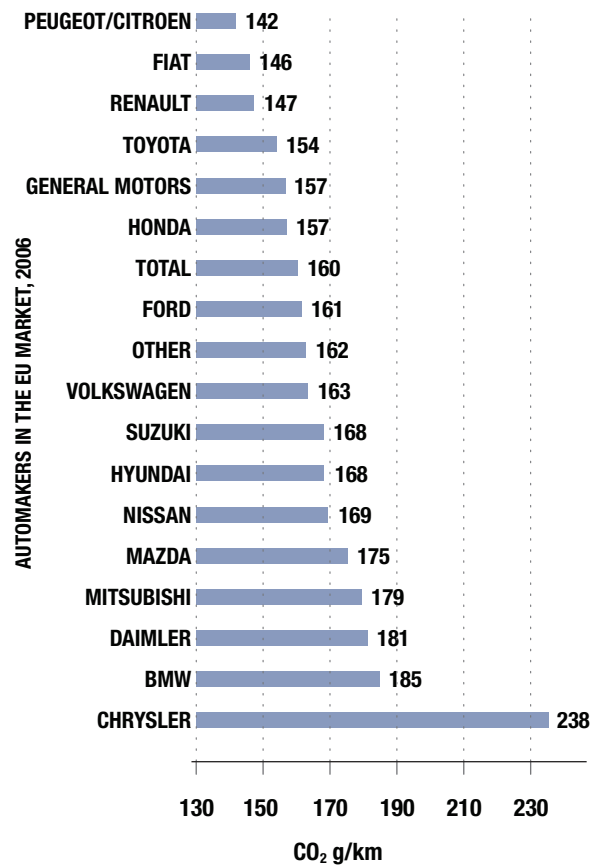


FIGURE 3. Average CO₂ Emission Rates (g/km) by Automakers, EU Market, 2006

g CO₂/km. Several European automakers—Peugeot/Citroen, Fiat, Renault, and Volkswagen—are currently selling vehicles with lower CO₂ emissions in the EU than most Asian manufacturers. This gives these European automakers an advantage in their own market under the forthcoming CO₂ standards. However, two of the three German auto manufacturers—BMW and Daimler—have relatively high CO₂ emissions, while Volkswagen is much closer to the 2006 EU fleet-wide average of 160 g/km. The recent sale of Chrysler has helped Daimler substantially lower its passenger fleet CO₂ emissions.

1.3 CHINA

China is one of the newest entrants to the field of regulating vehicular fuel economy. Since 2005, the country's rapidly growing new passenger vehicle market has been subject to fuel economy standards, which are geared toward reducing China's dependence on foreign oil and encouraging foreign automakers to bring more fuel-efficient vehicle technologies to the Chinese market. The new standards set up maximum fuel consumption limits by weight category and are implemented in two phases. Phase 1 took effect on July 1, 2005 for new models and a year later for continued models. Phase 2 is due to take effect on January 1, 2008 (new models) and January 1, 2009 (continued models). According to a recent study by CATARC, Phase 1 has increased overall passenger vehicle (including SUVs) fuel efficiency by approximately 9 percent, from 26 mpg in 2002 to 28.4 mpg in 2006, despite increases

in gross weight and engine displacement (CATARC 2007).

China has recently revised its taxation of motor vehicles to strengthen incentives for the sale and purchase of vehicles with smaller engines. The taxation has two components: an excise tax levied on automakers and a sales tax levied on consumers. The excise tax rates are based on engine displacement. In 2006, the Chinese government updated excise tax rates to further encourage the manufacture of smaller-engine vehicles. Specifically, the tax rate on small-engine (1.0-1.5 liter) vehicles was cut from 5 to 3 percent, while the tax rate on vehicles with larger-engines (more than 4 liters) was raised from 8 to 20 percent. Also, as the preferential 5 percent tax rate that applied to SUVs has been eliminated, all SUVs are now subject to the same tax schedule as other vehicles with the same engine displacement.

1.4 CANADA

Canada's Company Average Fuel Consumption (CAFC) program was introduced in 1976 to track the fuel consumption of the new light duty vehicle fleet. CAFC is similar to the U.S. CAFE program with the exception that the CAFC program does not distinguish between domestic and imported vehicles. Also, the CAFC program has been voluntary since Canadian automakers made a commitment to meet the targets in the early 1980s. The fuel consumption goals set out by the program have historically been equivalent to CAFE standards. Since Cana-

dian consumers tend to buy more fuel-efficient vehicles than U.S. consumers, the auto industry, as a whole, has consistently met or exceeded CAFC targets.

In 2000, the Government of Canada signaled its intention to seek significant improvements in GHG emissions under a voluntary agreement with automakers. Negotiations culminated in 2005 with the signing of a voluntary Memorandum of Understanding (MOU) between the government and automakers. Under the MOU, the automakers committed to reducing on-road GHG emissions from vehicles by 5.3 megatonnes CO₂ equivalent (CO₂eq) per year in 2010 (MOU 2005). The 5.3 Mt target is measured from a “reference case” level of emissions based on a 25 percent reduction target in fuel consumption that is designed to reflect the actions of automakers that would have occurred in the absence of action on climate change. Under the MOU, automakers can receive credits for reductions in: CO₂ achieved by reducing vehicle fuel consumption; exhaust N₂O and methane (CH₄) emissions; hydrofluorocarbon (HFC) emissions from air-conditioning systems; and reductions in the difference between lab-tested and actual in-use fuel consumption. Since the MOU covers all GHGs emitted by both the new and in-use vehicle fleet, the need to improve new vehicle fuel efficiency will depend on what other GHG reductions will be achieved by industry and counted towards the target. For this reason, the impact of the MOU on fuel

efficiency of the new fleet cannot be forecast with precision. The MOU includes three interim reduction goals for 2007, 2008 and 2009, and a report on progress to the 2007 goal is due in mid-2008.

In October 2006, the Canadian government announced a number of additional measures to reduce air pollutants and GHG emissions. Among these measures was a commitment to formally regulate motor vehicle fuel consumption beginning with the 2011 model year, signaling the end of the voluntary CAFC program. The government plans to issue a consultation paper on the development of these standards in the fall of 2007.

In the 2007 budget, the Canadian Government also introduced a program called the Vehicle Efficiency Incentive (VEI), which came into effect March 2007. The program includes a rebate and tax component, both of which are based on vehicle fuel efficiency. The performance-based rebate program, run by Transport Canada, offers \$1,000 to \$2,000 for the purchase or long-term lease (12 months or more) of an eligible vehicle. Transport Canada maintains a list of the eligible vehicles, which currently includes new cars achieving 6.5 L/100km (36 mpg) or better, new light trucks getting 8.3L/100km (28 mpg) or better, and new flexible fuel vehicles with combined fuel consumption E85 ratings of 13L/100km (18 mpg of combined fuel) or better (Transport Canada 2007). The new excise tax, called a “Green Levy”, is administered by the Canada Revenue

Agency on inefficient vehicles. The sliding tax of up to \$4,000 applies only to passenger cars with a weighted average fuel consumption of 302 g CO₂/km or greater and 18 mpg or less (Canada Revenue Agency 2007).

In addition to actions taken by the federal government, some Canadian provinces have also announced their own plans to further reduce GHG emissions from motor vehicles. The provinces of Québec, British Columbia and Nova Scotia have announced plans to adopt new vehicle standards that are consistent with California's GHG emission standard.

1.5 CALIFORNIA

In 2002, California enacted the first state law (AB 1493) requiring GHG emission limits from motor vehicles⁴. As directed by the statute, the California Air Resources Board (CARB) issued regulations in September 2004 limiting the "fleet average greenhouse gas exhaust mass emission values from passenger cars, light-duty trucks, and medium-duty passenger vehicles" (California Code of Regulations 2004). The fleet average caps first apply to model year 2009 vehicles. The standards become more stringent annually, so that by 2016, the new vehicle fleet average standard would be 30 percent below the 2009 level.

Baseline GHG emissions as of 2004 were estimated at 386,600 CO₂ equivalent tons per day. The California Air Resources Board (CARB) estimates that the proposed GHG

emission standards will reduce projected GHG emissions from the full light-duty vehicle fleet from baseline levels by 17 percent in 2020 and by 25 percent in 2030 (CARB 2004). After accounting for increases in vehicle miles traveled (VMT), GHG emissions are expected to stabilize around 2007 levels until 2020, with a modest increase from 2020 to 2030 as shown in Figure 4.

The California standards cover the whole suite of GHG emissions related to vehicle operation and use. These include:

- CO₂, CH₄ and N₂O emissions resulting directly from vehicle operation;
- CO₂ emissions resulting from energy consumption in operating the air conditioning (A/C) system;
- HFC emissions from the A/C system due to either leakage, losses during recharging, or release from scrapping of the vehicle at the end of life; and
- Upstream emissions associated with the production of the fuel used by the vehicle.

Reductions of non-fuel economy-related GHG emissions are expected to come from a variety of measures. Methane emissions are present in vehicle exhaust at low levels, and three-way catalysts are an effective means of lowering these emissions. Nitrous oxide (N₂O) emissions from mobile sources accounted for 13 percent of total U.S. N₂O

emissions in 2001. A recent pilot study of N₂O emissions from vehicles found that certain newer vehicles have substantially lower N₂O emissions than 1990s vintage vehicles, but the technical reason has not been determined (CARB 2004). The use of improved compressors, reduced refrigerant leakage systems, and alternative refrigerants in mobile air conditioners could also lead to substantial GHG reductions⁵. Alternative fuel vehicles, including plug-in hybrids, can generate credits for the vehicle manufacturer in proportion to the upstream emissions mitigated by an alternative fuel and the amount of that fuel used over a year (CARB 2004).

Since their passage, the California standards have been adopted by eleven other states.

If the program withstands legal challenge, these standards will reduce GHG emissions from more than one in three new vehicles sold in the U.S., impacting emissions from the entire U.S. vehicle fleet.

In December 2005, California requested a waiver from the U.S. Environmental Protection Agency (EPA), as required by Section 209 of the Clean Air Act, to promulgate GHG emission regulations. EPA delayed its response until the U.S. Supreme Court settled the question as to whether the Clean Air Act granted the Agency the authority to regulate CO₂. With the April 2007 Massachusetts v. EPA Supreme Court decision identifying CO₂ as an air pollutant recognized under the Clean Air Act, California's waiver has a greater likelihood of approval.

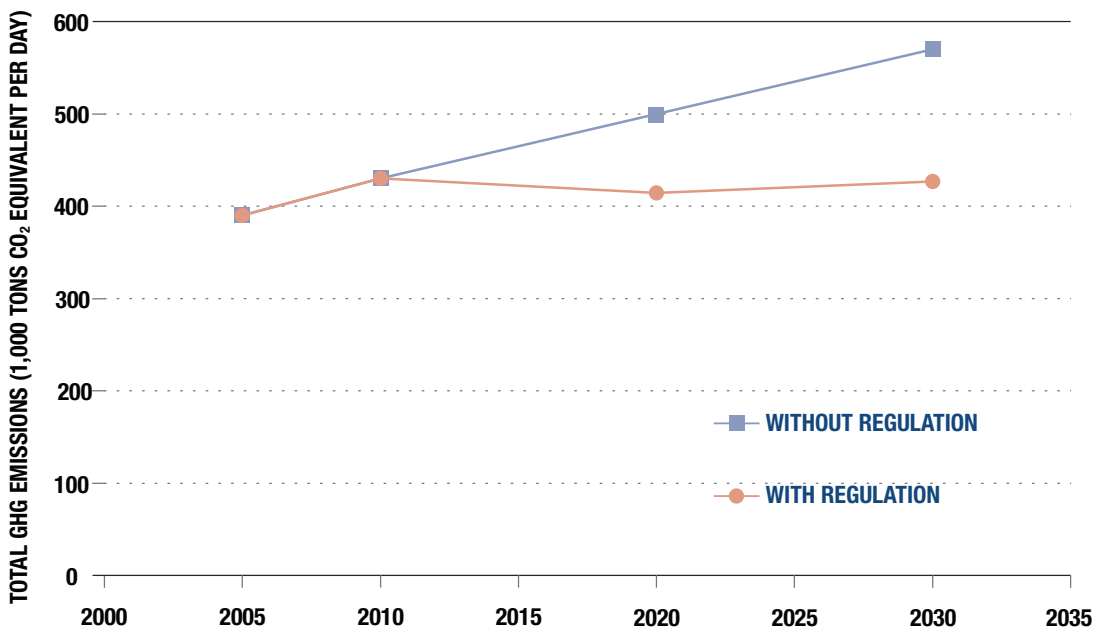


FIGURE 4. California Motor Vehicle Greenhouse Gas Emission Projections (CARB 2004)

1.6 THE UNITED STATES

The U.S. adopted its CAFE standards as part of a broad energy policy package in the wake of the 1973 oil crisis. At the time the standards were adopted, the expressed goal was to reduce the country's dependence on foreign oil; environmental outcomes were not an explicit policy goal. The CAFE standards are set by the National Highway Traffic and Safety Administration (NHTSA), while EPA is responsible for administering and reporting fuel economy tests procedures.

When CAFE standards were introduced, light trucks were a small percentage of the vehicle fleet used primarily for business and agricultural purposes. In order to protect small businesses and farmers, light trucks were subject to a less stringent fuel economy standard. Since that time, automakers have introduced a number of crossover vehicles, such as minivans and SUVs, that combine features of cars and light trucks. The use of these vehicles has shifted to primarily personal transport and market share has now surpassed passenger cars. As a result, there has been a 7 percent decrease in fuel economy of the overall light duty fleet since 1988 (EPA 2004).

Two separate CAFE standards remain in effect for passenger vehicles. The CAFE standard for passenger cars has remained unchanged since 1985 at 27.5 miles per gallon (mpg), although it was rolled back for several years in the late 1980s in response

to petitions filed by several automakers. The standard for light trucks was increased in two rulemakings from 20.7 mpg in 2004 to 24.0 mpg for 2011 over seven model years from 2005 to 2011. In its most recent rulemaking, NHTSA began setting CAFE standards for light trucks based on vehicle size as defined by their "footprint" (the bottom area between the vehicle's four wheels). The new standard is based on a complex formula matching fuel economy targets with vehicle sizes. For the first three years, manufacturers can choose between truck-fleet average targets of 22.7 mpg in 2008, 23.4 mpg in 2009, and 23.7 mpg in 2010, or size-based targets. Beginning in 2011, manufacturers will be required to meet the size-based standards that are expected to result in a fleetwide average of 24.0 mpg (NHTSA 2006).

An analysis by NHTSA shows that, due to a wide variety of size compositions of the light-duty truck fleet, each automaker would have its own fuel economy targets depending on the footprints of the vehicles they sell. As demonstrated in Table 1, the major U.S. automakers, DaimlerChrysler (DCX)⁶, General Motors (GM) and Ford, along with the Japanese automaker, Nissan, are expected to have the lowest fuel economy targets of all automakers while Hyundai, BMW and Toyota have the most stringent fuel economy standards in 2011 (NHTSA and DOT 2006).

Responding to consumer complaints, EPA recently readjusted the fuel economy test

procedures to more accurately report real world consumer experience. While this does not affect the CAFE standard or compliance by automakers, it does give consumers a more accurate reflection of expected fuel use. Designing tests that represent real-world driving styles and conditions is an issue in every nation that regulates fuel economy and GHG emissions. EPA's new testing method—which apply to model year 2008 and later vehicles—includes the city and highway tests used for previous models along with additional tests to represent faster speeds and acceleration, air conditioning use, colder outside temperatures, and wind and road surface resistance.

pollutants potentially subject to federal regulation under the Clean Air Act. In response, the Bush Administration signed an executive order directing the U.S. EPA, in collaboration with the Departments of Transportation and Energy, to develop regulations that could reduce projected⁷ oil use by 20 percent within a decade (Executive Order 2007). The Administration suggested that the “Twenty in Ten” goal be achieved by: (1) increasing the use renewable and alternative fuels, which will displace 15 percent of projected annual gasoline use; and (2) by further tightening the CAFE standards for cars and light trucks, which will bring about a further 5 percent reduction in projected gasoline use.

In April 2007, the U.S. Supreme Court ruled, in a 5-4 decision, that GHG emissions are air

The U.S. Congress is currently considering several bills that would increase car and

TABLE 1. Estimates of U.S. Light-Duty Truck Fuel Economy Targets and Projected Percentage Gains

	FUEL ECONOMY TARGETS (MILES PER GALLON)				PERCENTAGE GAINS 2008-2011
	2008	2009	2010	2011	
General Motors	21.9	22.6	22.9	23.2	5.94%
Isuzu	22.2	22.9	23.2	23.4	5.41%
Toyota	22.6	23.0	23.2	23.8	5.31%
Nissan	22.3	23.3	23.7	23.9	7.17%
Ford	22.7	23.2	23.8	23.9	5.29%
Volkswagen	23.1	23.7	24.0	24.2	4.76%
Porsche	23.0	23.7	24.0	24.2	5.22%
Daimler Chrysler	23.2	23.7	24.1	24.3	4.74%
Honda	23.3	24.0	24.4	24.6	5.58%
Hyundai	23.9	25.0	25.0	25.4	6.28%
BMW	24.5	25.1	25.5	25.8	5.31%
Subaru	25.4	26.4	26.3	26.8	5.51%
Mitsubishi	25.1	25.8	26.3	27.0	7.57%
Suzuki	25.5	26.3	26.6	27.1	6.27%

Source: National Highway Traffic Safety Administration (NHTSA), Department of Transportation, 2006

truck CAFE standards or establish federal GHG emissions standards for motor vehicles. For the first time in many years, the Senate passed a bill (S.357 “Ten in Ten”) that increasing passenger vehicle fuel economy standards by 10 mpg over a decade to 35 mpg in 2020.

1.7 SOUTH KOREA

South Korea established mandatory fuel economy standards in 2004 to replace a voluntary system. Starting in 2006 for domestic vehicles and 2009 for imports, standards are set at 34.4 CAFE-normalized mpg for vehicles with engine displacement under 1,500 cubic centimeters (cc) and 26.6 mpg for those over 1,500 cc. Credits can be earned to offset shortfalls. The program has shown encouraging progress in its early years. However, the market share of vehicles with larger engine size has been gradually increasing since recent years, while the standards remain static from 2006 and thereafter. As a result, the fleet average fuel economy in South Korea is projected to decline overtime.

This trend is shown in Table 2. The Korean Ministry of Commerce and the Ministry of Environment are discussing countermeasures such as redesigning the fuel economy standards or introducing passenger vehicle CO₂ emissions standards, according to Dr. Youngil Jeong, Director of Center for Environmentally Friendly Vehicles in Korea.

1.8 OTHER REGIONS

- In Australia, a voluntary agreement calls on the industry to reduce fleet average fuel consumption for passenger cars by 15 percent by 2010 (over a 2002 baseline). There are no specific enforcement mechanisms or non-compliance penalties identified under this agreement.
- Taiwan, China’s fuel economy standards, established before the mainland Chinese standards, are based on seven categories of engine size (measured in volume). The standards cover all gasoline and diesel passenger cars, light trucks, and commercial vehicles (<2,500 kg) and range

TABLE 2. Number of Registered Passenger Vehicles (current and projected) by Engine Size and Fleet Average Fuel Economy Levels in South Korea

CATEGORY BY ENGINE SIZE	NUMBER OF VEHICLES REGISTERED						
	2006	2007	2008	2009	2010	2011	2012
<1,500 cc	5,651,382	5,832,221	6,043,342	6,286,954	6,509,959	6,724,541	6,907,027
≥ 1,500 cc	4,744,232	5,032,690	5,322,161	5,608,959	5,901,817	6,180,446	6,450,052
	SHARE						
<1,500 cc	54.4%	53.7%	53.2%	52.8%	52.4%	52.1%	51.7%
≥ 1,500 cc	45.6%	46.3%	46.8%	47.2%	47.6%	47.9%	48.3%
	FLEET AVERAGE FUEL ECONOMY						
	30.8	30.8	30.7	30.7	30.7	30.7	30.6

Source: Youngil Jeong, Center for Environmentally Friendly Vehicles, 2007

from 16.9 mpg for vehicles with engine displacement over 4,201 cc to 36.2 mpg for vehicles less than 1,200 cc.

- Brazil put in place a fuel economy program called Escolha Certo (Right Choice) in the 1980s, which was discontinued in the early 1990s. In 1991, the country launched the National Program for the Rational Use of Oil and Gas (CONPET) to promote the efficient use of nonrenewable energy in all major economic sectors that consume oil derivatives, including transportation. A voluntary fuel economy labeling program for passenger vehicles is now under discussion as an important component of CONPET. Flex fuel vehicles, which can run on pure ethanol or gasohol (a blend of 75 percent gasoline and 25 percent ethanol—the only gasoline-based fuel sold in Brazil), now dominate new vehicle sales in Brazil. Because of its considerable use of non-gasoline fuels, Brazil's CO₂ emission from the light duty fleet is relatively low compared with other nations. For example, a recent study by Center for Clean Air Policy estimated that average CO₂ emissions from the 2004 light duty fleet are as low as 124 g/km (Krug et al 2006).

2. COMPARING VEHICLE STANDARDS AROUND THE WORLD

This section compares the passenger vehicle standards for both fuel economy and GHG emissions in Australia, California, Canada,

China, the European Union, Japan, South Korea, the United States, and Taiwan, China. Each standard's stringency is strongly influenced by the test procedure used to measure fuel economy or GHG emissions. Over the last several decades, Europe, Japan and the United States have developed unique test procedures reflecting local real world driving conditions; as a result, the same vehicle tested on the Japanese test procedure may generate a markedly different fuel economy rating or GHG emissions than the identical vehicle tested on the U.S. or European test cycle.

To allow for comparison on an equal basis, each national standard has been adjusted to common reference standards by the methodology originally developed in An and Sauer (2004). The appendix to this report outlines this methodology, while also describing how it was updated to include the new Japanese test procedure and refined to reflect a broader mix of vehicles sold in the European and Japanese markets.

2.1 OVERVIEW OF GLOBAL GHG EMISSION AND FUEL ECONOMY STANDARDS

Depending on the policy priorities in place, passenger vehicle standards are designed to either lower GHG emissions or reduce fuel consumption. GHG emission standards are intended to mitigate climate change and help achieve emission reduction goals associated with international agreements. Stated aims of fuel economy standards

include protecting consumers from rising fuel prices and price spikes, reducing oil imports, and reducing reliance on unstable oil-producing nations.

Policymakers are faced with many choices when drafting either type of standard: whether to set a single fleet-average standard or take a tiered approach, with multiple standards disaggregated according to vehicle footprint, weight, class, engine size, or interior size; which test cycle to adopt; and whether the standard should be voluntary or incorporate formal sanctions for non-compliance. Table 3 summarizes the specific policy approaches adopted by the countries included in this report.

While the regulations of the countries above display considerable diversity, common traits are evident from Table 3. The most common policy is a mandatory fuel economy standard affecting new vehicles only and measured in terms of distance traveled per volume of fuel consumed, generally under the composite CAFE test cycle or one of its subcomponents. Many of the new programs developed in recent years (e.g. California, Canada, Europe) display a preference for GHG or CO₂ emission standards. But the trend is not definitive as China recently adopted a fuel economy standard, and Canada seems poised to replace its GHG program with a fuel economy program.

TABLE 3. Fuel Economy and GHG Emissions Standards Around the World

COUNTRY/ REGION	STANDARD	MEASURE	STRUCTURE	TARGETED FLEET	TEST CYCLE	IMPLEMENTATION
Japan	Fuel	km/l	Weight-based	New	JC08	Mandatory
European Union*	CO ₂	g/km	Single standard	New	NEDC	Voluntary
China	Fuel	l/100-km	Weight-based	New	NEDC	Mandatory
Canada*	GHG (CO ₂ , CH ₄ , N ₂ O, HFCs)	5.3 Mt reduction	Vehicle class- based	In-use and new	U.S. CAFE	Voluntary
California	GHG (CO ₂ , CH ₄ , N ₂ O, HFCs)	g/mile	Vehicle class- based	New	U.S. CAFE	Mandatory
United States	Fuel	mpg	Single standard for cars and size- based standards for light trucks	New	U.S. CAFE	Mandatory
Australia	Fuel	l/100-km	Single standard	New	NEDC	Voluntary
South Korea	Fuel	km/l	Engine size-based	New	U.S. EPA City	Mandatory
Taiwan, China	Fuel	km/l	Engine size-based	New	U.S. CAFE	Mandatory

*Europe and Canada are shifting to mandatory regulatory programs.

2.2 COMPARISON OF PASSENGER VEHICLE STANDARDS

For this study, we adopted reference standards corresponding to two of the most common ways to measure and regulate fuel consumption and GHG missions from passenger vehicles: a GHG emission standard measured in terms of grams of carbon dioxide equivalent per kilometer measured on the EU NEDC cycle, and a fuel-economy based standard measured in terms of CAFE-adjusted miles per gallon.

meter adjusted to the European NEDC test cycle. Europe and Japan lead the world in reducing GHG emissions from their vehicle fleets. For most of years out to 2015, Japan's fuel efficiency targets translate to the most stringent passenger vehicle GHG emission standards in the world, with Europe as a close second. At the end of their regulatory periods, Japan's new passenger fleet CO₂ emissions are estimated to be equivalent to 125 g/km in 2015; Europe is projected to achieve 130 g/km three years earlier, in 2012.

Figure 5 compares country standards in terms of grams of CO₂-equivalent per kilo-

The U.S. new vehicle fleet is expected to remain the world's most carbon intensive for

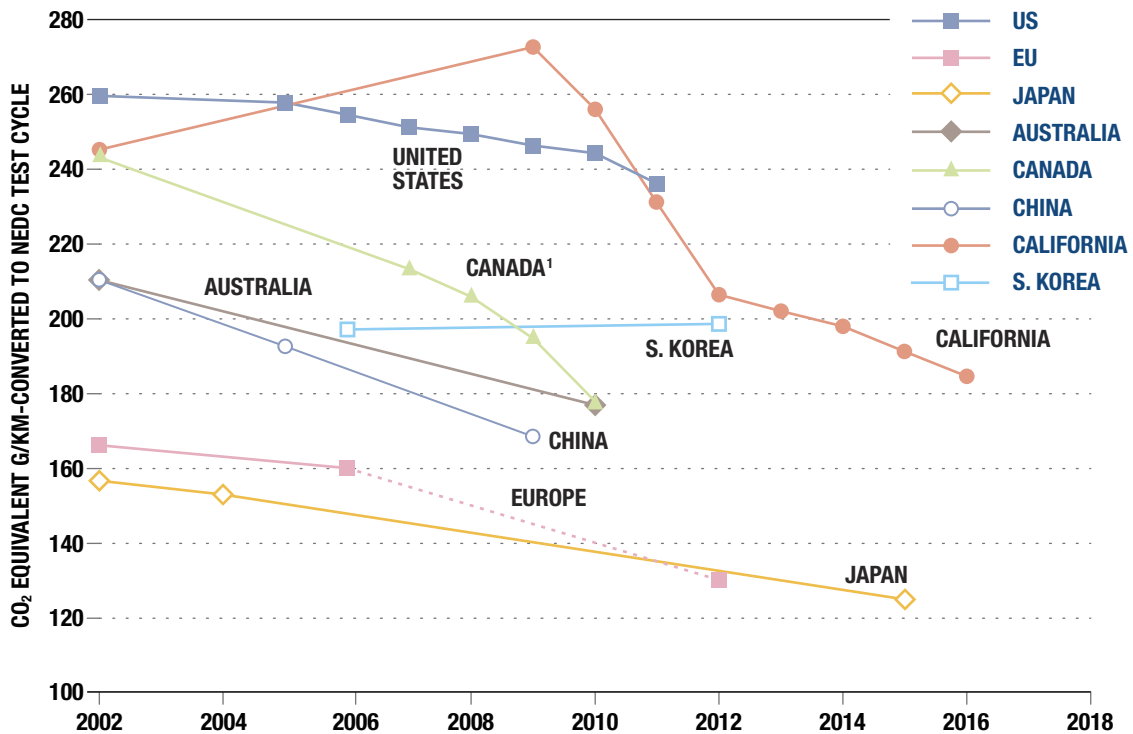


FIGURE 5. Actual and Projected GHG Emissions for New Passenger Vehicles by Country, 2002-2018.

Note: Solid lines denote actual performance or projected performance due to adopted regulations; dotted lines denote proposed standards; Values normalized to NEDC test cycle in grams of CO₂-equivalent per km.

[1] For Canada, the program includes in-use vehicles. The resulting uncertainty on new vehicle fuel economy was not quantified.

the foreseeable future, although significant improvements could be achieved should the U.S. government enact the U.S. Senate CAFE legislation or the President’s “Twenty in Ten” Executive Order. California is notable for its steep improvement in GHG emission standards, particularly in the early years of the program from 2009 to 2012. Interestingly, countries as diverse as China, Canada⁸, and Australia have adopted substantively equivalent regulations, with the carbon intensities of new vehicles sold in each country in the 2009-2010 time frame projected to be 168, 178, and 176 grams of CO₂-equivalent per kilometer, respectively.

Figure 6 shows actual and projected fleet average fuel economy from 2002 to 2018 for new vehicles in CAFE-normalized miles per gallon. In each case, we assume that a given country’s fleet exactly meets adopted or anticipated future standards. In 2006, Europe and Japan had the most stringent fuel economy standards for passenger vehicles in the world, with an estimated 40 mpg for both governments. Europe is expected to lead the world in fuel economy through at least 2015 if not longer, primarily due to the expanded use of efficient diesel engines in its light-duty vehicle fleet. The apparent discrepancy between Europe and Japan’s

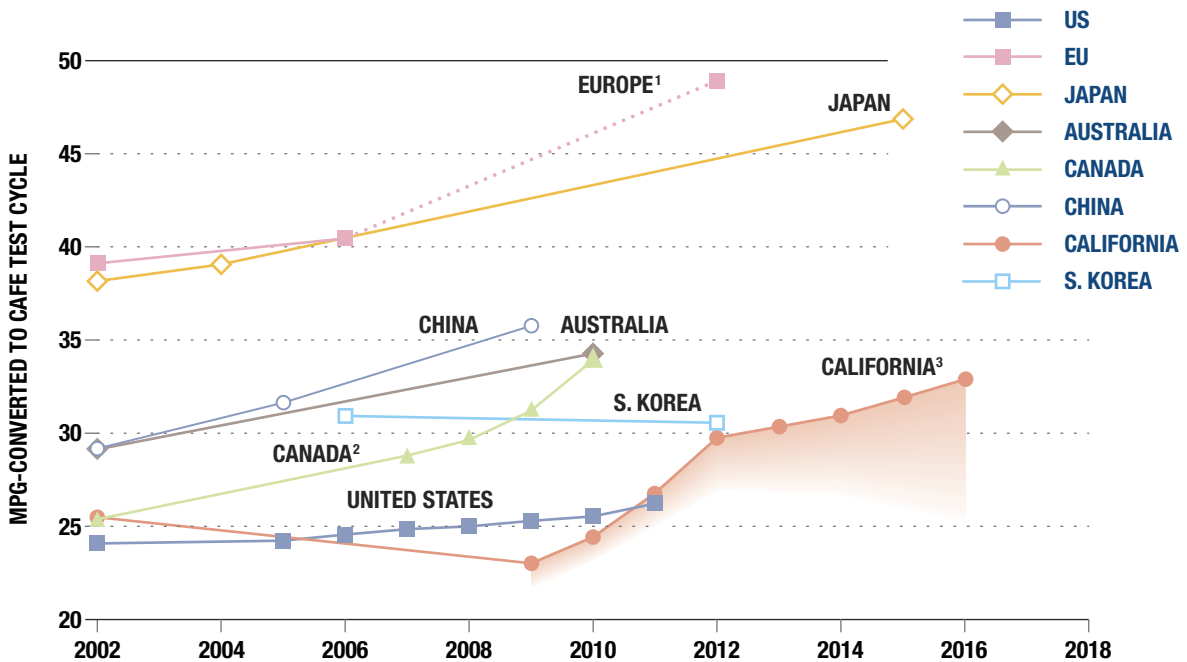


FIGURE 6. Actual and Projected Fuel Economy for New Passenger Vehicles by Country, 2002-2018.

[1] The relative stringency of Europe’s CO₂-based standards is enhanced under a fuel economy standard because diesel vehicles achieve a boost in fuel economy ratings due to the higher energy content of diesel fuel.

[2] For Canada, the program includes in-use vehicles. The resulting uncertainty of this impact on new vehicle emissions was not quantified.

[3] Shaded area under the California trend line represents the uncertain amount of non-fuel economy related GHG reductions (N₂O, CH₄, HFCs, and upstream emissions related to fuel production) that manufacturers will generate from measures such as low-leak, high efficiency air conditioners, alternative fuel vehicles, and plug-in hybrid electric vehicles.

performance on a mpg and grams of CO₂eq/km basis is due to the large numbers of diesel vehicles in the European fleet. Diesel fuel contains about 10 percent more carbon and more energy than gasoline. As a result, the fuel economy of diesel vehicles is augmented by both the energy efficiency and the greater energy content of the fuel when measured using miles per gallon. However, when considered under a GHG-basis, the higher carbon content of the fuel is taken into account and offsets the fuel-related improvement found on a mpg-basis⁹.

The shaded area under the California line in Figure 6 represents the range of uncertainty generated when those standards are converted to units of miles per gallon. There are two sources of this uncertainty: CARB's air conditioner credit, which allows automakers who have improved their A/C systems to "offset" some portion of measured exhaust emissions, and the use of biofuels in flex-fuel vehicles (FFVs) as a possible compliance mechanism. The air conditioner credit was calculated based upon data provided directly by CARB. The range of uncertainty attributable to biofuels is dependent on three variables: the sales rate of FFVs (assumed to be 50 percent in 2020); the biofuels use rate of the FFV buyers, and the relative GHG-intensity of those fuels. The uncertainty band shown in Figure 6 was determined by varying both the biofuels use rate and relative GHG savings of biofuels between 25 and 50 percent, which we have identified as

reasonable upper and lower bounds for those values; the resulting uncertainty range was then added to the A/C credit. In each case, the mileage of FFVs on E85 was assumed to be 75 percent that of the same vehicle operated on gasoline, which is consistent with the average of all FFVs in model years 2004-2007 according to the EPA test cycle.

In contrast to Europe and Japan, the United States has the most lax national standards included in our survey, a position that could change if either the President's Executive Order or the Senate Bill are adopted or enacted. As in Figure 5, China, Australia, and Canada represent intermediate cases: neither of the former two countries have changed standards since the 2004 report, but China has made substantial progress through changes in its tax code. The impact of Canada's GHG emissions standard, and the uncertainties surrounding it, were discussed above. Finally, South Korea is the only national government included in this survey where fleet average fuel economy is projected to fall through 2012, primarily due to growing sales of larger, more powerful vehicles.

Figures 5 and 6 provide an apples-to-apples comparison of passenger vehicle fuel economy and GHG emission standards in eight regions. This analysis demonstrates that, despite the substantial improvements that proposed standards would require, a large gap remains between the stringency of pas-

passenger vehicle standards in different parts of the world. A number of factors play important roles in determining vehicle fleet performance for these metrics, such as technology deployment, vehicle size and weight, engine size and horsepower, and local driving conditions. Some factors are well known. The sharp increase in sales of diesel passenger vehicles in Europe—now approximately 50 percent of new sales—has lowered CO₂ emissions from the fleet. By contrast, the increasing popularity of larger, heavier vehicles with large engines has degraded the efficiency of passenger fleets in several nations, including the U.S. and South Korea. While it is beyond the scope of this analysis to explore with analytical rigor the relationship between various factors affecting vehicle performance in different countries, this would certainly be

a useful area for further research.

One way to partially control for the impact of variations in vehicle size, weight, technology penetration, and engine performance across countries is to compare standards in terms of the absolute improvement required over each regulatory implementation period. Figure 7 shows the improvement required in passenger vehicle GHG emissions by country and/or region for each respective implementation period as measured under Europe’s NEDC test cycle.

As Figure 7 demonstrates, the largest absolute reductions are expected in countries and regions with relatively high baselines but which have recently adopted aggressive policies to reduce GHG emissions from light-

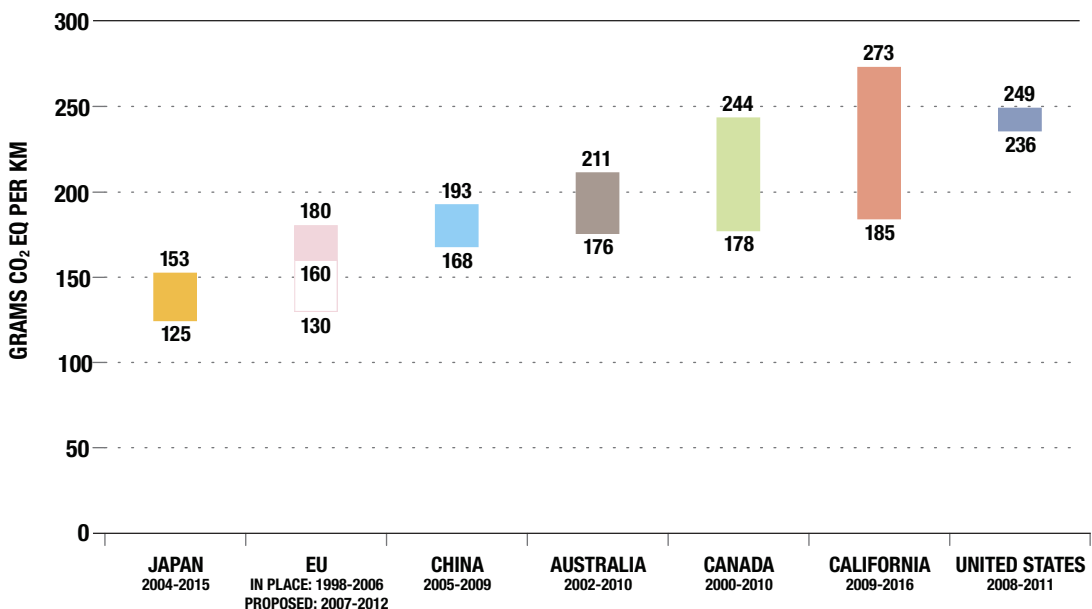


FIGURE 7. GHG Emission Reduction Associated with the Most Recent Regulations By Country

Note: Shaded bars denote in-place regulations; unshaded bars denote proposed regulations. Emissions data for Figure 7 are measured in grams CO₂-equivalent per kilometer under the NEDC test cycle. California and Canada’s programs include reductions in non-tailpipe and non-CO₂ emissions.

duty vehicles. When fully implemented, California's standards will cut average GHG emissions from new passenger vehicles by almost 90 grams of CO₂ equivalent per kilometer, by far the largest absolute reduction in our survey. Second to California is Canada's voluntary program, which, if successfully implemented, is expected to reduce GHG emissions by 66 g/km from 2000 to 2010. Other notable countries shown in Figure 7 include Japan, which is on target to reduce GHG emissions by 28 g/km off of its already low 2004 baseline, and the U.S., which, despite starting with the highest baseline, expects only meager reductions (13 g/km) under its CAFE program between 2008 and 2011.

FINDINGS AND CONCLUSIONS

A great deal of regulatory action has taken place, and will continue to evolve, as governments around the world work to reduce GHG emissions and fuel consumption from passenger vehicles. Japan and Europe are leading the way on GHG emission reductions and fuel economy improvements in their light-duty vehicle fleets. California's GHG emission regulations have now been adopted by 11 other states across the United States and received a legal boost from the U.S. Supreme Court. The EU is currently designing a legislative framework to deliver

ambitious reductions in tailpipe CO₂ emissions, partially by moving from a voluntary approach to formal standards. Fuel economy standards in the U.S. are also undergoing an important public debate. Canada is planning to issue new fuel economy regulations this fall. China has adopted new tax policies to dampen demand for larger, less efficient vehicles. The nations with the greatest motor vehicle GHG emissions and fuel consumption will be critical actors on global energy and environmental issues. Decisions on how to meet and enforce GHG and fuel economy goals will affect not only domestic affairs, but also worldwide conditions for generations to come.

APPENDIX: METHODOLOGY FOR ADJUSTING STANDARDS

Section 2 of the report compares eight government’s fuel economy and GHG emission standards. In order to correct for differences in test cycles, this report uses a methodology similar to that described in the appendix of An and Sauer (2004). This appendix summarizes that methodology and describes in detail several changes made for this report, including the following:

- The Japanese test cycle was updated to the new JC08 test cycle and two new multipliers were developed to translate Japanese vehicle standards: JC08 to U.S. CAFE and JC08 to the European NEDC test cycle.
- Additional vehicles were added to the simulation model to better capture the small-car bias of the Japanese and European fleets.
- A constant test cycle multiplier was replaced with a variable multiplier to reflect the fact that the leniency of the CAFE test cycle relative to other test cycles declines as vehicle fuel economy improves.

As Figure A-1 demonstrates, this analysis starts with regulatory fuel economy or GHG emissions standards for each of the eight regions. Each standard is converted to an adjusted fuel economy and GHG emission standard by a two-step process. First, all vehicle standards are converted to the same pair of units—CO₂ g/km and mpg. Second, multipliers are then used to normalize the stringency of each vehicle standard to the same test cycle. The original 2004 report used the European NEDC test cycle for CO₂ and the U.S. CAFE test cycle for miles per gallon, and we have continued that convention here. Of course, the U.S. fuel economy standard (CAFE-adjusted fuel economy standard) and the European CO₂ emission reduction target (NEDC-adjusted CO₂ standard) require no adjustment. A flowchart of the two-step conversion process is produced below.

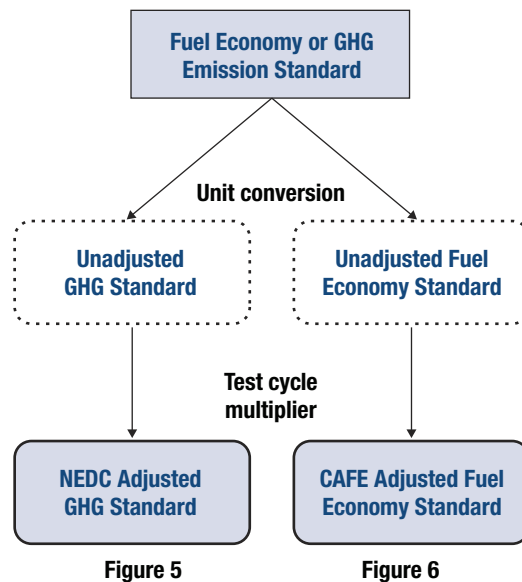


FIGURE A-1. Study Methodology

TABLE A-1. Important Unit Conversions

METRIC	STANDARD X	STANDARD Y	CONVERSION
Fuel economy	km/L	mpg	$Y = X * 2.35$
	L/100 km	mpg	$Y = 235.2/X$
	CO ₂ g/km	mpg*	$Y = 5469/X$
GHG standard	km/L	CO ₂ g/km	$Y = 2325/X$
	L/100 km	CO ₂ g/km	$Y = X * 23.2$
	mpg	CO ₂ g/km	$Y = 5469/X$

* For diesel vehicles, $Y = 6424/X$ was used to reflect the higher carbon content of diesel fuel.

In simplified mathematical form, a given country standard is converted to its CAFE-adjusted fuel economy and NEDC-adjusted GHG equivalent through the following process:

$$\text{Regulatory standard} \times \text{Unit conversion} \times \text{Test cycle multiplier} = \text{Adjusted standard}$$

Table A-1 shows the unit conversion factors used in this study. In each case, mpg refers to gasoline only.

Europe, Japan, and the United States have each developed their own test procedures to determine fuel economy and GHG emissions from new passenger vehicles. The U.S. test cycle is a combination of two cycles, one representing city driving and the other high-

way driving. Table A-2 summarizes salient characteristics from these five test cycles—the EPA city and highway test cycles, the composite CAFE cycle, the European NEDC cycle, and the JC08 test cycle. The European NEDC cycle is used to measure compliance under the EU’s voluntary CO₂ emission standards for passenger vehicles. The Japanese JC08 test cycle will be used starting in 2010 to measure progress toward Japan’s 2015 “Top Runner” fuel economy standards for light-duty passenger vehicles.

As the table indicates, significant differences exist between the five test cycles, which then translate into differences in measured fuel economy for identical vehicles. The EPA highway cycle is the shortest cycle and averages 48 miles per hour, or more than double

TABLE A-2. Summary of International Test Cycles

CYCLE	LENGTH (SECONDS)	AVERAGE SPEED (MPH)	MAX SPEED (MPH)	MAX ACCELERATION (MPH/S)
EPA Highway	766	48.2	59.9	3.3
EPA City	1375	19.5	56.7	3.3
CAFE	-----	32.4*	59.9	3.3
NEDC	1181	20.9	74.6	2.4
JC08	1204	15.2	50.7	3.8

* Based on 45/55 CAFE highway/city weighting, not test cycle length.

the average speed of the other cycles. Generally speaking, up to a point (approximately 55 mph) higher average speeds generate better fuel economy. As a result, a vehicle tested on the EPA highway test cycle (and thus under CAFE) will appear to have superior energy efficiency (i.e., a higher miles per gallon rating) compared to the same vehicle measured under the other cycles. A similar relationship is expected between the NEDC to JC08 cycles. NEDC has a higher average speed and more gentle acceleration and should result in a higher fuel economy rating compared to the same vehicles tested on the Japanese JC08.

This report, and the original 2004 report, uses the Modal Energy and Emissions Model (MEEM), a well-established model allowing for the simulation of fuel economy or CO₂ emissions across a wide variety of test cycles. Unlike the 2004 report, this study incorporates non-CO₂ greenhouse gas emissions through adjustments outside of the model. The MEEM inputs key physical and operating parameters for vehicles and engines (i.e. vehicle weight, engine size, rated power, vehicle air and tire resistance, etc.), uses those parameters to estimate engine power demand based on second-by-second speed-time traces of a given drive cycle, and converts the simulated power demand into vehicle fuel consumption and carbon dioxide emissions¹⁰. By inputting representative vehicles and modeling them

over a variety of test cycles, we have been able to estimate factors (here called multipliers to distinguish from unit-only conversion factors) by which to compare the standards of individual countries on an equal basis.

In the 2004 study, factors to convert the fuel economy of vehicles measured under European and Japanese test cycles to a CAFE equivalent were derived by modeling and comparing the fuel economies of six vehicles representative of the US fleet under the CAFE, NEDC, and Japanese test cycles. Those six vehicles included a small car, a large car, a minivan, a SUV, a pick-up truck and a crossover vehicle. Because this study includes a greater focus on the regulatory changes that have taken place recently in Europe and Japan, we have expanded the number of vehicles to include six additional makes and models of small cars which are more representative of the European and Japanese fleets. Particular effort was made to include vehicles sold internationally and in the same general fuel economy range of current and future standards in Europe and Japan.

Table A-3 shows the vehicles included in our analysis, their mpg fuel economies as estimated by the MEEM model under the NEDC, CAFE, and JC08 test cycles, and the multiplier required to normalize the results between test cycles.

As the table indicates, the expectation that testing under the CAFE cycle will result in higher fuel economies than under the NEDC and JC08 cycles is supported by the modeling results. The simple (non-sales weighted) average fuel economy gap between the JC08 and CAFE cycles is around 30% (i.e. a CAFE-JC08 multiplier of 1.29). The gap between JC08 and the European NEDC cycle is estimated to be on the order of 15%, and the gap between CAFE and NEDC is about 12%. At the same time, Table A-3 suggests that the discrepancy between test cycles is not constant, but tends to rise and fall depending on vehicle fuel economy. For example, the smallest difference between the CAFE-JC08 test cycles is 1.17, which belongs to the most efficient vehicle, the 42 mpg Toyota Yaris. Consis-

tent with the trend, the highest ratio of 1.39 belongs to the least efficient vehicle, the 19 mpg Chevrolet Silverado.

There is a technical basis for the modeled relationship between vehicle fuel economy and differences in test cycle results. In general, vehicles with higher fuel economies have smaller engines that operate more frequently under higher efficiency conditions. As a result, the fuel economy of those vehicles is less sensitive to driving conditions – thus the smaller test cycle multiplier. Many advanced engines not included in this report, notably hybrid electric drivetrains, also perform better than conventional internal combustion engines under the stop-and-go driving conditions simulated by the NEDC and JC08 test cycles.

TABLE A-3. Simulation Results for Gasoline Vehicle Fuel Economy Ratings Under Various Test Cycles

TYPE	MAKE	MODEL	TEST CYCLE FE (MPG)			TEST CYCLE MULTIPLIER		
			NEDC	CAFE	JC08	NEDC-JC08	CAFE-JC08	CAFE-NEDC
Small Car	Ford	Focus	26.0	29.8	22.9	1.14	1.30	1.15
	Toyota	Corolla	32.4	34.8	27.6	1.17	1.26	1.08
	Toyota	Yaris	40.6	42.2	36.1	1.12	1.17	1.04
	Honda	Fit	36.0	40.1	31.8	1.13	1.26	1.11
	Hyundai	Accent	35.1	39.0	32.1	1.09	1.21	1.11
	Kia	Rio	35.4	39.1	32.2	1.10	1.21	1.10
	Daewoo	Aveo	31.2	35.5	26.1	1.19	1.36	1.14
Large Car	Toyota	Camry	24.7	26.6	21.5	1.15	1.24	1.08
Minivan	Dodge	Grand Caravan	20.5	23.9	17.2	1.19	1.39	1.17
SUV	Ford	Explorer	17.6	20.2	14.6	1.20	1.38	1.15
Pickup	Chevrolet	Silverado	15.9	18.8	13.5	1.18	1.39	1.18
Crossover	Saturn	Vue	23.0	26.3	19.8	1.16	1.33	1.14
Simple Average						1.15	1.29	1.12

Figure A-2 plots vehicle fuel economy against the MEEM test cycle ratio, or test cycle multiplier, for the CAFE-JC08 test cycles. Also shown on the graph is the approximate location of the 2004 Japanese passenger vehicle fleet average, and the 2015 standard in km/L (solid vertical lines). The numbers located to the right of the right axis indicate the CAFE adjusted fuel economy of the Japanese passenger fleet emission standards at different test cycle multipliers¹¹. The logarithmic correlation of the vehicle models is shown as a dotted line ($R^2 = 0.75$) extrapolated out two units for illustrative purposes.

Figure A-2 clearly shows the inverse relationship between the CAFE-JC08 multiplier and fuel economy, with more fuel efficient vehicles performing relatively better on the JC08 cycle than less efficient models. For vehicles representative of the 2015 standard

of 16.8 km/L, the multiplier is in the range of 1.19, corresponding to a CAFE adjusted standard of 47 mpg. This value compares to an unadjusted (multiplier of 1.0) fuel economy of 40 mpg, and 55 mpg for a conversion factor of 1.4, corresponding to the least fuel efficient vehicles included in this report.

The finding that the CAFE-JC08 test cycle multiplier falls as vehicles become more fuel efficient means that care must be taken when adjusting a fleet average fuel economy to a different cycle: as fuel economy improves, the multiplier changes, so using a constant multiplier over time will introduce bias into the analysis. Table A-4 shows the four equations used to estimate the test cycle multipliers for this study.

As the table indicates, the sensitivity of a given multiplier to increasing fuel economy

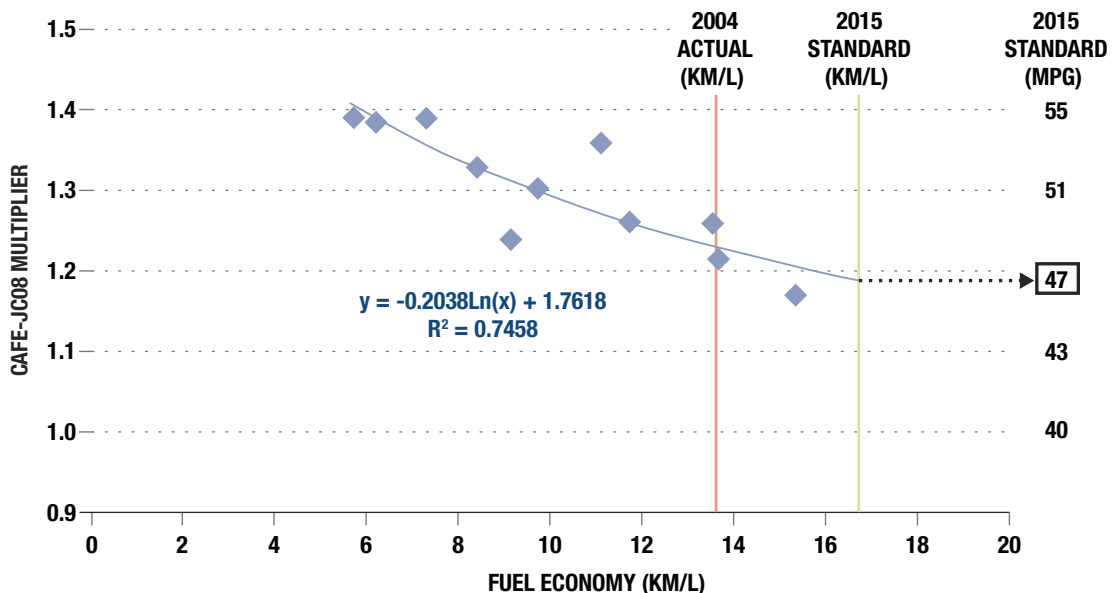


FIGURE A-2. Modeled Fuel Economy, CAFE-JC08 Multiplier, and CAFE Adjusted 2015 Japanese Fuel Economy Standard

TABLE A-4. Driving Test Cycle Multiplier Equations

TEST CYCLE CONVERSION	MULTIPLIER	CORRELATION
CAFE-JC08	$-0.2038 \times \ln(\text{JC08}) + 1.7618$	0.7458
NEDC-JC08	$-0.0841 \times \ln(\text{JC08}) + 1.3464$	0.5607
NEDC-CAFE	$0.0816 \times \ln(\text{CAFE}) + 0.6243$	0.5622
CAFE-NEDC	$0.1021 \times \ln(\text{NEDC}) + 0.5787$	0.5800

Units: JC08 = km/L; CAFE =mpg; NEDC = g/km. The multiplier itself is dimensionless.

varies between different test cycles. The largest sensitivity is between the JC08 and CAFE test cycles, which is more than double that the NEDC-CAFE multiplier. This is perhaps not surprising given that, as summarized in Table A-1, the JC08 and composite CAFE test cycles are the most divergent in terms of average test speed. Furthermore, the sensitivity of test cycle multipliers to changes in fuel economy suggests that each cycle-to-cycle conversion must be conducted independently.

Figure A-3 shows how the current and projected fuel economy for new vehicles in Japan from 2005 to 2015 was adjusted to units of CAFE mpg in this report, a methodology that was adopted for all other countries and test cycles. Three lines are shown. The solid line represents the fuel economy adjusted year by year using the log relationship derived in Figure A-2. The dotted red line represents the adjusted fuel economy based on a static multiplier equal to the most fuel efficient vehicle in our sample. The third, the dotted green line, represents the adjusted fuel economy based on a static multiplier factor derived from the least fuel efficient vehicle in our sample. The approximate multiplier factor used in each time period is provided in the boxes next to the appropriate line.

Several conclusions can be drawn. First, Figure A-3 demonstrates that Japan’s fleet

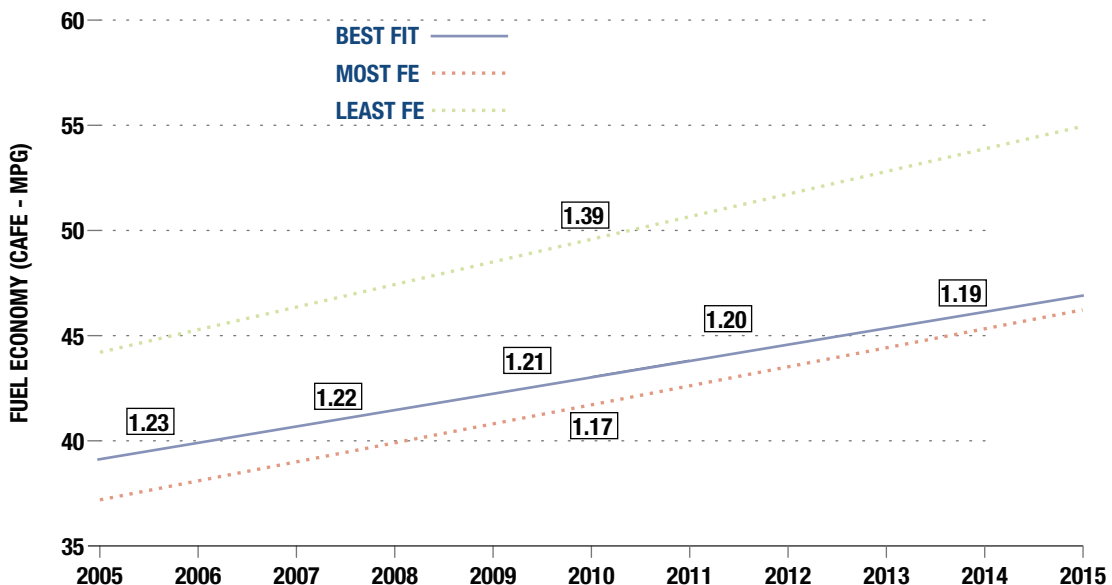


FIGURE A-3. CAFE Adjusted Projected New Vehicle Average Fuel Economy in Japan, 2005-2015

* Boxed numbers denote test cycle multiplier.

was already relatively fuel efficient in 2005, with a test cycle multiplier close to the lower bound set by the most fuel-efficient vehicle included in this report, the Toyota Yaris. In addition, the figure shows the slight “bend” that occurs in the best fit line as the fleet average fuel efficiency improves further over time. Finally, Figure A-3 illustrates the conservative nature of our methodology, with the adjusted standard value of 47 mpg presented in the main body of this report falling well on the low side of the 46 to 55 mpg range delineating by the most and least fuel-efficient vehicles included in our survey.

REFERENCES

- Agency for Natural Resources and Energy (ANRE) and the Ministry of Land, Infrastructure and Transport (MLIT). 2007.** *Concerning Revisions of Evaluation Standards for Automobile Manufacturers with Regard to Energy Efficiency: Joint Final Report of the Automobile Evaluation Standards Subcommittee of the Advisory Committee for Natural Resources and Energy and the Automobile Fuel Efficiency Standards Subcommittee of the Council for Transport Policy.* February. (Japanese)
- Agency for Natural Resources and Energy (ANRE) and the Ministry of Land, Infrastructure and Transport (MLIT). 2006.** *Concerning Revisions of Evaluation Standards for Automobile Manufacturers with Regard to Energy Efficiency: Joint Interim Report of the Automobile Evaluation Standards Subcommittee of the Advisory Committee for Natural Resources and Energy and the Automobile Fuel Efficiency Standards Subcommittee of the Council for Transport Policy.* December. (Japanese)
- An F. and Rousseau A. 2001.** SAE Paper No. 2001-01-0954, SAE Special Publication (SP-1607) on Advanced Hybrid Vehicle Powertrains. Society of Automotive Engineers, Warrendale, PA.
- An F. and Sauer A. 2004.** *Comparison of Passenger Vehicle Fuel Economy and Greenhouse Gas Emission Standards Around the World.*
- Automotive News: Global Market Data Book.** Issue: June 25, 2007, pp. 8.
- Barth, M., An F., Younglove T., Scora G., Wensel T., and Ross M. 2000.** *NCHRP Project 25-11: Development of a Comprehensive Modal Emissions Model—The Final Report.* Transportation Research Board, National Academy of Science, Washington, DC.
- Canada Revenue Agency. 2007.** Web access: <http://www.cra-arc.gc.ca/agency/budget/2007/excise-e.html>.
- California Air Resources Board (CARB). 2004A.** *Staff Proposal Regarding the Maximum Feasible and Cost-Effective Reduction of Greenhouse Gas Emissions from Motor Vehicles.*
- CARB. 2004B.** *Climate Change Emission Control Regulations.* Web access: http://arb.ca.gov/cc/factsheets/cc_newfs.pdf.
- California Code of Regulations. 2004.** Title 13, Section 1961.1.
- China Automotive Technology and Research Center (draft). 2007.** (Chinese)
- Code of Federal Register (CFR). 2006.** *Average Fuel Economy Standards for Light Trucks, Model Years 2008-2011.* National Highway Traffic Safety Administration, 49 CFR Parts 523, 533, 537, Docket No. 2006-24306, NIN 2127-AJ61.
- CFR. 2005.** *29 CFR Part 533, Table 7, Light Trucks, Average Fuel Economy; Model Years 2008-2011; Proposed Rules.*
- Commission of the European Communities. 2007.** *Communication from the Commission to the Council and the European Parliament: Results of the Review of The Community Strategy To Reduce CO2 Emissions from Passenger Cars and Light-Commercial Vehicles.*
- Cornell University News Service, Susan Lang. 2005.** *Cornell Ecologist's Study Finds That Producing Ethanol and Bio-Diesel from Corn and Other Crops Is Not Worth The Energy.* Web access: <http://www.news.cornell.edu/stories/July05/ethanol.toocostly.ssl.html>.
- Japanese Automobile Manufacturers Association (JAMA). 2007.** *Taxes and Automobiles (Japanese).* Web access: http://www.jama.or.jp/tax/tax_system/tax_system_3t1.html. (Japanese)
- Krug, T., et al. 2006.** *Greenhouse Gas Mitigation in Brazil: Scenarios and Opportunities through*

2025. Center for Clean Air Policy, November 2006.

Lutsey, Nicholas. 2001. *Impact of Canada's Voluntary Agreement on Greenhouse Gas Emissions from Light Duty Vehicles*. Institute of Transportation Studies (University of California, Davis) Paper RR-06-02, 2006.

Memorandum of Understanding Between the Government of Canada and the Canadian Automotive Industry Respecting Automobile Greenhouse Gas Emissions. 2005.

MLIT. 2006. *2006 Survey of Automobile Fuel Economy*. Web access: <http://www.mlit.go.jp/jidosha/nenpi/nenpilist/nenpilist0603.pdf>. (Japanese)

President Bush's Executive Order "Twenty in Ten". 2007. Web access: <http://www.whitehouse.gov/stateoftheunion/2007/initiatives/energy.html>.

Senate Bill 357, 2007.

Transport Canada. 2007. Web access: <http://ecoaction.gc.ca/ecotransport/ecoauto-eng.cfm>.

U.S. Environmental Protection Agency (EPA). 2004. *Light-Duty Automotive Technology and Fuel Economy Trends: 1975 through 2004*.

U.S. National Highway Traffic Safety Administration (NHTSA) and Department of Transportation (DOT). 2006.

ENDNOTES

¹ Starting as an option in model year (MY) 2008 and required in MY2011, the fleet average standards in light truck CAFE will change to a size-based, continuous function standard. See section 1.6 for more detail.

² Because Japanese vehicles are calibrated to slower driving conditions, increases in test speeds are claimed to increase fuel consumption, in contrast to results for vehicles sold in the U.S. market.

³ The ACEA included BMW, DaimlerChrysler, Fiat, Ford, GM, Porsche, PSA Peugeot Citroen, Renault, and VW Group. The Korean Automobile Manufacturers Association (KAMA) includes Daewoo, Hyundai, Kia, and Sangyong. The Japanese Automobile Manufacturers Association (JAMA) includes Diahatsu, Honda, Isuzu, Mazda, Mitsubishi, Nissan, Subaru, Suzuki, Toyota.

⁴ AB 1493, also known as the California Vehicle Global Warming Law, was signed into law by Governor Gray Davis on July 22, 2002.

⁵ The industry-standard mobile air conditioner refrigerant HFC-134a has a Global Warming Potential of 1300; alternative refrigerants such as HFC 152a and CO₂ have GWPs of 120 and 1, respectively (CARB 2004).

⁶ Daimler and Chrysler merged in 1998. On May 14, 2007, Daimler sold Chrysler to Cerberus Capital Management. The data in Table 1 are drawn from the final CAFE rule in 2006, when the transaction had not occurred. Later in this report, Chrysler will be split out from Daimler.

⁷ Choosing to set reductions goals from a baseline of projected emissions rather than a firm baseline, such as the year in which the policy was adopted or a point in the past, can limit the total expected emission reductions substantially.

⁸ The Canada GHG emissions trend shown in Figure 5 is based on the 2005 Memorandum of Understanding between the Canadian government and the auto manufacturers to achieve a 5.3 Mt GHG emissions reduction by 2010. The Canadian program cannot be forecast with precision since the MOU covers all GHG emissions from new and existing passenger vehicles. The actual reductions in GHG emissions from new vehicles, and the improvements in fuel economy shown in Figure 6, may be lower depending on the reductions achieved by the means discussed in the Section 1.4.

⁹ Historically, diesels have required some tradeoff between fuel economy and pollutant emissions. Diesel vehicles sold in Europe continue to have higher emissions of nitrogen oxide and particulate matter, which can negatively impact both local air quality and climate change. Stricter emissions standards have thus far played a significant role in restricting the market share of diesels in light-duty fleets in the U.S. and Japan. However, new emissions control technologies are expected to allow diesels to meet the strictest passenger vehicle standards currently in place.

¹⁰ For further information regarding the MEEM model, see Barth, M., et. al, 2000; An and Rousseau. 2001.

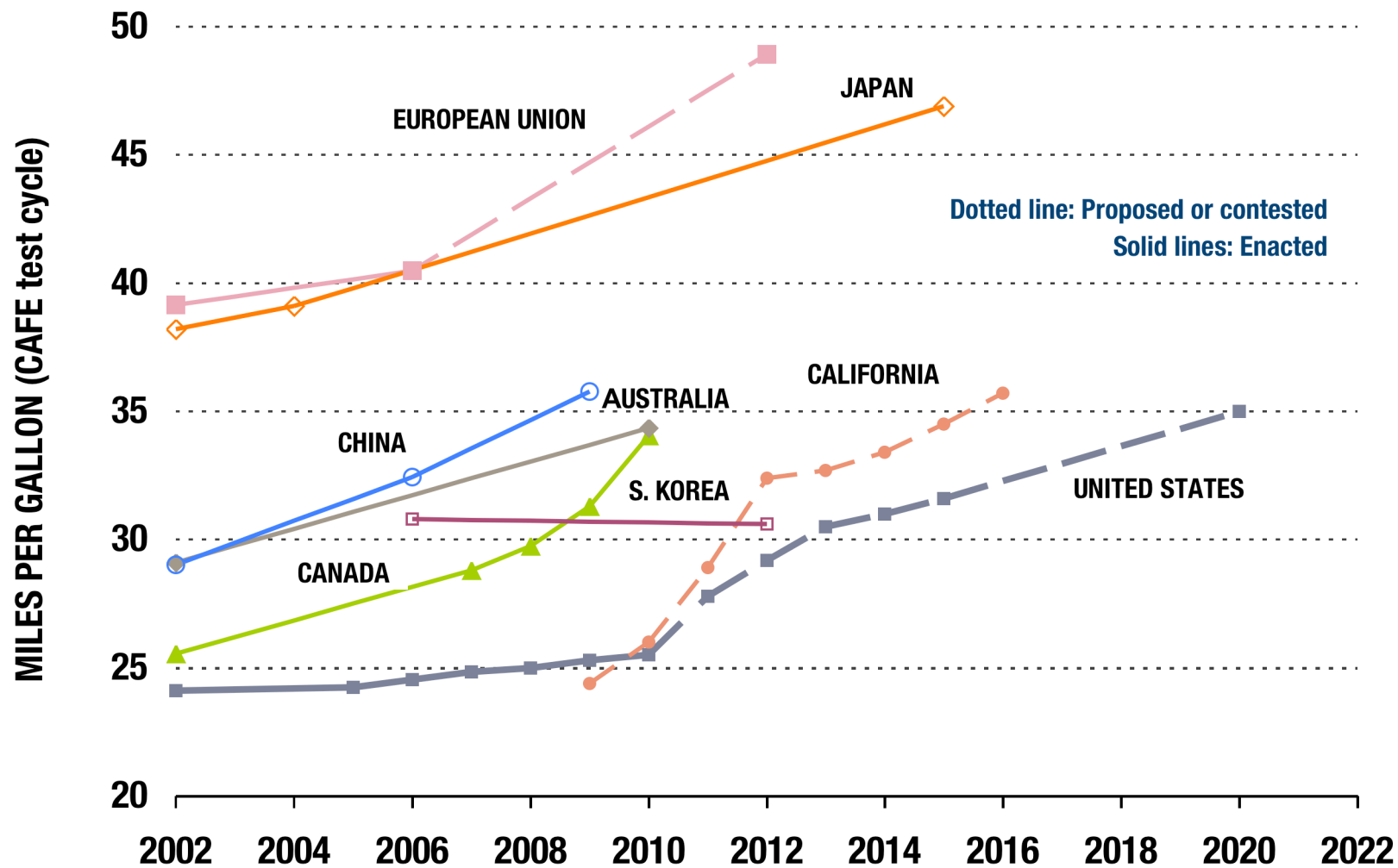
¹¹ Note that mpg equivalent numbers at the far right of the graph are specific to the 2015 standard. As such, the CAFE equivalent for the 2004 fleet average (39 mpg) cannot be read directly off this graph.



Washington DC
1225 I St., Suite 1000, NW,
Washington, DC 20005
United States of America
phone: +1 (202) 347-8932

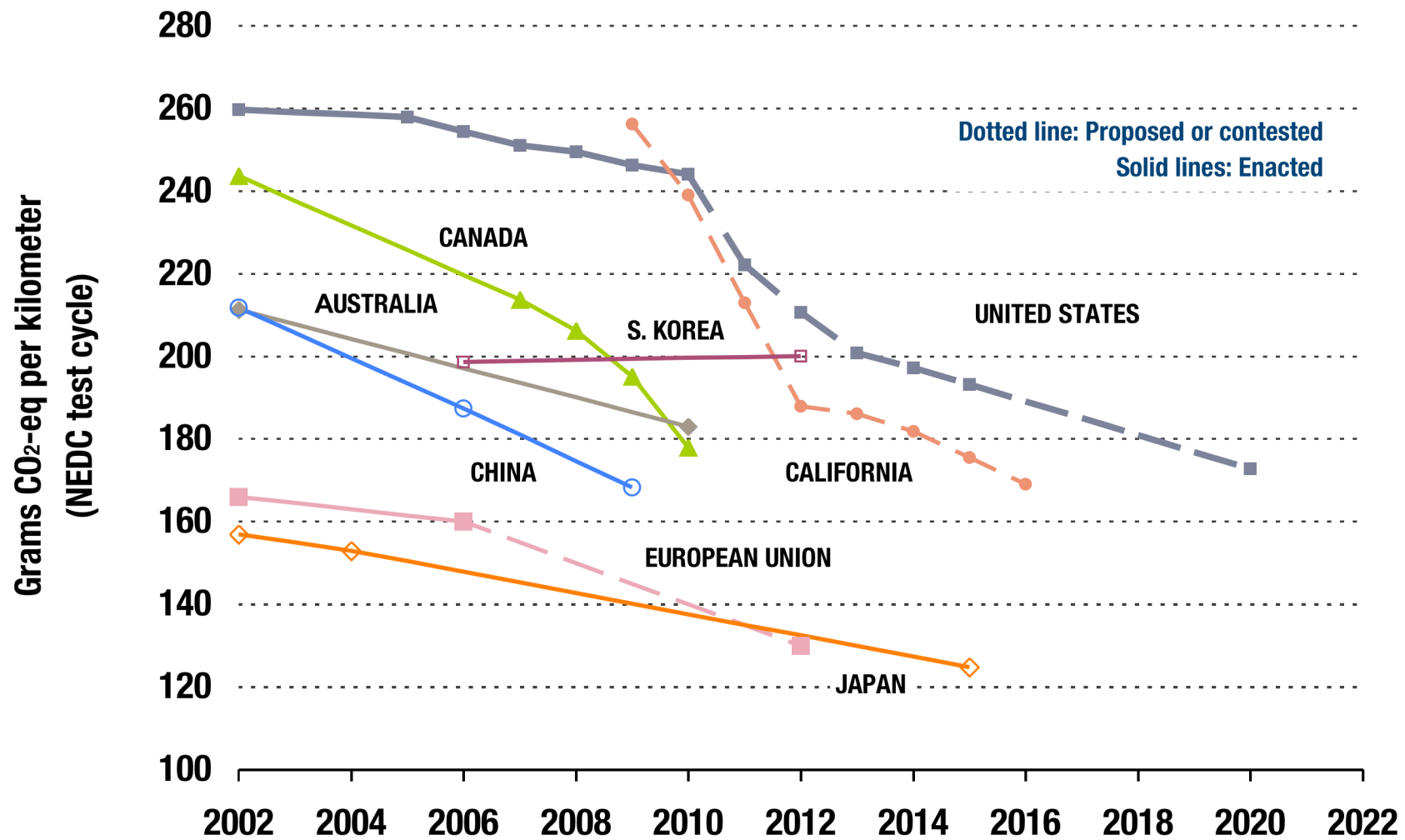
San Francisco
1 Hallidie Plaza, Suite 503
San Francisco, California 94102
United States of America
phone: +1 (415) 399-9019

Actual and Projected Fuel Economy for New Passenger Vehicles by Country/Region, 2002-2022



Source: *Passenger Vehicle Greenhouse Gas and Fuel Economy Standards: A Global Update*, ICCT. 7 August 2008 update.

Actual and Projected GHG Emissions for New Passenger Vehicles by Country/Region, 2002-2022



Source: *Passenger Vehicle Greenhouse Gas and Fuel Economy Standards: A Global Update*, ICCT. 7 August 2008 update.

example, this is the case for water. This is consistent with the negative slope dP/dT of the crystal–liquid transition line for water, that implies that $\Delta S/\Delta V < 0$ since, according to the Clausius–Clapeyron equation, $dP/dT = \Delta S/\Delta V$, where ΔS and ΔV are the entropy and volume differences between the two coexisting phases.

For our system, we expect the reverse: $(\partial V/\partial T)_P > 0$ so $(\partial S/\partial V)_T > 0$, consistent with the positive slope of the LDL–HDL transition line dP/dT (see Fig. 2b). We confirm that $(\partial S/\partial V)_T > 0$ by explicitly calculating S for our system by means of thermodynamic integration.

Our results show that the presence of two critical points and the occurrence of the density anomaly are not necessarily related, suggesting that we might seek experimental evidence of a liquid–liquid phase transition in systems with no density anomaly. In particular, a second critical point may also exist in liquid metals that can be described by soft-core potentials. Thus the class of experimental systems displaying a second critical point may be broader than previously hypothesized. □

Received 6 October; accepted 18 December 2000.

1. Katayama, Y. *et al.* A first-order liquid–liquid phase transition in phosphorus. *Nature* **403**, 170–173 (2000).
2. Debenedetti, P. G. *Metastable Liquids: Concepts and Principles* (Princeton Univ. Press, Princeton, 1998).
3. Wilding, M. C., McMillan, P. F. & Navrotsky, A. The thermodynamic nature of a phase transition in yttria–alumina liquids. *J. Cryst. Noncryst. Solids* (in the press).
4. Brazhkin, V. V., Popova, S. V. & Voloshin, R. N. High-pressure transformations in simple melts. *High Pressure Res.* **15**, 267–305 (1997).
5. Brazhkin, V. V., Gromnitskaya, E. L., Stalgorova, O. V. & Lyapin, A. G. Elastic softening of amorphous H₂O network prior to the HDA–LDA transition in amorphous state. *Rev. High Pressure Sci. Technol.* **7**, 1129–1131 (1998).
6. Mishima, O. Liquid–liquid critical point in heavy water. *Phys. Rev. Lett.* **85**, 334–336 (2000).
7. Bellissent-Funel, M.-C. Evidence of a possible liquid–liquid phase transition in super-cooled water by neutron diffraction. *Nuovo Cimento* **20D**, 2107–2122 (1998).
8. Soper, A. K. & Ricci, M. A. Structures of high-density and low-density water. *Phys. Rev. Lett.* **84**, 2881–2884 (2000).
9. Lacks, D. J. First-order amorphous–amorphous transformation in silica. *Phys. Rev. Lett.* **84**, 4629–4632 (2000).
10. van Thiel, M. & Ree, F. H. High-pressure liquid–liquid phase change in carbon. *Phys. Rev. B* **48**, 3591–3599 (1993).
11. Poole, P. H., Sciortino, F., Essmann, U. & Stanley, H. E. Phase behavior of metastable water. *Nature* **360**, 324–328 (1992).
12. Glosli, J. N. & Ree, F. H. Liquid–liquid phase transformation in carbon. *Phys. Rev. Lett.* **82**, 4659–4662 (1999).
13. Saika-Voivod, I., Sciortino, F. & Poole, P. H. Computer simulations of liquid silica: Equation of state and liquid–liquid phase transition. *Phys. Rev. E* **63**, 011202-1–011202-9 (2001).
14. Mon, K. K., Ashcroft, M. W. & Chester, G. V. Core polarization and the structure of simple metals. *Phys. Rev. B* **19**, 5103–5118 (1979).
15. Stell, G. & Hemmer, P. C. Phase transition due to softness of the potential core. *J. Chem. Phys.* **56**, 4274–4286 (1972).
16. Silbert, M. & Young, W. H. Liquid metals with structure factor shoulders. *Phys. Lett.* **58A**, 469–470 (1976).
17. Levesque, D. & Weis, J. J. Structure factor of a system with shouldered hard sphere potential. *Phys. Lett.* **60A**, 473–474 (1977).
18. Kincaid, J. M. & Stell, G. Structure factor of a one-dimensional shouldered hard-sphere fluid. *Phys. Lett.* **65A**, 131–134 (1978).
19. Cummings, P. T. & Stell, G. Mean spherical approximation for a model liquid metal potential. *Mol. Phys.* **43**, 1267–1291 (1981).
20. Velasco, E., Mederos, L., Navascués, G., Hemmer, P. C. & Stell, G. Complex phase behavior induced by repulsive interactions. *Phys. Rev. Lett.* **85**, 122–125 (2000).
21. Voronel, A., Paperno, I., Rabinovich, S. & Lapina, E. New critical point at the vicinity of freezing temperature of K₂Cs. *Phys. Rev. Lett.* **50**, 247–249 (1983).
22. Behrens, S. H., Christl, D. I., Immerzael, R., Schurtenberger, P. & Borkovec, M. Charging and aggregation properties of carboxyl latex particles: Experiments versus DLVO theory. *Langmuir* **16**, 2566–2575 (2000).
23. Debenedetti, P. G., Raghavan, V. S. & Borick, S. S. Spinodal curve of some supercooled liquids. *J. Phys. Chem.* **95**, 4540–4551 (1991).
24. Sadr-Lahijany, M. R., Scala, A., Buldyrev, S. V. & Stanley, H. E. Liquid state anomalies for the Stell–Hemmer core-softened potential. *Phys. Rev. Lett.* **81**, 4895–4898 (1998).
25. Jagla, E. A. Core-softened potentials and the anomalous properties of water. *J. Chem. Phys.* **111**, 8980–8986 (1999).
26. Stillinger, F. H. & Head-Gordon, T. Perturbational view of inherent structures in water. *Phys. Rev. E* **47**, 2484–2490 (1993).
27. Caccamo, C. Integral equation theory description of phase equilibria in classical fluids. *Phys. Rep.* **274**, 1–105 (1996).
28. Berendsen, H. J. C., Postma, J. P. M., van Gunsteren, W. F., DiNola, A. & Haak, J. R. Molecular dynamics with coupling to an external bath. *J. Chem. Phys.* **81**, 3684–3690 (1984).
29. Rein ten Wolde, P. & Frenkel, D. Enhancement of protein crystal nucleation by critical density fluctuations. *Science* **277**, 1975–1978 (1997).
30. Hagen, M. H. J., Meijer, E. J., Mooij, G. C. A. M., Frenkel, D. & Lekkerkerker, H. N. W. Does C₆₀ have a liquid phase? *Nature* **365**, 425–426 (1993).

Acknowledgements

We wish to thank L. A. N. Amaral, P. V. Giaquinta, E. La Nave, T. Lopez Ciudad, S. Mossa, G. Pellicane, A. Scala, F. W. Starr, J. Teixeira, and, in particular, F. Sciortino for helpful suggestions and discussions. We thank the NSF and the CNR (Italy) for partial support.

Correspondence and requests for materials should be addressed to G.F. (e-mail: franzese@argento.bu.edu).

Strong radiative heating due to the mixing state of black carbon in atmospheric aerosols

Mark Z. Jacobson

Department of Civil & Environmental Engineering, Stanford University, Stanford, California 94305-4020, USA

Aerosols affect the Earth’s temperature and climate by altering the radiative properties of the atmosphere. A large positive component of this radiative forcing from aerosols is due to black carbon—soot—that is released from the burning of fossil fuel and biomass, and, to a lesser extent, natural fires, but the exact forcing is affected by how black carbon is mixed with other aerosol constituents. From studies of aerosol radiative forcing, it is known that black carbon can exist in one of several possible mixing states; distinct from other aerosol particles (externally mixed^{1–7}) or incorporated within them (internally mixed^{1,3,7}), or a black-carbon core could be surrounded by a well mixed shell⁷. But so far it has been assumed that aerosols exist predominantly as an external mixture. Here I simulate the evolution of the chemical composition of aerosols, finding that the mixing state and direct forcing of the black-carbon component approach those of an internal mixture, largely due to coagulation and growth of aerosol particles. This finding implies a higher positive forcing from black carbon than previously thought, suggesting that the warming effect from black carbon may nearly balance the net cooling effect of other anthropogenic aerosol constituents. The magnitude of the direct radiative forcing from black carbon itself exceeds that due to CH₄, suggesting that black carbon may be the second most important component of global warming after CO₂ in terms of direct forcing.

This work was motivated by studies^{1–7} that found different black-carbon (BC) forcings when different BC mixing states were assumed. In one study⁷ the mixing state was found to affect the BC global direct forcing by a factor of 2.9 (0.27 W m⁻² for an external mixture, +0.54 W m⁻² for BC as a coated core, and +0.78 W m⁻² for BC as well mixed internally). Because BC is a solid and cannot physically be well mixed in a particle, the third case was discarded as unrealistic, and it was suggested that the real forcing by BC probably fell between that from an external mixture and that from a coated core. Here I report simulations that were performed among multiple aerosol size distributions to estimate which of these two treatments, if either, better approximates BC forcing in the real atmosphere.

The global model that I used was GATOR-GCMM, which treated gas, aerosol, radiative, meteorological and transport processes (see Supplementary Information for details). Aerosol processes included emissions, homogeneous nucleation, condensation, dissolution, coagulation, chemical equilibrium, transport, sedimentation, dry deposition, and rainout among 18 aerosol size distributions, 17 size bins per distribution, one number concentration, and an average of seven mole concentrations per bin per distribution. The 18 distributions (Supplementary Information) consisted of four ‘primary’ size distributions (sea spray (A), soil (B), black carbon (E1) and organic

matter (F)) into which emissions occurred, one 'primary' distribution (sulphate (D)) into which homogeneous nucleation occurred, two additional BC distributions (E2 and E3) into which primary BC grew, 10 'binary' distributions (AB, AD, AE, AF, BD, BE, BF, DE, DF and EF) that resulted from heterocoagulation among A, B, D, E1, E2, E3 and F distributions, and a completely mixed distribution (MX) that resulted from all higher heterocoagulation interactions. Distributions A, B, D, E1 and F were initialized, and the aerosol population was relaxed with continuous emissions that were allocated to distributions A, B, E1 and F, homogeneous nucleation that was allocated to distribution D, and coagulation, growth, chemistry, transport and deposition among all distributions until a near global-scale steady state was obtained.

Figure 1 shows the variation with time of the globally averaged mass per cent of BC-containing particles that obtained a non-BC coating of various mass percentages when (simulation a; Fig. 1a) coagulation alone and when (simulation b; Fig. 1b) coagulation, condensation, dissolution and equilibrium water uptake were the only forms of internal mixing. In the simulation shown in Fig. 1a, coagulation caused about 35% by mass of initial and emitted externally mixed BC to obtain a coating > 20% by mass within five days. In the simulation shown in Fig. 1b, growth processes and coagulation together caused 63% of BC by mass to obtain a coating

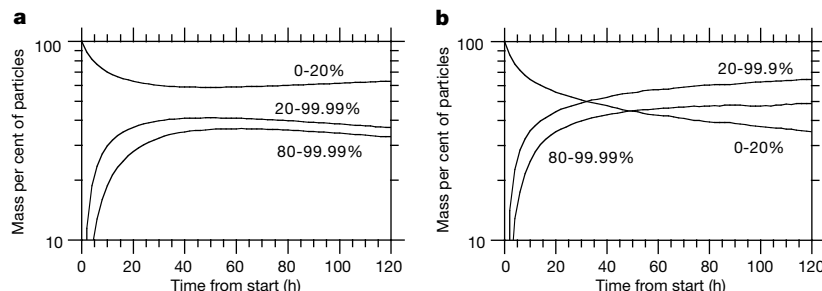


Figure 1 Coating of BC-containing particles over time. The figure shows the time-variation of the globally averaged mass per cent of BC-containing particles that obtain a non-BC coating of 0–20%, 20–99% and 80–99% by mass when (a) coagulation alone and (b) coagulation, condensation, dissolution, and equilibrium water uptake affect internal mixing. In both cases, emissions, homogeneous nucleation, transport, dry

> 20% by mass within five days. The difference indicates that growth and coagulation caused BC internal mixing at similar rates.

Coagulation has been calculated to affect the number and volume concentrations of particles primarily less than 0.2- μm diameter in urban air⁸. In that study, only one size distribution was considered. When multiple distributions are treated, the net effect of coagulation on the total number and volume concentrations of particles, summed over all distributions, is the same as that over one distribution if the initial number and volume concentrations are the same in both cases. The difference is that, in the multiple-distribution case, coagulation moves components among distributions (heterocoagulation), having a notable effect on particle composition not evident when only one distribution is simulated. Figure 2 shows such an effect. It shows the time-varying globally averaged mass per cent of BC in different distributions from the Fig. 1b simulation. Initially, all BC was externally mixed in distribution E1. BC then self-coagulated and grew into BC distributions E2 and E3 and heterocoagulated with sulphate, organic matter, soil and/or sea spray to form binary and higher mixtures. The difference between 100% and E1+E2+E3 in Fig. 2 represents the mass fraction of BC (50%) that heterocoagulated. Since this fraction is large, heterocoagulation appears to be important in the global-scale internal mixing of BC.

The mixing results that I report here seem to be consistent with

deposition, sedimentation, and rainout of aerosols were also treated. Initially, 100% by mass of BC-containing particles were externally mixed (containing 0% coating by mass). The percentages in the figure were obtained by summing, over all BC-containing distributions, the mass of BC-containing particles of a given shell mass fraction and normalizing by the total mass of BC-containing particles.

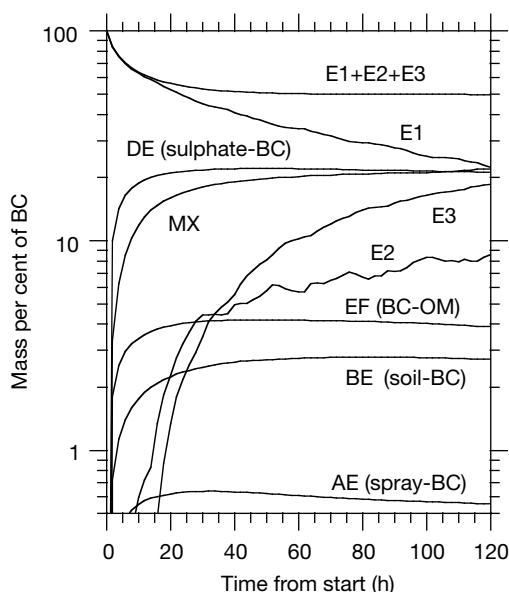


Figure 2 Shift of BC among particle distributions over time. The figure shows the globally averaged change in mixing state of BC among the 8 out of 18 size distributions in which BC was present, when coagulation, condensation, dissolution, and equilibrium water uptake affected internal mixing. Emissions, transport, dry deposition, sedimentation, and

rainout of aerosols were also accounted for. Initially, all BC was externally mixed in distribution E1. Coagulation moved BC from distribution E1 to binary mixtures of sulphate-BC, BC-organic matter (OM), soil-BC and spray-BC, to ternary and higher mixtures (MX) and to distributions E2 and E3. Growth also contributed to moving material from E1 to E2 and E3.

observations. Andreae *et al.*⁹ found that 80–90% of silicate particles over the Pacific Ocean between Ecuador and Hawaii contained sea spray. Here, by five days, 70–85% of soil particles in this region contained sea spray. Murphy *et al.*¹⁰ found that almost all particles > 0.13 μm over the remote Southern Pacific Ocean contained sea spray. Here, > 95% of all near-surface particles in that region contained sea spray. Posfai *et al.*¹¹ found that almost all soot particles over the North Atlantic contained sulphate. Here, > 93% of BC-containing particles in this region contained sulphate.

Simulations were run to estimate the yearly and globally averaged radiative effects of treating BC in three ways: as a coated core in multiple distributions; as a single externally mixed distribution; and as a coated core in a single internally mixed distribution (Fig. 3). In the multiple-distribution case, modelled mid-visible optical depths (0.1–0.4) and single-scattering albedos (0.86–0.97) over the eastern United States and the western Atlantic Ocean during TARFOX were in the range of measured values (0.06–0.7 and 0.85–0.98, respectively; refs 12, 13). Modelled optical depths (0.16–0.44) in the Arabian Sea, and optical depths (0.07–0.17) and single-scattering albedos (0.88–0.94) in the Indian Ocean during INDOEX were similarly close to observations (0.2–0.4 (ref. 14), ≤ 0.1 (ref. 14) and 0.88–0.90 (ref. 15), respectively). Modelled mid-visible single-scattering albedos over biomass-burning regions of Brazil (0.86–0.94) were in the range of measurements obtained during the same time of year (0.82–0.94 (ref. 16), 0.79–0.95 (ref. 17)). Modelled single-scattering albedos over biomass-burning regions of Africa (0.85–0.92) were close to those over biomass-burning regions of Brazil. The modelled annually averaged mid-visible optical depth over the global oceans (0.13) compares with a measured value of 0.12 (ref. 18).

Figure 3 shows that, within five days, the BC forcing from the multiple-distribution coated-core case was within 24% of that from the single-distribution coated-core case. This implies that the single-distribution coated-core assumption appears to be a better approximation of BC direct forcing than is the external-mixture assumption. As all studies to date have used the external-mixture assumption for determining lower bounds or average values of global direct forcing by anthropogenic aerosols, such lower bounds or average values must be higher (closer to zero) than all previous studies have predicted.

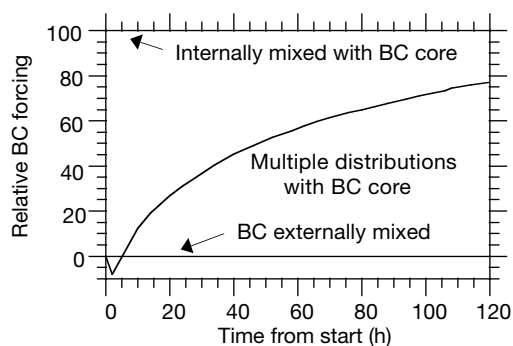


Figure 3 Time-dependent relative global BC direct forcing (at the tropopause) obtained when 18 size distributions were modelled. The relative forcing is $(F_{\text{mult}} - F_{\text{ext}}) / (F_{\text{int}} - F_{\text{ext}})$, where F_{mult} , F_{ext} and F_{int} are the forcings obtained with multiple distributions with BC as core, a single externally mixed BC distribution, and a single internally mixed distribution with BC as core, respectively. Each of the three forcing values at each time was calculated by averaging results from 24 simulations (6 days per year and 4 start times per day). For each simulation, the multiple-distribution forcing was obtained by initializing externally mixed distributions and relaxing towards a steady state with continuous emissions and nucleation of externally mixed particles and physical/chemical/deposition processes among all particles. The single externally and internally mixed distributions were derived from the multiple-distribution cases each time step in a mass-conserving manner to guarantee that the mass of BC and other components were exactly the same in each size bin each time step. Radiative calculations were then performed over the single distributions.

The final yearly averaged direct forcing due to BC in the external mixture, the multiple-distribution coated-core, and the single internally-mixed, coated-core distribution cases from Fig. 3 were 0.31, 0.55 and 0.62 W m^{-2} , respectively. The multiple-distribution BC direct forcing (0.55) falls between direct-forcing estimates for CH_4 (0.47 W m^{-2}) and CO_2 (1.56 W m^{-2}) from IPCC¹⁹. Thus, subject to uncertainties, BC may be the second most important component of global warming in terms of direct forcing, after CO_2 . For this reason, controls on BC emissions, not treated under the Kyoto Protocol of December 1997, need to be considered. Major sources of BC include the burning of diesel fuel, coal, jet fuel, natural gas, and biomass.

Previous studies have implied⁷ or suggested²⁰ that BC controls would be beneficial (studies have also shown that controls on non- CO_2 greenhouse-gas emissions would be beneficial²¹). The present study suggests that BC controls may be as—or more—beneficial than methane controls. Nevertheless, to obtain the true effect on rising global temperatures of controls on BC, CH_4 and CO_2 , comparative time-dependent simulations of the response of climate to these pollutants are needed. □

Received 24 July; accepted 23 November 2000.

- Haywood, J. M., Roberts, D. L., Slingo, A., Edwards, J. M. & Shine, K. P. General circulation model calculations of the direct radiative forcing by anthropogenic sulfate and fossil-fuel soot aerosol. *J. Clim.* **10**, 1562–1577 (1997).
- Haywood, J. M. & Ramaswamy, V. Global sensitivity studies of the direct radiative forcing due to anthropogenic sulfate and black carbon aerosols. *J. Geophys. Res.* **103**, 6043–6058 (1998).
- Myhre, G., Stordal, F., Restad, K. & Isaksen, I. S. A. Estimation of the direct radiative forcing due to sulfate and soot aerosols. *Tellus B* **50**, 463–477 (1998).
- Cooke, W. F., Liousse, C., Cachier, H. & Feichter, J. Construction of a $1^\circ \times 1^\circ$ fossil fuel emission data set for carbonaceous aerosol and implementation and radiative impact in the ECHAM4 model. *J. Geophys. Res.* **104**, 22137–22162 (1999).
- Hansen, J. E. *et al.* Climate forcings in the industrial era. *Proc. Natl Acad. Sci. USA* **95**, 12753–12758 (1998).
- Penner, J. E., Chuang, C. C. & Grant, K. Climate forcing by carbonaceous and sulfate aerosols. *Clim. Dyn.* **14**, 839–851 (1998).
- Jacobson, M. Z. A physically-based treatment of elemental carbon optics: Implications for global direct forcing of aerosols. *Geophys. Res. Lett.* **27**, 217–220 (2000).
- Jacobson, M. Z. Development and application of a new air pollution modeling system - II. Aerosol module structure and design. *Atmos. Environ.* **31**, 131–144 (1997).
- Andreae, M. O. *et al.* Internal mixture of sea salt, silicates, and excess sulfate in marine aerosols. *Science* **232**, 1620–1623 (1986).
- Murphy, D. M. *et al.* Influence of sea-salt on aerosol radiative properties in the Southern Ocean marine boundary layer. *Nature* **395**, 62–65 (1998).
- Posfai, M., Anderson, J. R., Buseck, P. R. & Sievering, H. Soot and sulfate aerosol particles in the remote marine troposphere. *J. Geophys. Res.* **104**, 21685–21693 (1999).
- Hegg, D. A., Livingston, J., Hobbs, P. V., Novakov, T. & Russell, P. Chemical apportionment of aerosol column optical depth off the mid-Atlantic coast of the United States. *J. Geophys. Res.* **102**, 25293–25303 (1997).
- Russell, P. B., Hobbs, P. V. & Stowe, L. L. Aerosol properties and radiative effects in the United States East Coast haze plume: An overview of the tropospheric aerosol radiative forcing observational experiment (TARFOX). *J. Geophys. Res.* **104**, 2213–2222 (1999).
- Jayaraman, A. *et al.* Direct observations of aerosol radiative forcing over the tropical Indian Ocean during the January–February 1996 pre-INDOEX cruise. *J. Geophys. Res.* **103**, 13827–13836 (1998).
- Satheesh, S. K. *et al.* A model for the natural and anthropogenic aerosols over the tropical Indian Ocean derived from Indian Ocean Experiment data. *J. Geophys. Res.* **104**, 27421–27440 (1999).
- Eck, T. F., Holben, B. N., Slutsker, I. & Setzer, A. Measurements of irradiance attenuation and estimation of aerosol single scattering albedo for biomass burning aerosols in Amazonia. *J. Geophys. Res.* **103**, 31865–31878 (1998).
- Dubovik, O. *et al.* Single-scattering albedo of smoke retrieved from the sky radiance and solar transmittance measured from ground. *J. Geophys. Res.* **103**, 31903–31923 (1998).
- Husar, R. B., Prospero, J. M. & Stowe, L. L. Characterization of tropospheric aerosols over the oceans with the NOAA advanced very high resolution radiometer optical thickness operational product. *J. Geophys. Res.* **102**, 16889–16909 (1997).
- Houghton, J. T. *et al.* (eds) *Climate Change 1995, The Science of Climate Change* (Cambridge University Press, New York, 1996).
- Hansen, J., Sato, M., Ruedy, R., Lacis, A. & Oinas, V. Global warming in the twenty-first century: An alternative scenario. *Proc. Natl Acad. Sci.* **97**, 9875–9880 (2000).
- Hayhoe, K. *et al.* Costs of multigreenhouse gas reduction targets for the USA. *Science* **286**, 905–906 (1999).

Supplementary information is available on Nature's World-Wide Web site (<http://www.nature.com>) or as paper copy from the London editorial office of Nature.

Acknowledgements

This work was supported by the NASA New Investigator Program, the NSF, the David and Lucile Packard Foundation, and Hewlett-Packard.

Correspondence and requests for information should be addressed to author (e-mail: jacobson@ce.stanford.edu).